Imperial College London
Department of Chemical Engineering

Modelling, Optimisation and Explicit Model Predictive Control of Anaesthesia Drug Delivery Systems

Alexandra Krieger

December 2013

Supervised by Professor Stratos Pistikopoulos

Submitted in part fulfilment of the requirements for the degree of
Doctor of Philosophy in Chemical Engineering of Imperial College London
and the Diploma of Imperial College London

Declaration

I herewith certify that all material in this dissertation which is not my own work has been properly acknowledged.

Alexandra Krieger

Abstract

The contributions of this thesis are organised in two parts. Part I presents a mathematical model for drug distribution and drug effect of volatile anaesthesia. Part II presents model predictive control strategies for depth of anaesthesia control based on the derived model.

Closed-loop model predictive control strategies for anaesthesia are aiming to improve patient's safety and to fine-tune drug delivery, routinely performed by the anaesthetist.

The framework presented in this thesis highlights the advantages of extensive modelling and model analysis, which are contributing to a detailed understanding of the system, when aiming for the optimal control of such system. As part of the presented framework, the model uncertainty originated from patient-variability is analysed and the designed control strategy is tested against the identified uncertainty.

An individualised physiologically based model of drug distribution and uptake, pharmacokinetics, and drug effect, pharmacodynamics, of volatile anaesthesia is presented, where the pharmacokinetic model is adjusted to the weight, height, gender and age of the patient. The pharmacodynamic model links the hypnotic depth measured by the Bispectral index (BIS), to the arterial concentration by an artificial effect site compartment and the Hill equation. The individualised pharmacokinetic and pharmacodynamic variables and parameters are analysed with respect to their influence on the measurable outputs, the end-tidal concentration and the BIS. The validation of the model, performed with clinical data for isoflurane and desflurane based anaesthesia, shows a good prediction of the drug uptake, while the pharmacodynamic parameters are individually estimated for each patient.

The derived control design consists of a linear multi-parametric model predictive controller and a state estimator. The non-measurable tissue and blood concentrations are estimated based on the end-tidal concentration of the volatile anaesthetic. The designed controller adapts to the individual patient's dynamics based on measured data. In an alternative approach, the individual patient's sensitivity is estimated on-line by solving a least squares parameter estimation problem.

Acknowledgements

This thesis was funded by the European Research Council (MOBILE, ERC Advanced Grant, No: 226462). Further I would like to acknowledge the financial support by the CPSE Industrial Consortium. I would like to thank Dr. med. Rainer Röhrig and the Department of Medical Informatics in Anesthesiology and Intensive Care Medicine of the University of Gießen in Germany for providing the anonymised patient data used in this study. I would like to thank my supervisor Stratos Pistikopoulos for his guidance and encouragement during the time in his group at Imperial College London. Further, I would also like to thank my examiners, Prof. Robin de Keyser and Prof. Claire Adjiman, who provided detailed comments and constructive feedback on my thesis. A great thank you to all my colleagues for their good friendship, fruitful discussions and occasional weekend activities. My time in London would not have been the same without participating actively in the volleyball community. Thanks to all of you. You truly kept me fit and busy. I met so many amazing personalities from all over the world during my PhD. You all made my time worthwhile. Most of all I would like to thank my flatmates. You were my family abroad and always there for me. We are truly "the best flat ever". I also would like to thank my friends back home in Germany, who kept in touch and dropped me occasional visits. You gave me the feeling nothing changed although I was away. Finally I would like to thank my sister and my parents for their support. You were always there for me. Danke.

Contents

List of Tables

List of Figures

Notation

Modelling, Model Analysis and Model Validation

List of Acronyms

BIS	Bispectral index
BMI	Body mass index
F	Adipose tissue/ Fat group
M	Muscle group
MAC	Mean alveolar concentration
P	Patient
PBPK	Physiologically based pharmacokinetics
PD	Pharmacodynamic
PK	Pharmacokinetic
SI	Sensitivity index
VPG	Vessel poor group
VRG	Vessel rich group

List of Variables and Parameters

Symbol	Denotation	Units
C	Concentration of volatile anaesthetic	vol%
C_{50}	Drug concentration at 50% effect	vol%
f_R	Respiratory frequency	$\frac{1}{\text{min}}$
γ	Slope of Hill equation	-
λ	Solubility	-
m	Tissue mass	kg
m_{liv}	Metabolism liver	$\frac{\text{mL}}{\text{min}}$
$\dot{Q}$	Cardiac output	$\frac{\text{mL}}{\text{min}}$
$\dot{Q}_i$	Blood flow	$\frac{\text{mL}}{\text{min}}$
$\dot{Q}_s$	Shunt flow	-
ρ	Tissue density	$\frac{\text{kg}}{\text{mL}}$
$r_{\dot{Q}}$	Ratio of cardiac output	-
r_{V_B}	Ratio of total blood volume	-
r_{V_t}	Ratio of total tissue/body volume	-
u	Uptake	$\frac{\text{mL}}{\text{min}}$
V	Volume	mL
$\dot{V}$	Minute ventilation	$\frac{\text{mL}}{\text{min}}$
V_A	Alveolar volume	mL
$\dot{V}_A$	Alveolar ventilation	$\frac{\text{mL}}{\text{min}}$
V_B	Blood volume	mL
V_D	Dead space	% V_T
$\dot{V}_D$	Dead space ventilation	$\frac{\text{mL}}{\text{min}}$
V_L	Lung volume	mL
V_T	Tidal volume	mL

List of Subscripts

Symbol	Denotation
A	Alveoli
a	Arterial
b	Blood
e	Effect compartment
E	Expired
est	Estimated value
F	Fat group, adipose tissue
f	Female
i	Compartment
I	Inspired
L	Lungs
l	Lower bound
liv	Liver
M	Muscle group
m	Male
$meas$	Measured value
t	Tissue
u	Upper bound
$\bar{v}$	Mixed venous return
VPG	Vessel poor group
VRG	Vessel rich group

Optimisation and Model Predictive Control

List of Acronyms

CD	Control design
LPV	Linear parameter varying
LTI	Linear time invariant
MHE	Moving horizon estimation
mp	multi-parametric
MPC	Model predictive control
ODE	Ordinary differential equation
QP	Quadratic programming
RSME	Root mean squared error

List of Variables

Symbol	Denotation
A	State matrix
B	Input matrix
B_d	Input disturbance matrix
C	Output matrix
C_d	Output disturbance matrix
CR	Critical Region
d	Disturbance
E	Constraint matrix of mp-QP problem
F	Weight matrix of mp-QP problem
G	Disturbance matrix
G	Constraint matrix of mp-QP problem
H	Weight matrix of mp-QP problem
M	Control horizon
N	Output horizon
P	Weight matrix on the final states
Q	Weight matrix on the states
$\hat{Q}$	Process noise covariance matrix of Kalman filter
Q_R	Weight matrix on reference tracking error
R	Weight matrix on inputs
$\hat{R}$	Measurement noise covariance matrix of Kalman filter
R_1	Weight matrix on rate of change in control input
t_s	Sampling time
θ	Parameter vector of mp-QP problem
u	Input vector
U	Optimisation vector of mp-QP problem
Δu	Step change in control input, (ΔC_I)
v	Measurement noise
w	Process noise
W	Constraint matrix of mp-QP problem
x	State vector
y	Output vector
Y	Weight matrix of mp-QP problem
y^R	Reference point

1. Motivation and Introduction

During surgery, the anaesthetist faces the task of providing safe anaesthesia for the patient, while maintaining the vital functions. A mix of administered drugs leads to the desired effects of hypnosis, amnesia, analgesia and muscle relaxation. The drug side-effects on the cardiovascular system, the respiratory system and the central nervous system, if not monitored closely, can have such a high impact that they are life threatening. Given an enormous variety of (i) patients differing in weight, height, age, sex and race, (ii) requirements for surgeries with distinctive impact on the patient and (iii) interactions of administered agents, the anaesthetist has to keep all these covariates and influences in mind, while providing anaesthesia with possible complications.

Currently anaesthetists rely on common practice and their personal experience to determine simultaneous drug administration rates. High-fidelity modelling and optimised control for drug administration could (i) pave the way for personalised health care, taking into account the individual patient characteristics for optimal and flexible drug administration, (ii) guarantee the safety of the patient minimising side-effects, as well as (iii) provide the anaesthetist with additional information about the current anaesthetic state of the patient, the patient's vital functions and more time to focus on critical issues.

The modelling and automatic control of anaesthesia is believed to benefit the safety of the patient undergoing surgery and provide anaesthetists and researchers with valuable insights, (Bibian *et al.*, 2005; Glass and Rampil, 2001; Hardman and Ross, 2006; Morari and Gentilini, 2001; Struys *et al.*, 2006).

Motivated by various challenges in automation of anaesthesia, this thesis focuses on the automation of the hypnotic state of the patient. The presented steps in this thesis towards a validated control strategy starting with the model development via model analysis, uncertainty identification and robust control design are pointed out in the framework in Figure 1.1.

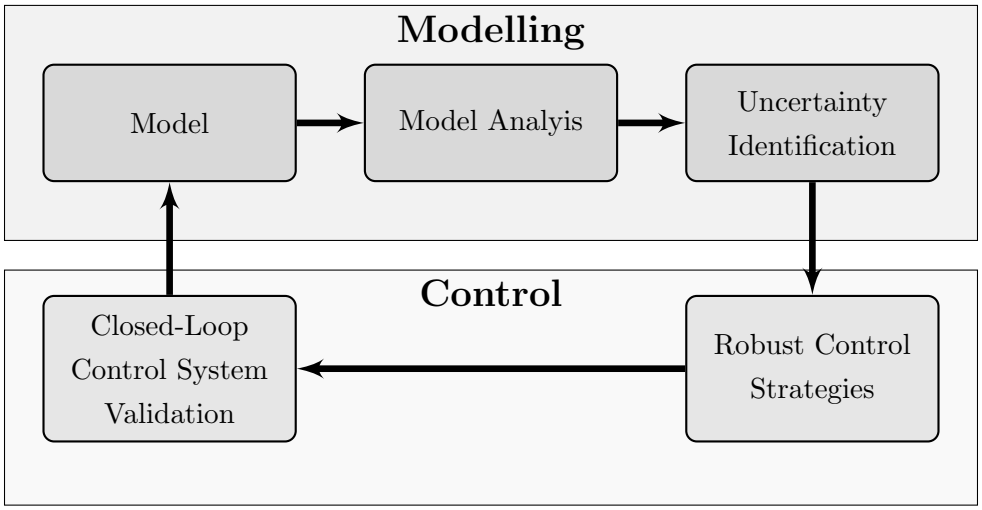

Figure 1.1.: Framework illustrating the work presented in this thesis.

Anaesthesia is either both induced and maintained by the continuous infusion of an intravenous anaesthetic agent, e.g. propofol, or maintained by admixture of a volatile anaesthetic agent, e.g. isoflurane or desflurane, to the inhaled air. Volatile anaesthesia is preferred by most anaesthetists, because the end-tidal concentration of the volatile anaesthetic is standardly measured and widely used as an indicator of the hypnotic depth, (Miller *et al.*, 2010) and (Chapter 2, Figure 2.2). For intravenous anaesthesia, the anaesthetist relies on the measurement of the hypnotic depth by, for example, the Bispectral Index (BIS), because on-line plasma concentration measurements are not available. The Bispectral index (BIS) is an empirically derived signal based on a real-time electroencephalography (EEG) trace acquired from a frontotemporal montage. The BIS value indicates the responsiveness of the patient and ranges from 100 to 0, where 100 describes normal cortical electrical activity of a fully awake patient, 85-65 sedation, 65-45 general anaesthesia, 45 deep hypnosis, 40 near suppression, 30-0 increasing burst suppression and 0 cortical electrical silence, (Miller *et al.*, 2010).

In brief, the objective for control of anaesthesia can be summarised by a fast and stable maintenance of the hypnotic level, measured by the BIS. The BIS target values for general anaesthesia lie in-between 40-60, but might be modified by the anaesthetist. A summary of the control objective is depicted in Figure 1.2, where C_I denotes the concentration of the inhaled volatile anaesthetic or the bolus of the infused intravenous anaesthetic. BIS denotes the measure of the anaesthetic depth and C_E the exhaled or end-tidal anaesthetic concentration, only available for volatile anaesthesia.

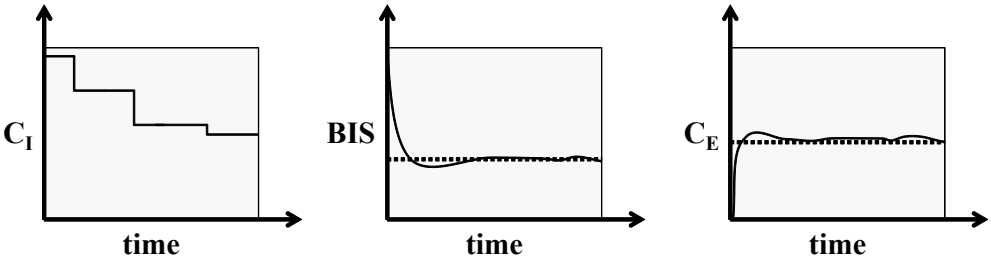

Figure 1.2.: Control objective for intravenous and volatile anaesthesia.

The closed loop state feedback control design for drug delivery of anaesthesia is illustrated in Figure 1.3. The controller, MPC block in Figure 1.3, computes the optimal drug concentration or dose u (C_I) for the patient to maintain the reference point y^R on the BIS or C_E, which is illustrated in Figure 1.2.

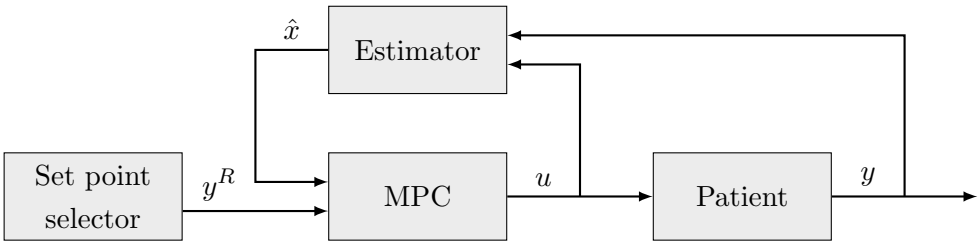

Figure 1.3.: Closed loop control design structure.

The first essential step towards such closed loop control strategy is the derivation of a mathematical model that adequately describes the system. Here the challenge is to find the balance between a very complex model and an over-simplified model. The very complex model is likely to contain too many parameters that cannot be determined or estimated independently, mainly due to the lack of measurements and adequate sensors. The over-simplified model might neither capture the systems dynamics nor allow insights and understanding of the system. During the modelling process and model design, the objective of the model development plays a crucial role; in this thesis, the focus lies on model development for explicit MPC. Hence, the model should be of a reasonable size to enable the computation of an explicit controller, but still represent the individual patient's characteristics.

The pharmacokinetic-pharmacodynamic (PK-PD) model presented in this thesis contains 7 ordinary differential equations (ODE), presented in Chapter 3. The state space representation (1.1) of the equation system, built based on this model, has two fixed inputs, one variable input, one output and 7 state

variables, resulting in a 7-dimensional state vector $x \in \mathbb{R}^n$ with n=7.

$$\begin{aligned} x_{k+1} &= \mathbf{A}x_k + \mathbf{B}u_k \\ y_k &= f(x_k), \end{aligned} \tag{1.1}$$

where k denotes the discrete time points. The state vector, x_k, contains the concentrations in the blood and tissue compartments of the model, u_k denotes the variable input, C_I, and y_k is the output, BIS. An illustration is given in Figures 1.2 - 1.3. The non-linearity, $f(x_k)$, is introduced by the Hill equation, which relates the effect-site concentration to the BIS. For the design of a linear explicit MPC strategy a discrete linear state space system is required:

$$\begin{aligned} x_{k+1} &= \mathbf{A}x_k + \mathbf{B}u_k \\ y_k &= \mathbf{C}x_k \end{aligned} \tag{1.2}$$

The strategies to obtain a liner system are (i) the algebraic inverse of the Hill equation (Gentilini *et al.*, 2001; Ionescu *et al.*, 2008) or alternatively (ii) piecewise affine approximations of the Hill equation (Chapter 7).

The derived model is implemented and simulated in gPROMS (PSE, 2011) and shows a good approximation of the pharmacokinetics of isoflurane and desflurane, whereas the pharmacodynamic parameters were individually estimated for each patient applying the gPROMS (PSE, 2011) parameter estimation entity (Chapter 5). To gain further understanding, all parameters of the model are analysed with respect to the measurable outputs: the end-tidal concentration and the BIS. For a global sensitivity analysis parameters and variables were divided into a pharmacokinetic and pharmacodynamic group and analysed separately. A further analysis was performed by changing the parameters one at a time in-between specified bounds to observe the effect on the output of interest. In the final part of the model analysis, a correlation analysis of the most influential parameters and variables is presented. This extensive analysis leads to a very good understanding of the model and its dynamics and, more importantly, the envelope of uncertainty the MPC has to handle (Chapter 4). In addition, the model with individually adjusted variables and parameters can be applied for closed loop control validation, where the patient block in Figure 1.3 represents a patient of the clinical study.

Given this validated and analysed model, an anaesthesia drug delivery system consisting of an explicit MPC is designed that calculates the optimal drug dose as a function of the derived model. The MPC is designed as a state feedback controller. The optimal control input, the drug dose C_I, is calculated based on the system's states, which are the drug concentrations in the tissue

and blood compartments. Not all drug concentrations can be easily measured; hence, a state estimator is required to predict the non-measurable states. The straightforward choice is to apply the derived state space model and simulate it simultaneously with the process for identical inputs to obtain the states. As a second strategy the states are estimated by a Kalman filter based on the measurement of the end-tidal anaesthetic concentration (Chapter 7).

The choice for the design of an explicit controller via multi-parametric quadratic programming (mp-QP) is motivated by the possibility of testing the controller in advance for all occurring scenarios and the full parameter space, (Bemporad *et al.*, 2002), which complies with the high safety standards for drug delivery systems of anaesthesia. The mp-MPC is derived in the POP toolbox for MATLAB, (ParOS, 2004), and designed to adjust to the individual patient's dynamics by an output feedback strategy. As an add-on to the explicit MPC, an on-line parameter estimation of the PD parameter C_{50}, which shows the highest sensitivity towards the BIS is presented. Here a least squares optimisation problem is solved in GAMS (2013) (Chapter 10).

Structure of this Thesis

The structure of this thesis is organised in two parts guided by the framework presented in Figure 1.1. Part I is concerned with modelling of the drug distribution and drug effects during volatile anaesthesia, model analysis and validation studies. Part I has been partly published in Krieger *et al.* (2013). Part II is illustrating the control design and closed-loop control validation of the drug delivery system for depth of anaesthesia. Each part contains a separate literature review.

Part I:
Modelling, Model Analysis and Model Validation

Objective and Summary

The objective of this part is to fundamentally understand and analyse the dynamics of the system: the model for volatile anaesthesia.

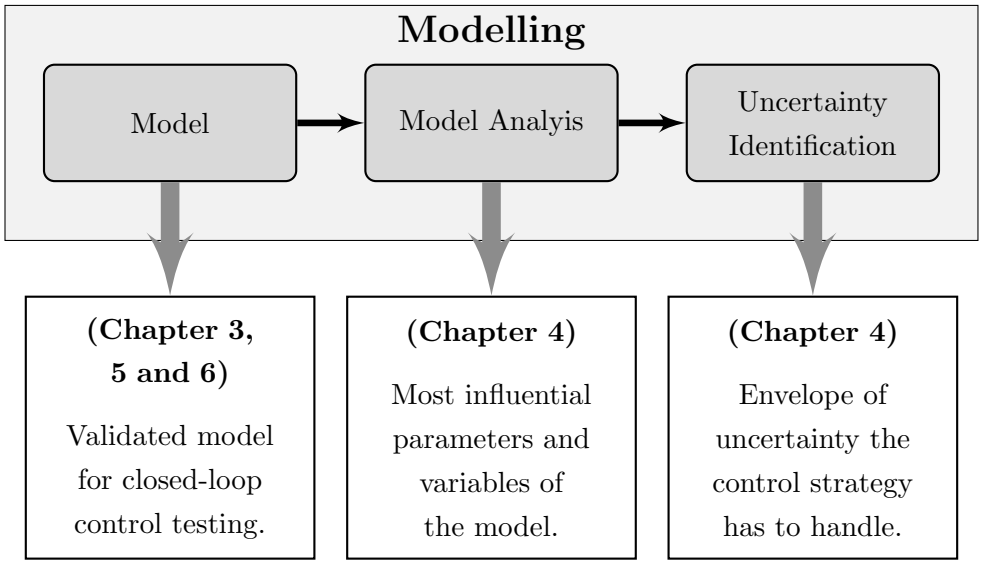

Figure 1.4.: Modelling framework and contributions presented in Part I.

The objectives and contributions of an extensive analysis leading to a well-established understanding of the dynamic system model in Figure 1.4 are further defined as follows:

I) Validated model with clinical data for closed loop control evaluation.
   - Validated model for uptake and distribution of isoflurane and desflurane based anaesthesia.

II) In-depth understanding of the influence of the model's parameters and variables.
   - Cardiac output and lung volume are the parameters with the highest influence on the distribution and uptake of the volatile anaesthetic agent.
   - The pharmacodynamic parameters have the highest influence with respect to the drug effect; particularly C_{50} defined as the effect site concentration at 50% drug effect.

III) Identify the uncertainty for the design of a robust control strategy.
   - The inter-patient variability is very high; particularly for the pharmacodynamic parameters; hence an off-set free robust control method or on-line parameter estimation is required to provide safe control.

2. Fundamentals of Mathematical Modelling for Anaesthesia

The mathematical modelling of drug distribution and drug effect for a wide number of drugs, e.g. chemotherapeutic agents, hypnotics and analgesics is a well established method to help understanding and predicting the mechanisms occurring during and after drug administration. In this context, the aim is to describe the time course of drug concentrations in the tissues and the effect on the body by mathematical equations, (Dingemanse and Appel-Dingemanse, 2007). Equations describing the distribution, absorption, elimination and metabolism are referred to as pharmacokinetics, whereas the link of the concentration to the effect is described by pharmacodynamic equations.

2.1. Pharmacokinetic Modelling

Pharmacokinetics describe the distribution of the drug in the human body. Here, two approaches for pharmacokinetic models dominate the literature, (i) mammillary compartmental models, where several peripheral compartments are connected to one central compartment, and (ii) physiologically based pharmacokinetic models, where organs and tissues are interconnected and arranged copied from physiology. The approach of physiologically based pharmacokinetic (PBPK) modelling for drug delivery, uptake and distribution models gains increasing attention of researchers, (Hall *et al.*, 2012), and may be very detailed down to a systems biology level, (Ghosh *et al.*, 2011).
The probably oldest idea of of describing the human body as a complex interaction of flows and plants processing nutrients originates from Kahn (1926), who imagined the man as a complex industrial machine. In the 1930s Teorell derived first physiologically based models for drug distribution, uptake and elimination (Teorell, 1937a,b). Pioneering work towards individual patient variables of volatile agents for a model mapping the circulation to describe the uptake of ether in a dog goes back to Haggard, (Haggard, 1924a,b,c).

Regarding the prediction of the uptake of volatile anaesthetics most models are either based on the work of Mapleson or Eger. Both authors were aiming to match the measured uptake of the anaesthetic gas by mathematical equations

to understand the anaesthetic uptake of their patients. The basic idea was to group tissues with similar properties, such as the well perfused organs, into one compartment and describe the uptake based on these tissues' properties, e.g. drug solubility and perfusion.

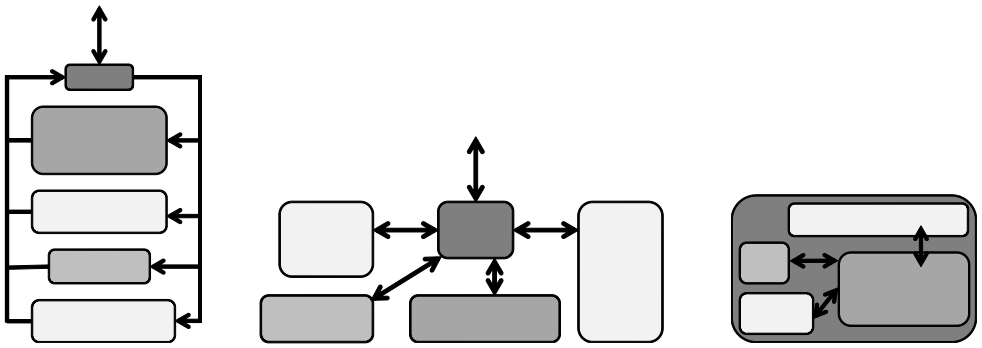

(a) PBPK model Mapleson.

(b) Mammillary PK model Eger.

(c) Further subdivision of one compartment.

Figure 2.1.: Generic structures of pharmacokinetic models for volatile anaesthesia.

Mapleson described the blood flows and body tissues analogously to an electrical circuit, where the tissue compartments are represented by capacitors and the blood vessels by resistances, illustrated in Figure 2.1(a), (Mapleson, 1962, 1963, 1964a,b). The derived compartmental physiologically based model was further tested and validated for halothane uptake in a dog by Allott *et al.* (1976).

Eger described the uptake of the anaesthetic agent by a hydraulic model, where different tissue groups are characterized by tanks of different diameters and connected to one central tank, which represents the alveolar gas, and is illustrated in Figure 2.1(b), (Cromwell *et al.*, 1971; Eger, 1974; Eger and Guadagni, 1963).

Based on the work of Mapleson, Zwart *et al.* and Smith *et al.* derived an eight compartmental physiologically based model for the uptake of halothane, (Smith *et al.*, 1972; Zwart *et al.*, 1972). Goldberg *et al.* applied this model for closed loop anaesthesia of halothane, (Goldberg *et al.*, 1978). Fiserova-Bergerova *et al.* extended the model by adding additional tissue groups, i.e. subcutaneous and inner adipose tissue, the liver and additional anaesthetic agents, i.e. isoflurane, enflurane and methoxyflurane, (Fiserova-Bergerova, 1992; Fiserova-Bergerova and Holaday, 1979; Fiserova-Bergerova *et al.*, 1974, 1980). Also Lerou *et al.* extended the Mapleson model to a 14 compartment model for teaching and research purposes describing the simultaneous uptake

of isoflurane, nitrous oxide and oxygen, which was then validated with clinical data, (Lerou and Booij, 2001a,b, 2002; Lerou *et al.*, 1991a,b, 2002; Vermeulen *et al.*, 1995).
Eger's hydraulic model was further extended by Carpenter *et al.* (1986) to a five compartmental mammillary model connected by one central compartment, Figure 2.1(b). This approach was further applied and extended by Yasuda *et al.* for uptake of desflurane, isoflurane and halothane, (Yasuda *et al.*, 1991a,b).
Kety was the pioneer towards characterisation of individualised drug uptake depending on (i) drug solubilities or partition coefficients in the tissues and (ii) the physiological variables such as the cardiac output, (Kety, 1950, 1951).

The description of one compartment itself in either the mammillary model or the physiological based model can be described by complex interactions and flows between e.g. blood cells, plasma, intestinal fluid, a rapid interactive pool, and a slow interactive pool, illustrated in Figure 2.1(c). Bischoff (1975) gives a comprehensive summary of physiologically based pharmacokinetic models. Furthermore the concept of a flow-limited and/or a diffusion-limited model can be applied to describe the uptake and distribution within one compartment, (Thompson and Beard, 2011). Given a fast drug diffusion in the capillaries from blood to tissue, in most approaches the compartments are assumed to be flow-limited. In the perfusion-limited approximation the uptake of the tissues is restricted by the permeability of the membranes separating blood and tissue, (Bischoff, 1975, 1986).

2.2. Pharmacodynamic Modelling

The individualized characterisation of the pharmacodynamics, which link the drug concentration to the drug effect, is more challenging because of higher inter- and intra-patient variability, (Mertens and Vuyk, 1998).

To determine the hypnotic depth, anaesthetists commonly apply the Minimum Alveolar Concentration (MAC) as a guideline. MAC is defined as the concentration required to prevent movement in response to surgical incision in 50% of the patients. During general anaesthesia conventionally 1.3 MAC is the target value, which assures sufficient anaesthesia in 90% of the patients, (Eger *et al.*, 1965). The resulting cumulative probability curve is shown in Figure 2.2, (Krieger *et al.*, 2012).

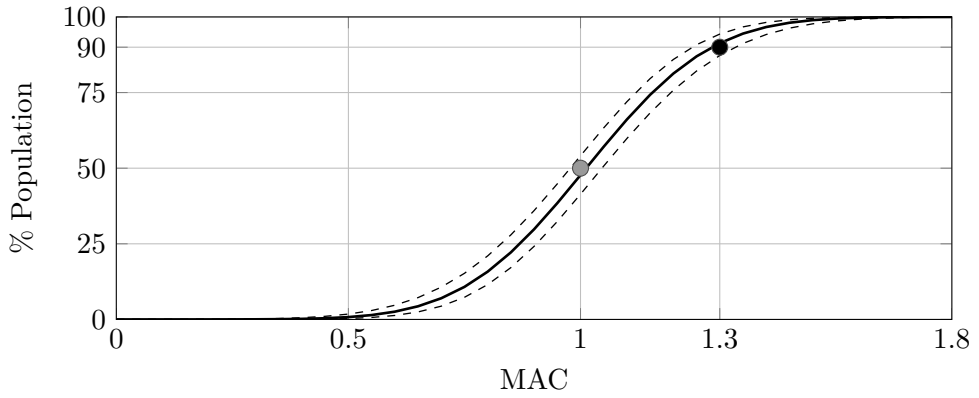

Figure 2.2.: Population distribution of MAC for sufficient hypnosis with 95% confidence interval. The gray dot denotes 1 MAC for 50% and the black dot denotes 1.3 MAC for 90% of the population.

Figure 2.2 highlights the challenge of identifying the individual patient's sensitivity and anaesthetic state to avoid awareness or overdosing.

Already by definition the guideline for dosing of volatile anaesthetic agents during anaesthesia is based on probability. This highlights the challenge of identifying the individual patient's sensitivity and consecutively the hypnotic depth to avoid awareness or overdosing. Parameters influencing the individual patient's sensitivity are for example the age. Studies by Brunner *et al.* (1994) investigated the correlation of MAC with patient characteristics or analgesics administered simultaneously during anaesthesia. Mapleson (1996) and Eger (2001) found that MAC decreases with age and that elderly patients are more sensitive to anaesthetics. Furthermore the patient's sensitivity towards the anaesthetic agent changes depending on surgical stimulation and simultaneously administered drugs during anaesthesia, such as muscle relaxants and analgesics, (Glass *et al.*, 1997; Rosow, 1997). Recent advances investigate the pharmacogenomic variability as an indicator of individual patient's sensitivity to anaesthetic agents, (Searle and Hopkins, 2009). The challenge is to include the entire pharmacodynamic variability, which is estimated to vary up to 400% by Mertens and Vuyk (1998), in the model. This task might be very complex if not impossible.

2.3. Applications

Applications of mathematical models for drug delivery systems lie in the area of patient simulators or mannequins for training of nurses, medical students or anaesthetists and in on-line computation of the current drug concentrations and effect during surgery.

2.3.1. Patient Simulators and Simulation Tools for Teaching and Training

The idea of using computer programs to simulate and predict the uptake of the anaesthetic agent originates from the work of Tanner *et al.* (1986).

Training and teaching with patient simulators and mannequins is becoming more common in modern medical education. One of the most advanced patient simulators on the market is the CAE Healthcare© HPS® (CAE Healthcare, 2013). This patient simulator shows all vital functions and inhales and exhales oxygen and anaesthetic agents according to a mathematical model, (Van Meurs, 2011).

Several software tools for training are available, the most well known tool is Gas Man®(MMSI, 2006), a computer tool for teaching, simulating and experimenting with anaesthesia uptake and distribution.

2.3.2. On-line Monitoring and Prediction

The SmartPilot View by Dräger (Herbst, 2010) or the Navigator Applications Suite software by GE Healthcare (2013) are software tools that enable a frequently updated state of the patient calculated based on drug infusions and boluses and the measured variables e.g. the exhaled and inhaled gases and the vital functions. The aim of these tools is to provide the anaesthetist with a decision support. The anaesthetist can follow the moving state of the patient in a 2D graph and see the future states for the given infusions and inhalations, (Grünberg, 2009).

3. Model for Volatile Anaesthesia

The first and essential step for any model predictive control design is the derivation and validation of a model that is describing the system's behaviour accurately. The physiologically based model for the uptake, distribution and effect of volatile anaesthetic agents presented in this section is based on the work published in Krieger *et al.* (2013) and our previous work in Krieger *et al.* (2011, 2012).

In this thesis the physiologically based pharmacokinetic modelling approach is applied to describe the pharmacokinetics (PK) and address patient variability by including patient-specific characteristics in the mathematical description, (Hall *et al.*, 2012). The variability of the PK uncertainty is included analogously to Fiserova-Bergerova (1992), where all volumes for blood tissue and gas compartments are assigned specific to the individual patient's weight, height and age. By including these factors the aim is to reduce significantly the variability in the PK, which is estimated to be around 60-80%, (Mertens and Vuyk, 1998).

The challenge is to find the balance between a too complex but reasonably simple model with respect to application in model predictive control and still aim for the required detail, (Tanner, 1982).

3.1. Pharmacokinetics

The physiologically based compartmental model for volatile anaesthetics, Figure 3.1(a), is based on Eger's compartmental model for volatile anaesthesia, where the tissues with similar properties are lumped together resulting in three body compartments representing the Vessel Rich Group (VRG), the Muscle Group (M) and the Adipose Tissue (F), (Eger, 1974). Each body compartment is further divided into an ideally mixed blood and ideally mixed tissue part. This approach is based on a model for cancer chemotherapeutic drugs first presented by Bischoff (1986). The gas, blood and tissue volumes are individually adjusted to the weight, height, gender and age of the patient.

A detailed list of all variables and their units can be found in the notation lists in the beginning of this thesis.

The compartments are described assuming a flow-limited formulation. Hence, the diffusion through the capillary vessel walls is assumed to be rapid and the mass transfer of the drug into the tissue is restricted by the perfusion of the compartment. This approximation is not fundamental to the physiological pharmacokinetic approach, but commonly used due to the lack of sufficient physiological information of e.g. membrane permeabilities, diffusion coefficients and tissue surfaces, (Bischoff, 1986). No inter-tissue diffusion between the compartments e.g. from the VRG to the adipose tissue is included, (Zwart *et al.*, 1972). This implies that mass exchange only occurs through the blood vessels. The transport time and the pulsatile character of the blood flow are neglected, because the equilibration times are large compared to the cardiac cycle, (Zwart *et al.*, 1972). All fluxes leaving a gas, blood or tissue compartment are in equilibrium with the compartment.

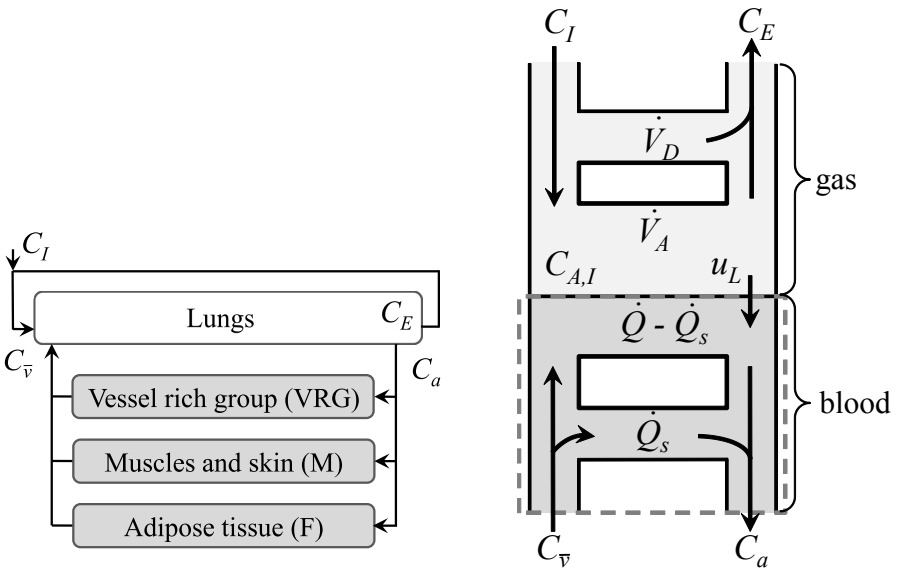

(a) Patient body. (b) Fluxes in the lungs.

Figure 3.1.: Structure of the physiologically based patient model.

The uptake of the anaesthetic agent is determined by two factors: the ventilation of air through the lungs and the perfusion of blood through the lungs. The ventilation is given by the product of the respiratory frequency f_R and the tidal volume V_T. Only a part of the total minute ventilation $\dot{V}$, usually two thirds, take part in the gas exchange in the lungs and reach the alveoli. This alveolar ventilation $\dot{V}_A$ is given by the total ventilation $\dot{V}$ less the dead space ventilation $\dot{V}_D$:

$$\dot{V}_A = \dot{V} - \dot{V}_D = f_R(V_T - V_D) \tag{3.1}$$

Here f_R and V_T are set by the anaesthetic machine and the anaesthetist, respectively. Analogously to (3.1) the alveolar volume V_A is determined by the lung volume V_L less the dead space volume V_D.

$$V_A = V_L - V_D \tag{3.2}$$

The applied mass balances and assumptions, the fluxes of gas and blood in the lungs are shown in Figure 3.1(b).
The input variable of the model, to be optimised by the controller, is the concentration of the inhaled volatile anaesthetic agent C_I, routinely set by the anaesthetist.

To map the respiratory cycle and the changing gas concentration in the lungs, the concentration in the alveoli just after inspiration C_{A_I} is given in (3.3) analogous to the Bohr equation for carbon dioxide, (Miller *et al.*, 2010), where the amount of inhaled anaesthetic gas is ideally mixed with the gas left in the lungs after expiration. This equation aims to represent the time-varying process of inspiration and expiration by a time invariant equation.

$$C_{A_I}\,(V_A + V_T) = C_I\,V_T + C_E\,V_A \tag{3.3}$$

The concentration during expiration is given by the assumption of an equilibrium between the end-tidal expired concentration C_E and the mixed venous blood concentration $C_{\bar{v}}$. The concentrations are linked via the blood gas partition coefficient λ, (Eger, 1974).

$$C_E = \frac{C_{\bar{v}}}{\lambda} \tag{3.4}$$

The anaesthetic uptake takes place in the alveoli of the lungs alongside with the uptake of oxygen and the removal of carbon dioxide. The driving force for all fluxes is the concentration difference between the mixed venous blood and the arterial blood, (Miller *et al.*, 2010). Additionally, the amount of gas in the lungs and in the pulmonary capillaries, which are perfusing the alveoli, is determined by the cardiac output $\dot{Q}$. A part of the total cardiac output, the shunt flow $\dot{Q}_s$, does not reach the alveoli and therefore is excluded from the gas exchange, see Figure 3.1(b). This results in the following equation for the uptake of the volatile anaesthetic in the lungs

$$u_L = (\dot{Q} - \dot{Q}_s)\,(\lambda C_{A_I} - C_{\bar{v}}) \tag{3.5}$$

with the blood gas partition coefficient λ. The concentration in the arterial

blood C_a is determined by a mass balance of inlet and outlet fluxes indicated in Figure 3.1(b) by the dashed line and u_L in (3.5).

$$C_a\dot{Q} = C_{\bar{v}}\dot{Q} + u_L \tag{3.6}$$

The mixed venous blood concentration is given by an average of all blood concentrations in the compartments multiplied with the perfusion of the respective compartment. To account for the venous shunt, diversion of blood from the artery directly to the vein, the last term in (3.7) is added.

$$C_{\bar{v}} = \sum_i r_{\dot{Q},i}\, C_{b,i} + (1 - \sum_i r_{\dot{Q},i})\, C_a \tag{3.7}$$

The tissue compartments in Figure 3.1(a) are further divided into blood and tissue sub-compartments, shown in Figure 3.2.

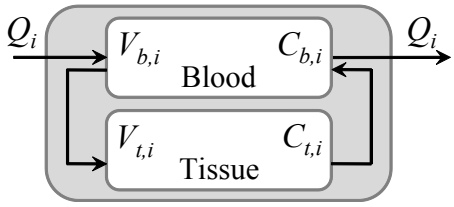

Figure 3.2.: Structure of one tissue compartment.

The concentrations of the anaesthetic agent in the individual compartments are given by mass balances for each blood and tissue compartment.

$$V_{b,i}\frac{dC_{b,i}}{dt} = \dot{Q}_i(C_a - C_{b,i}) - u_{t,i}\,, \quad i = VRG, M, F \tag{3.8}$$

$$V_{t,i}\frac{dC_{t,i}}{dt} = u_{t,i}\,, \quad i = M, F \tag{3.9}$$

The mass balance of VRG tissue includes an additional term for the metabolism of the anaesthetic agent in the liver m_{liv}, where $\dot{Q}_{liv}$ describes the perfusion of the liver, (Saltzman, 2001).

$$V_{t,VRG}\frac{dC_{t,VRG}}{dt} = u_{t,VRG} - \dot{Q}_{liv}\, C_{t,VRG}\, m_{liv} \tag{3.10}$$

The driving force of the anaesthetic uptake by the tissue $u_{t,i}$ in each compartment is the difference of the concentration in the tissue at equilibrium for the given concentration in the blood $C_{b,i}$ and the actual concentration in the tissue $C_{t,i}$, (Eger, 1974; Enderle *et al.*, 2005). The partition coefficients λ_i relate the concentrations in the tissue $C_{t,i}$ to the concentrations in the blood $C_{b,i}$ at equilibrium. Analogously to (3.5) the uptake of the tissue in the body

compartments is described in (3.11).

$$u_{t,i} = \dot{Q}_i(\lambda_i C_{b,i} - C_{t,i}) \tag{3.11}$$

The perfusion of each compartment $\dot{Q}_i$ is given by the cardiac output $\dot{Q}$ and the ratio of the cardiac output $r_{\dot{Q},i}$ perfusing the compartment.

$$\dot{Q}_i = r_{\dot{Q},i} \cdot \dot{Q} \tag{3.12}$$

Similarly, the parameter $r_{V_b,i}$ describes the ratio of the total blood volume V_b in compartment i and $r_{V,i}$ to the ratio of total body tissue volume V, respectively.

$$V_{t,i} = r_{V,i} \cdot V \tag{3.13}$$

$$V_{b,i} = r_{V_b,i} \cdot V_b \tag{3.14}$$

3.2. Individualised Pharmacokinetics

In the following sections the PK variables and parameters in (3.1) - (3.14) are given as functions of the patient's physiology, i.e. age, weight, height and gender, to account for patient-variability.

3.2.1. Lumped Tissue Compartments

The volumes of the body compartments are given as a part of the total body volume. The mass of the adipose tissue is a function of the Body Mass Index (BMI), age and gender of the patient, (Deurenberg *et al.*, 1991). The percentage of the body mass of VRG and the Vessel Poor Group (VPG) are not primarily depending on the BMI of the patient. Thus, they are assigned as a percentage of the ideal body weight for a person with the patient's height, BMI = 22 [kg/m^2] for both genders, (Lemmens *et al.*, 2006). The ideal body weight for a patient with height h is given in (3.15).

$$m_{ideal} = 22 \cdot h^2 \qquad \text{with BMI} = \frac{m\,[kg]}{(h\,[m])^2} \tag{3.15}$$

The body mass, which is neither allocated to the adipose tissue, nor to VPG or VRG, is assigned to the muscle group. The mass and volume of VPG is calculated to determine the volume of the muscle group and not further considered in the mathematical model, as the perfusion and anaesthetic uptake of the VPG tissue is negligible for short term anaesthesia. The equations for

the patient-specific tissue compartment mass are given in Table 3.1.

Table 3.1.: Calculation of patient-specific tissue mass.

Parameter	Description	Equation	Unit	Ref
m_F	Adipose mass	$(1.2\,\mathrm{BMI} - 10.8\,\mathrm{gender}^{\lozenge} + 0.23\,\mathrm{age} - 5.4) \cdot 0.01m$	kg	Deurenberg *et al.* (1991)
m_{VPG}	VPG mass	$0.2 \cdot m_{ideal}$	kg	Miller *et al.* (2010)
m_{VRG}	VRG mass	$0.1 \cdot m_{ideal}$	kg	Miller *et al.* (2010)
m_M	Muscle mass	$m - m_F - m_{VPG} - m_{VRG}$	kg	

$^{\lozenge}$female: gender $= 0$, male: gender $= 1$

The volume of the compartments is determined by the average density of the tissue of the compartment, (Heymsfield *et al.*, 2005).

$$V_i = \frac{m_i}{\rho_i} \tag{3.16}$$

3.2.2. Blood Volume

The blood volume is adapted to height h in [cm], weight m in [kg] and gender of the patient published by Nadler *et al.* (1962), where f denotes a female and m a male patient.

$$V_{B,f} = 0.3561\,h^3 + 0.03308\,m + 0.1833 \tag{3.17a}$$

$$V_{B,m} = 0.3669\,h^3 + 0.03219\,m + 0.6041 \tag{3.17b}$$

3.2.3. Cardiac Output

The cardiac output $\dot{Q}$ in [L/min] as a function of the patient's BMI, age and gender is adapted from Stelfox *et al.* (2006); gender $= 1$ for a female patient and gender $= 0$ for a male patient.

$$\dot{Q} = 5.84 + 0.08\,\mathrm{BMI} - 0.03\,\mathrm{age} - 0.62\,\mathrm{gender} \tag{3.18}$$

Further coefficients for additional predictors such as simultaneously administered agents or the patient's health state and be found in Stelfox *et al.* (2006).

3.2.4. Lung Volume

The ventilated lung volume less the dead space determines the distribution volume of the inspired anaesthetic in (3.2) and (3.3). On average, men have larger lungs than women. During anaesthesia the ventilated lung volume reduces to approximately the functional residual capacity, altered by atelectasis and anaesthetic side-effects. The patient-specific functional residual capacity as a function of the BMI in litres is given by Pelosi *et al.* (1998).

$$V_L = 11.97 \exp(-0.096\,\mathrm{BMI}) + 0.46 \tag{3.19}$$

3.3. Pharmacodynamics

Pharmacodynamics (PD) describe the link of the concentration of the anaesthetic agent to the effect of the drug. In a common modelling approach for drugs with response delays a hypothetical effect-compartment, which describes the mathematical link between the plasma concentrations and drug effects, is added to the equation system. This hypothetical compartment is solely applied to describe the delay of the drug action by a mathematical equation and does not contribute towards the pharmacokinetics of the drug. Therefore it is not reflected in the pharmacokinetic equations, (Mager *et al.*, 2003; Sheiner *et al.*, 1979). The effect-site concentration C_e in this hypothetical effect site compartment is given as follows:

$$\frac{dC_e}{dt} = k_{e0}\,(C_a - C_e) \tag{3.20}$$

Here, C_a denotes the concentration in the arterial blood calculated in (3.6), C_e denotes the effect site concentration and k_{e0} denotes the first order rate constant describing the delay of drug action.

The hypnotic effect, which is of interest in our case, is measured by the BIS and calculated as a function of the concentration in the effect site compartment, C_e, by the Hill equation. Originally, the Hill equation was first used by Hill (1910) to describe the equilibrium relationship between the partial pressure of oxygen in the blood and the saturation of haemoglobin. Now it is known as a standard equation in pharmacology, (Goutelle *et al.*, 2008).

$$\mathrm{BIS} = \mathrm{BIS}_0 + (\mathrm{BIS}_{max} - \mathrm{BIS}_0)\,\frac{C_e^{\gamma}}{C_{50}^{\gamma} + C_e^{\gamma}}, \tag{3.21}$$

where C_{50} is the concentration triggering 50% of the total effect or the potency of the drug and γ the slope of the Hill equation in (3.21). BIS_0 describes the

initial effect at no anaesthetic concentration $\mathrm{BIS}_0 = 100$ and BIS_{max} describes the maximum effect $\mathrm{BIS}_{max} = 0$. The three PD parameters k_{e0}, C_{50} and γ are individual patient characteristics and might change during the course of anaesthesia triggered by e.g. surgical stimulation or drug interaction.

3.4. Individual Patient Variables and Parameters

In this section the range of the PK and PD variables and parameters as a function of the patient's physiology, i.e. age, weight, height and gender, are calculated. Here, variables refer to values that might change over time, whereas parameters are constant. All PK and PD variables and parameters, their nominal values and range are summarised in Table 3.2.

In the presented model the individual PK variables are the cardiac output, the shunt flow, the distribution of the cardiac output on the compartments, the lung shunt, the dead space volume and the lung volume. All variables are likely to change during the course of anaesthesia as a function of the concentration of the anaesthetic agent, other simultaneously administered drugs or surgical stimulation.

The deviation for the cardiac output $\dot{Q}$ is calculated for patients with a body weight of 45-100 kg, body height of 1.50-1.90 m, age of 18-90 years and both genders in (3.18).

The shunt flow $\dot{Q}_s$ results from a 0% to 30% shunt of the cardiac output increased by atelectasis, which is often occurring during anaesthesia, (Miller *et al.*, 2010).

For the distribution of the cardiac output on the different compartments no deviation was found in the open literature. The baroreflex is still active during light to moderate anaesthesia and aims to provide the essential, well perfused organs, with oxygen. Therefore the ratio of the vessel rich group is assumed to increase slightly, whereas the perfusion of the fat and muscle group decreases, (Miller *et al.*, 2010).

The dead space is altered from a normal value of V_D=150 mL $\approx 30\% V_T$ to V_D=600 mL $\approx 60\% V_T$ caused by atelectasis, (Miller *et al.*, 2010).

The deviation in the lung volumes is given by (3.19) for patients with a BMI in the range of 20 to 40 covered in the study by Pelosi *et al.* (1998).

The PK parameters are the partition coefficients, the tissue volumes and the blood volumes, which are constant during the entire course of anaesthesia.

The deviation for the blood gas partition coefficient λ and the tissue partition coefficients λ_i were summarised and published by Eger *et al.* (2002) from different sources.

The tissue volumes are calculated for patients with a body weight of 45-100 kg, a body height of 1.50-1.90 m and both genders applying the equations in Table 3.1. The blood volumes are calculated based on the assumptions that the blood volume V_b is proportional to the perfusion of the compartment and that 60% of the total blood volume is distributed on the systematic tissue, (Saltzman, 2001).

$$V_{b,i} = 0.6\, V_b\, r_{\dot{Q},i} \tag{3.22}$$

The PD parameters are k_{e0}, C_{50} and γ in (3.20) and (3.21). The variation in the PD parameters was published in a study by Gentilini *et al.* (2001). The values at the boundary of the estimation problem were excluded. In Gentilini *et al.* (2001) the effect site concentration C_e is linked to the alveolar gas concentration, whereas in the model presented here the effect site concentration is linked to the arterial blood concentration (3.20). To ensure consistency between these two models, the value of $C_{50,A}$ found by Gentilini *et al.* (2001) is multiplied with λ to scale C_e from alveolar to arterial concentration, analogously to (3.4).

$$C_{50,a} = \lambda\, C_{50,A} \tag{3.23}$$

Table 3.2.: Range and nominal values for PK and PD parameters and variables; partition coefficients at 37°C for isoflurane.

	Symbol	Nominal value	Deviation	Unit	Ref.
PK	λ	1.4	1.38-1.46	-	Eger *et al.* (2002)
	λ_F	50	43.84-55.8	-	Eger *et al.* (2002)
	λ_M	2.57	1.44-3.19	-	Eger *et al.* (2002)
	λ_{VRG}	1.65	1.45-1.86	-	Eger *et al.* (2002)
	$\dot{Q}$	5 000	3 520-7 300	mL/min	Stelfox *et al.* (2006)
	$\dot{Q}_s$	150	0-1 500	mL/min	Miller *et al.* (2010)
	$r_{\dot{Q},F}$	0.054	0.045-0.054	-	Eger (1974)
	$r_{\dot{Q},M}$	0.181	0.1-0.181	-	Eger (1974)
	$r_{\dot{Q},VRG}$	0.75	0.75-0.765	-	Eger (1974)
	V_b	4 900	2 875-6 339	mL	Nadler *et al.* (1962)
	$V_{b,F}$	160	69-205	mL	Eger (1974), Nadler *et al.* (1962)
	$V_{b,M}$	410	276-688	mL	Eger (1974), Nadler *et al.* (1962)
	$V_{b,VRG}$	1495	1 293-2 910	mL	Eger (1974), Nadler *et al.* (1962)
	V_D	150	150-600	mL	Miller *et al.* (2010)
	V_L	2 000	770-2 200	mL	Pelosi *et al.* (1998)
	$V_{t,F}$	14 500	4 563-4 5300	mL	Eger (1974)
	$V_{t,M}$	33 000	20 010-55 789	mL	Eger (1974)
	$V_{t,VRG}$	6 000	4 950-7 942	mL	Eger (1974)
PD	$C_{50,A}$	0.7478	0.2959-1.094	vol%	Gentilini *et al.* (2001)
	γ	1.534	0.2-2.351	-	Gentilini *et al.* (2001)
	k_{e0}	0.3853	0.0248-2.895	1/min	Gentilini *et al.* (2001)

3.5. Concluding Remarks

The presented mathematical model for volatile anaesthesia provides an update with modifications of the standardly applied models for control of volatile anaesthesia, (Eger, 1974; Yasuda *et al.*, 1991a; Zwart *et al.*, 1972). The uptake of the tissue compartments and in the lungs is described separately by explicit equations and the PK parameters and variables are calculated based on the patient's physiology.

In the next section this model is analysed and the most influential variables and parameters are identified.

4. Model Analysis

This section presents an extensive analysis of parameters and variables in the physiologically based model described in Chapter 3. The aim is to identify the uncertainty the controller has to cope with. This uncertainty is originated by inter-patient variability. In a consecutive step the model is analysed towards its most influential parameters and variables. The methods used to gain an in-depth understanding of the model are global sensitivity analysis, parameter estimation and parameter correlation. The results presented in this chapter were published in Krieger *et al.* (2013).

4.1. Uncertainty by Inter-patient Variability

The outcome of this section is to identify the imposed uncertainty, which is, or may be, originated by patient variability with respect to the output of interest, the BIS.

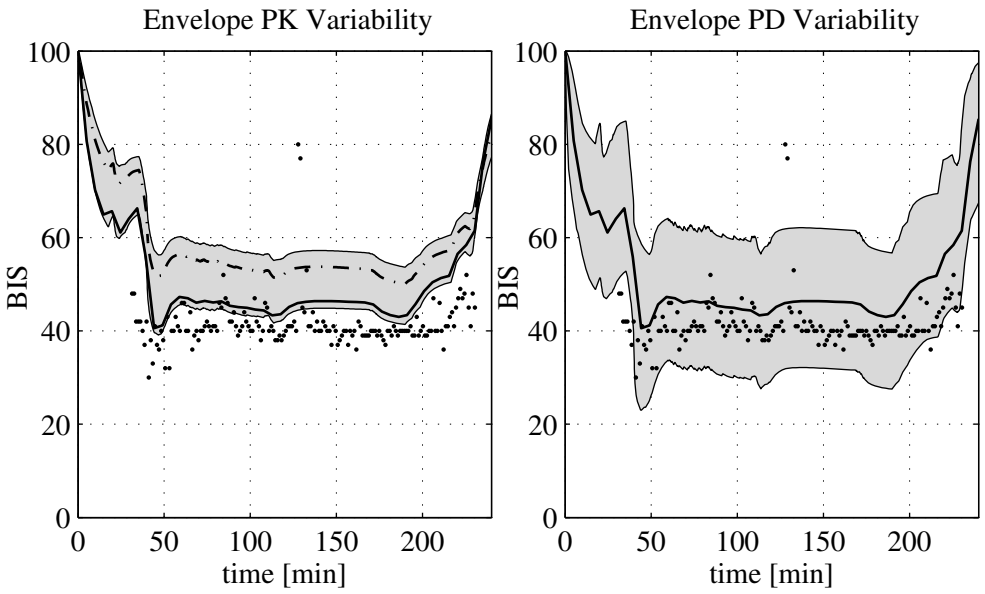

Figure 4.1.: BIS for PK (left) and PD (right) variability summarised in Table 3.2; dash dotted line: BIS nominal PKs; solid line: BIS individualised PKs for Patient 1; black dots: measured BIS.

For this purpose, separate simulations for the full range of PK and PD variability in Table 3.2 were performed for isoflurane based anaesthesia with set time-varying inputs for f_R, V_T and C_I. Details about the patient and the inputs are given in Section 5.1, Patient 1: Figure 5.1, Table 5.1. The resulting envelopes of uncertainty with respect to the BIS by PK and PD variability are shown in Figure 4.1. By comparison of the envelopes of uncertainty in Figure 4.1 the uncertainty introduced by PD variability is identified more profound than the uncertainty introduced by PK variability. More specifically, the maximum deviation from the BIS for nominal PK values is 25%, whereas the maximum deviation of the BIS including PD variability and PK values adjusted to Patient 1 is 56%.

Additionally, the improved model prediction, given individual pharmacokinetics, is illustrated in Figure 4.1. For this purpose, the model is simulated for nominal patient variables given in Table 3.2, denoted by the dash dotted line, and for individualised pharmacokinetics presented in Section 3.2, denoted by the solid line, in Figure 4.1. A comparison of the two simulation results with the measurements, denoted by the black dots, shows a significant improvement of the prediction achieved by calculating the PK variables and parameters based on the patient's physiology.

Normally during anaesthesia the anaesthetist modifies the inhaled concentration according to the obtained measurements in order to maintain adequate anaesthesia. The high deviation in the variables clearly support the need for additional information about the patient in order to assure adequate hypnosis.

4.2. Global Sensitivity Analysis

In this section the relative influence of the uncertain PK and PD parameters and variables on the measurable outputs is investigated via global sensitivity analysis. For volatile anaesthesia the measurable outputs are the end-tidal volatile anaesthetic concentration C_E and the BIS. The results of the global sensitivity analysis are several sensitivity indices between 0 and 1, with 0 being non-influential. The sensitivity index (SI) represents the relative influence of the parameter or variable on the output of interest at the given time; the sum of all sensitivity indices for the applied Sobol method converges to one. The sensitivity indices of the PK and PD parameters and variables presented in this section were calculated with the GUI-HDMR software, (Ziehn and Tomlin, 2009). To perform the analysis all PK and PD parameters and variables were varied between their bounds; the resulting output and the scaled input from 0 to 1 for a large number of sampling points are required by the GUI-HDMR soft-

ware. The method applied in the GUI-HDMR software uses random sampling high dimensional model representation (RS-HDMR) to construct an expression for the output as a function of the parameters with orthogonal polynomials. This expression accounts for up to second order interactions and corresponds to the ANOVA decomposition truncated to second order. From the coefficients of the representation the SI is derived. The sensitivity indices are calculated based on partial variances, which themselves are calculated by the approximation of the model by orthonormal polynomials. For further details on how the sensitivity indices are derived consult: Li *et al.* (2002) and Ziehn and Tomlin (2009).

In total, four sensitivity analyses for the PK and PD variables and parameters with 26 000 sampling points were performed. The samples were created by simulating the model in gPROMS via the gOMATLAB interface.

In *Case 1* the influence of the PK variables and parameters on the end-tidal concentration C_E is investigated, because the PK variables and parameters describe the distribution of the anaesthetic agent in the human body. In *Case 2* the influence of the PK variables and parameters on the BIS is investigated. The PK variables and parameters influence the BIS via their effect on the arterial concentration linked to the effect site concentration and to the BIS, (3.20) and (3.21). In *Case 3* the influence of the PD parameters, which characterise the link of the arterial blood concentration to the BIS is investigated. In *Case 4* all PK and PD variables and parameters were analysed with respect to the BIS. For *Case 1* and *Case 2* all PD parameters were fixed at their nominal values, while in *Case 3* the PK parameters were fixed at their nominal values. In *Case 4* all PK and PD variables and parameters were varied between their lower and upper bounds in Table 3.2. The four cases are summarised in Table 4.1.

Table 4.1.: Cases of the sensitivity analyses.

	Fixed	Varied	Output
Case 1	PD	PK	C_E
Case 2	PD	PK	BIS
Case 3	PK	PD	BIS
Case 4	-	PK, PD	BIS

For the sensitivity analysis the inspired concentration, the respiratory frequency and the tidal volume, were kept constant: $C_I = 1.1$ vol%, $f_R = 12\,\text{min}^{-1}$, $V_T = 500$ mL. All concentrations were initialised with zero. The sensitivity indices of all PK and PD variables and parameters for *Case 1*-*Case 4* are sum-

marised in Table 4.2.

Table 4.2.: Relative Sobol' SIs using GUI-HDMR (Ziehn and Tomlin, 2009) of *Case 1*-*Case 4* in Table 4.1 after 5 min and 20 min.

		Case 1: C_E		*Case 2*: BIS		*Case 4*: BIS	
	Variable	5 min	20 min	5 min	20 min	5 min	20 min
PK	λ	0.0	0.0	0.0094	0.0134	0.0018	0.0031
	λ_F	0.0	0.0	0.0	0.0	0.0	0.0
	λ_M	0.0104	0.0259	0.0030	0.0127	0.0005	0.0028
	λ_{VRG}	0.0312	0.0144	0.0097	0.0101	0.0020	0.0020
	$\dot{Q}$	**0.1812**	**0.1428**	**0.0462**	**0.0919**	0.0101	0.0187
	$\dot{Q}_s$	**0.1665**	**0.1763**	**0.2362**	**0.2134**	**0.0400**	**0.0457**
	$r_{\dot{Q},F}$	0.0017	0.0034	0.0005	0.0016	0.0002	0.0005
	$r_{\dot{Q},M}$	0.0568	0.0937	0.0175	0.0489	0.0033	0.0111
	$r_{\dot{Q},VRG}$	0.0002	0.0004	0.0002	0.0006	0.0	0.0
	$V_{b,F}$	0.0024	0.0027	0.0034	0.0023	0.0	0.0
	$V_{b,M}$	0.0078	0.0085	0.0006	0.0001	0.0	0.0
	$V_{b,VRG}$	0.0132	0.0043	0.0060	0.0030	0.0010	0.0006
	V_D	0.0055	0.0054	0.0076	0.0065	0.0013	0.0013
	V_L	**0.4595**	**0.4766**	**0.6539**	**0.5663**	**0.1101**	**0.1215**
	$V_{t,F}$	0.0003	0.0003	0.0001	0.0001	0.0	0.0
	$V_{t,M}$	0.0043	0.0067	0.0267	0.0265	0.0001	0.0003
	$V_{t,VRG}$	0.0753	0.0559	0.0162	0.0369	0.0038	0.0071
				Case 3: BIS		*Case 4*: BIS	
PD	C_{50}	-	-	**0.4241**	**0.7709**	**0.3124**	**0.5698**
	γ	-	-	0.2840	0.1224	**0.2813**	**0.0851**
	k_{e0}	-	-	0.2809	0.0815	**0.1947**	**0.0638**

The time-varying PK and PD sensitivity indices of all cases defined in Table 4.1 are shown in Figure 4.2. The PK variables and parameters with an average SI < 0.01 were excluded for the purpose of clarity.

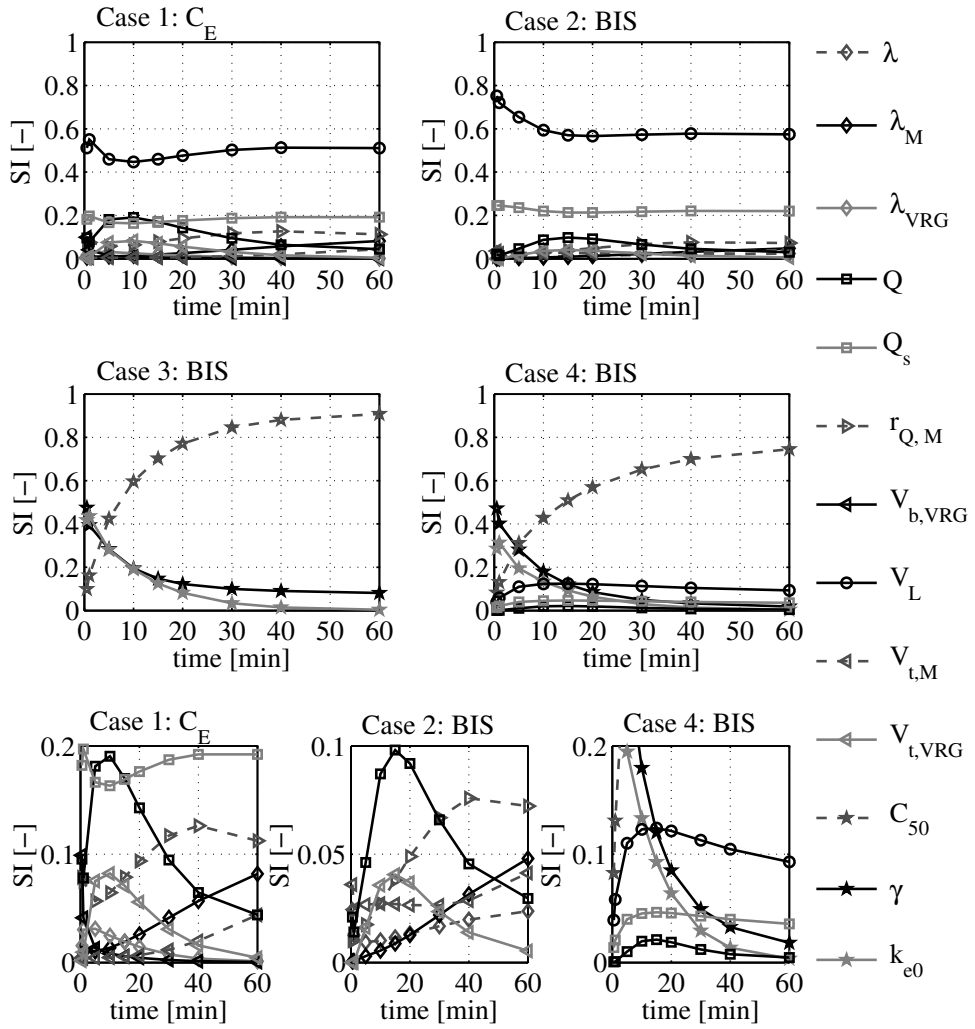

Figure 4.2.: Time-varying relative Sobol' SIs of *Case 1*-*Case 4*. The three bottom plots denote a zoomed in scope of *Case 1*, *Case 2* and *Case 4*.

In *Case 1* the distribution volume of the anaesthetic agent, the lung volume V_L, has the highest SI with respect to the end-tidal concentration C_E during the entire course of anaesthesia. The PK variables with the next highest sensitivity indices are the cardiac output and the shunt flow. Hence, as expected, the ventilation and perfusion have the highest influence on the uptake of the volatile anaesthetic agent.

For *Case 2*, lung volume, cardiac output and lung shunt are identified, analogously to *Case 1*, as the crucial variables with respect to the BIS, and hence

the arterial blood concentration to which the BIS is linked via the effect site concentration C_e in (3.20).

Case 3 shows that at the beginning the sensitivity indices of the PD parameters γ and k_{e0} are approximately identical, while C_{50} has the highest index and hence the highest influence on the BIS. Under the assumption of a constant inspired concentration, the sensitivity of C_{50} increases to approximately 90% after 60 min. The results of *Case 3* in Figure 4.2 are in accordance with the formulation of equations (3.20) and (3.21). Only C_{50} relates the BIS to a specific effect site concentration. The parameter γ changes the slope of the Hill equation and defines the necessary change in the effect site concentration to achieve the desired change in the BIS. The PD parameter k_{e0} determines how fast the BIS is responding to a change in the inputs and determines the delay of the effect. Neither γ nor k_{e0} are affecting the steady state BIS value.

In *Case 4*, the PD parameters are identified to have the highest sensitivity during the beginning of anaesthesia, whereas for a longer course of anaesthesia, especially the lung volume's SI is increasing.

From a physiological aspect and as a conclusion of the sensitivity analysis of *Case 1* and *Case 2*, the cardiac output and the shunt flow determine the anaesthetic uptake in the circulation and the lung volume determines the anaesthetic uptake in the ventilation. All other PK parameters have a considerably lower SI and can be regarded as negligible compared to the lung volume, the cardiac output and the lung shunt flow. *Case 3* and *Case 4* illustrate that C_{50} is the most important parameter in order to obtain the correct depth of anaesthesia for the individual patient.

4.3. Variability Analysis

In this section the influence of the individual parameters and variables on the outputs is further investigated. The sensitivity analysis in Section 4.2 gives a measure of the relative influence of each parameter on the output. This does not include whether a higher or lower value of the parameter or variable of interest is increasing or decreasing the output. The variability analysis further expands the understanding of the model and the influence of each parameter and variable. For an understanding of the actual physical influence of the PK and PD variables and parameters, it was investigated whether an increase in the PK or PD variable or parameter increases or decreases the output y, here C_E and/or BIS. For this study the calculated nominal outputs y_{nom} of C_E and BIS were compared to the outputs of C_E and BIS when changing the respective PK or PD variable or parameter one by one to the upper $y_{\max}$ and

the lower bound $y_{\min}$, while keeping all other variables and parameters at their nominal values.

$$P_{\%,i} = \frac{y_{\max,i} - y_{\min,i}}{y_{\text{nom}}}. \tag{4.1}$$

The percentage of change $P_{\%,i}$ of C_E and BIS are obtained with gPROMS, (PSE, 2011) and the gOMATLAB interface. The results are summarised in Table 4.3.

Table 4.3.: $P_{\%,i}$ of C_E and BIS after 5, 20 and 60 min; $C_I = 1.1$ vol%, f_R =12 and V_T =500 mL.

		C_E			BIS		
	Variable	5 min	20 min	60 min	5 min	20 min	60 min
PK	λ	0.0	0.0	0.0	-2.01	-3.60	-4.12
	λ_F	-0.08	-0.10	-0.16	0.01	0.04	0.08
	λ_M	-9.59	-11.27	-13.97	1.46	4.29	6.73
	λ_{VRG}	-12.24	-5.03	-0.81	1.96	2.34	0.43
	$\dot{Q}$	**28.89**	**17.34**	**8.97**	-4.11	-7.71	-4.46
	$\dot{Q}_s$	**-26.10**	**-21.25**	**-17.11**	**9.43**	**14.38**	**13.25**
	$r_{\dot{Q},F}$	-2.70	-2.86	-3.11	0.42	1.11	1.52
	$r_{\dot{Q},M}$	-18.42	-17.67	-12.64	2.90	6.75	6.19
	$r_{\dot{Q},VRG}$	-0.44	0.10	0.01	0.14	-0.04	0.00
	$V_{b,F}$	0.0	0.0	0.00	0.0	0.0	0.0
	$V_{b,M}$	-0.26	-0.12	-0.10	0.06	0.05	0.05
	$V_{b,VRG}$	-8.26	-3.06	-0.47	1.50	1.44	0.25
	V_D	5.39	4.09	3.14	-1.92	-2.56	-2.24
	V_L	**-77.81**	**-50.87**	**-36.32**	**25.79**	**27.63**	**23.06**
	$V_{t,F}$	-0.06	-0.24	-0.88	0.01	0.08	0.41
	$V_{t,M}$	-1.07	-4.02	-11.35	0.12	1.39	5.41
	$V_{t,VRG}$	-19.24	-10.59	-1.61	2.59	4.84	0.87
PD	C_{50}	-	-	-	**28.06**	**49.25**	**56.19**
	γ	-	-	-	**27.71**	**14.34**	4.55
	k_{e0}	-	-	-	**-37.69**	**-52.55**	**-23.98**

The results in Table 4.3 and the sign of $P_{\%}$ show how an increase or decrease of a parameter or variable generates a lower or higher anaesthetic uptake. The BIS is a function of the arterial concentration C_a. Hence, for an increased uptake the BIS is increasing, see V_L. Simultaneously, the end-tidal concentration, C_E, is decreasing given a higher anaesthetic uptake.

The simulations clearly confirm the results obtained by the previous sensitivity analysis, as the PK and PD variables with the highest SI also show the highest absolute value on the outputs in terms of $P_{\%,i}$.

4.4. Parameter Estimation and Correlation

The envelope of BIS uncertainty by PK variability is significantly smaller than the envelope of uncertainty by PD variability in Figure 4.1. This motivates an attempt to estimate the PD parameters in order to capture the uncertainty as a consequence of PK variability. This statement is investigated for the envelope of PK variability in Figure 4.1.

The parameter estimation problem is evaluated by the correlation matrix C of the estimated parameters. An entry in the off-diagonal elements of the correlation matrix C close to one ($|C_{ij}| \approx 1$) indicates a high correlation of the corresponding parameters i and j, whereas an entry of zero ($|C_{ij}| \approx 0$) indicates no correlation. The entries of the correlation matrix are calculated based on the variance-covariance matrix V. The variance of a parameter is given on the diagonal (V_{ii}) and the covariance of two parameters i and j on the off-diagonal elements (V_{ij}). Further details can be found in the gPROMS user guide, (PSE, 2011).

$$C_{ij} = \frac{V_{ij}}{\sqrt{V_{ii}V_{jj}}}, \quad i \neq j \tag{4.2a}$$

$$C_{ii} = 1 \tag{4.2b}$$

During the following analysis the upper bound of the envelope shown in Figure 4.1 is referred to as PK_u, while the lower bound is referred to as PK_l. The evaluation of the quality of the estimates is performed for both cases.

The correlation matrix of V_L and the three PD parameters obtained using gPROMS (PSE, 2011) is given in Table 4.4.

Table 4.4.: Correlation matrix C of C_{50}, γ, k_{e0} and V_L for the parameter estimation problem PK_u and PK_u; PK_u above diagonal and PK_l below diagonal.

	C_{50}	γ	k_{e0}	V_L
C_{50}	1	0.644	-0.691	**-0.993**
γ	0.662	1	-0.312	-0.713
k_{e0}	-0.753	-0.368	1	0.697
V_L	**-0.992**	-0.663	0.791	1

The results show that V_L and the PD parameters are highly correlated, in particular C_{50} and V_L, where $C_{C_{50},V_L} \approx$ - 0.99. As a consequence C_{50} and V_L cannot be estimated independently or, for this case, the uncertainty imposed by variability in the PK variables and parameters can be captured and a sufficiently accurate BIS can be reproduced by the adjustment of the PD parameters only. This statement is investigated for PK_l and PK_u; this time only estimating the PD parameters.

The correlation matrix of the PD parameters for PK_l and PK_u for all PD parameters obtained using gPROMS (PSE, 2011) are summarised in Table 4.5.

Table 4.5.: Correlation matrix of the PD parameters, entries for PK_u above diagonal and PK_l below diagonal.

	C_{50}	γ	k_{e0}
C_{50}	1	-0.759	-0.0033
γ	0.0563	1	0.383
k_{e0}	0.431	0.348	1

Here, the PD parameters γ and C_{50} show minor correlation originated by the formulation of (3.21).

All values of the PD parameters are obtained solving a maximum likelihood parameter estimation problem with gPROMS and lie within their respective bounds in Table 3.2, (Bard, 1974; PSE, 2011).

Table 4.6.: Estimated PD parameters for PK_l and PK_u.

	PK_l	PK_u
$C_{50,A}$	0.6177	0.8962
γ	1.4458	1.6369
k_{e0}	0.4308	0.2978

The results of the fit are shown in Figure 4.3. Here PK_l and PK_u denote the upper and lower bound of the PK uncertainty envelope and $PK_{l,est}$ and $PK_{u,est}$ the BIS for the estimated PD parameters given in Table 4.6.

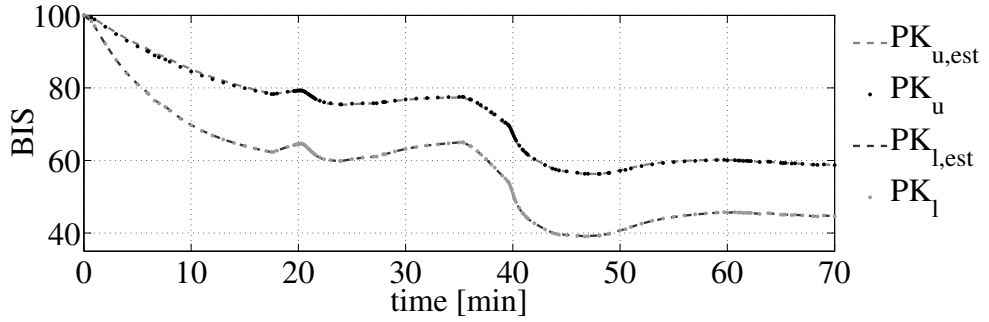

Figure 4.3.: BIS output for estimated PD parameters in Table 4.5 capturing PK variability Figure 4.1. PK_l and PK_u denote the upper and lower bound of the PK uncertainty envelope and $PK_{l,est}$ and $PK_{u,est}$ the output for values of the PD parameters given in Table 4.5.

This analysis shows that via PD parameter estimation it is possible to capture the uncertainty introduced by potential PK variability. Hence, the PD parameters C_{50}, k_{e0} and γ are sufficient to predict the BIS under uncertainty in the PK and PD variables and parameters. This statement is further investigated for a set of clinical patient data in the next section.

4.5. Concluding Remarks

This chapter provides a framework for a structured analysis of the parameters and variables that influence the measurable outputs, which results in an in-depth understanding of the model.

The PD parameters are clearly identified as the parameters with the highest variability and highest influence on the BIS.

In the next section the model is validated with clinical data for isoflurane and desflurane based volatile anaesthesia.

5. Model Validation

A simulation study for isoflurane based anaesthesia of three patients and for desflurane based anaesthesia of eight patients is presented in this section. The anonymised data were provided by the Department of Medical Informatics in Anesthesiology and Intensive Care Medicine of the University of Gießen in Germany. Isoflurane and desflurane concentrations were measured with an anaesthesia ventilator (Primus, Draeger medical) and BIS was measured by patient monitoring (IntelliVue MP70, Phillips). The data were recorded on-line with an anaesthesia information management system (NarkoData®, IMESO GmbH). Anaesthesia was induced by propofol and maintained with isoflurane and desflurane respectively, simultaneously administered analgesics were fentanyl and/or sufentanil. Cisatracurium was used for muscle relaxation. The results for isoflurane based anaesthesia were published in Krieger *et al.* (2013).

5.1. Isoflurane Based Anaesthesia

In this section measured data of isoflurane based anaesthesia are compared to the simulated data obtained by the model presented in Chapter 3 and simulated in gPROMS. Anaesthesia was induced with propofol and maintained with isoflurane. The details and drug doses are summarised in Table 5.1.

The individual PD parameters for each of the three patients were obtained by a parameter estimation problem. For comparison, the expected BIS for the nominal PD parameters in Table 3.2 were computed. All simulation results and measurements are shown in Figure 5.1.

The characteristics of the three patients for isoflurane based anaesthesia and the values of the estimated PD parameters are also summarised in Table 5.1.

Table 5.1.: Patients' characteristics; calculated values of the lung volume (3.19) and cardiac output (3.18) and estimated PD parameters; details of the surgery and simultaneously administered drugs.

	Patient 1	Patient 2	Patient 3	Units
age	61	65	66	yrs
BMI	31.5	14.5	26.0	kg/m^2
h	1.69	1.7	1.63	m
m	90	42	69	kg
gender	m	m	f	m/f
V_L	1041	2200†	1449	mL
$\dot{Q}$	6530	5052	5317	mL/min
$C_{50,A}$	0.3981	0.3600	0.5660	vol %
γ	0.4920	0.6169	1.9974	-
k_{e0}	1.117	0.0248‡	0.3832	1/min
ASA status	2	2	3	
surgery	urology	urology	general surg.	
Propofol$^\blacktriangle$	200	120	200	mg
Fentanyl$^\lozenge$	1	0.5	1	mg
Sufentanyl$^\lozenge$	-	55	-	μg
Cisatracurium$^\lozenge$	22	28	30	mg

$^\dagger V_L$ at upper bound; ‡estimate at lower bound.

$^\blacktriangle$Dose of 1% solution propofol for induction of anaesthesia.

$^\lozenge$Sum of single doses during entire course of surgery.

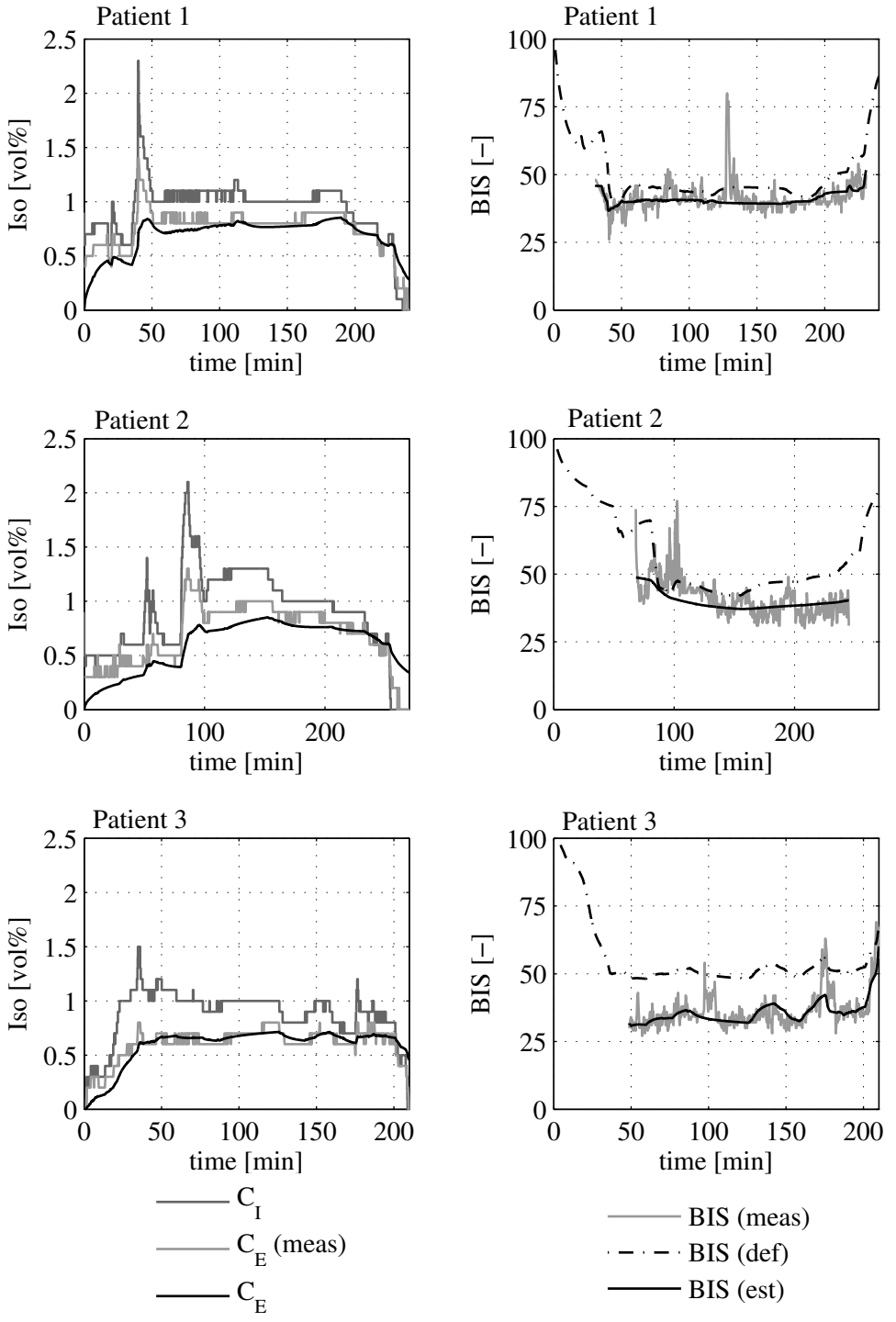

Figure 5.1.: Inspired and expired isoflurane concentrations and BIS for three patients. The measured data points are denoted with (meas), the BIS for individually estimated PD parameters is denoted with (est) and the expected BIS for the PD nominal values is denoted with (def).

The simulation results of the end-tidal concentration C_E for Patient 1 and Patient 3 are in good accordance with the measurements C_E (meas). Hence, the PK model shows a good fit of the data. However, for Patient 2 the model is not predicting the measured end-tidal concentration as close. This might be related to the underweight of the patient, BMI=14.5, for which the PK parameters have to be modified with additional knowledge about the patients health state. The expected BIS for the PD nominal variables, BIS (def), show the best match with the measured BIS for Patient 1. Especially for Patient 3 a considerable off-set between the measurement and the predicted BIS is observed. For individually estimated PD parameters the predicted BIS is in good accordance with the measurement for all three patients.

The prediction of the end-tidal concentration C_E by adjusting the PK variables and parameters according to the pharmacokinetic model presented in 3.1 shows good results. However, the PD parameters need to be estimated to fit the measured data.

5.2. Desflurane Based Anaesthesia

In this section measured data of eight patients undergoing desflurane based anaesthesia are compared to the simulated data obtained by the model presented in Chapter 3 and simulated in gPROMS. Anaesthesia was induced with propofol and maintained with desflurane. The characteristics of the eight patients are summarised in Table 5.4.

For the simulations the solubilities of desflurane published by Eger *et al.* (2002) were used. All other variables were calculated as described in Chapter 3 Table 3.2.

Table 5.2.: Solubilities of desflurane in tissue and blood, (Eger *et al.*, 2002).

Solubility	Value
λ	0.45
λ_F	29
λ_M	1.73
λ_{VRG}	1.3

The individual PD parameters for each of the eight patients were obtained by a parameter estimation problem. PD values for desflurane based anaesthesia were reported as a function of the end-tidal anaesthetic concentration, $C_a \triangleq C_E$ in (3.20), by Rehberg *et al.* (1999) and Röpcke *et al.* (2001). Röpcke

et al. (2001) found different PD parameters during surgical stimulation of the patient and during times without surgical stimulation. The range of the PD parameters for desflurane based anaesthesia for the parameter estimation problem are taken from Rehberg *et al.* (1999).

Table 5.3.: PD parameter range for desflurane, (Rehberg *et al.*, 1999).

	min	max
$C_{50,A}$	1	8
γ	0.5	2
k_{e0}	0.2	1.6

All simulation results and measurements are shown in Figures 5.2 - 5.3.

Table 5.4.: Patients' characteristics; calculated values of the lung volume (3.19) and cardiac output (3.18) and estimated PD parameters; P denotes Patient.

	P 4	P 5	P 6	P 7	P 8	P 9	P 10	P 11	Units
age	55	27	83	54	64	68	32	76	yrs
BMI	28.3	23.5	23.7	21.4	31.0	27.4	21.9	31.7	kg/m^2
h	1.88	1.75	1.79	1.81	1.74	1.76	1.85	1.83	m
m	100	72	76	70	94	85	75	106	kg
gender	m	f	m	m	m	m	m	m	m/f
V_L	1252	1713	1688	1999	1068	1319	1920	1033	mL
$\dot{Q}$	6680	6479	5437	6100	6652	6215	6808	6345	mL/min
$C_{50,A}$	3.60	1.57	1.56	1.12	2.16	1.31	2.24	2.19	vol %
γ	$0.50^{\ddagger}$	0.90	$0.50^{\ddagger}$	$0.50^{\ddagger}$	0.77	$0.50^{\ddagger}$	$0.50^{\ddagger}$	$0.50^{\ddagger}$	-
k_{e0}	$0.20^{\ddagger}$	$0.20^{\ddagger}$	0.25	$0.20^{\ddagger}$	0.28	$0.20^{\ddagger}$	0.36	$1.60^{\dagger}$	-
ASA	1	1	3	3	3	2	1	2	-

†Estimate at upper bound; ‡Estimate at lower bound.

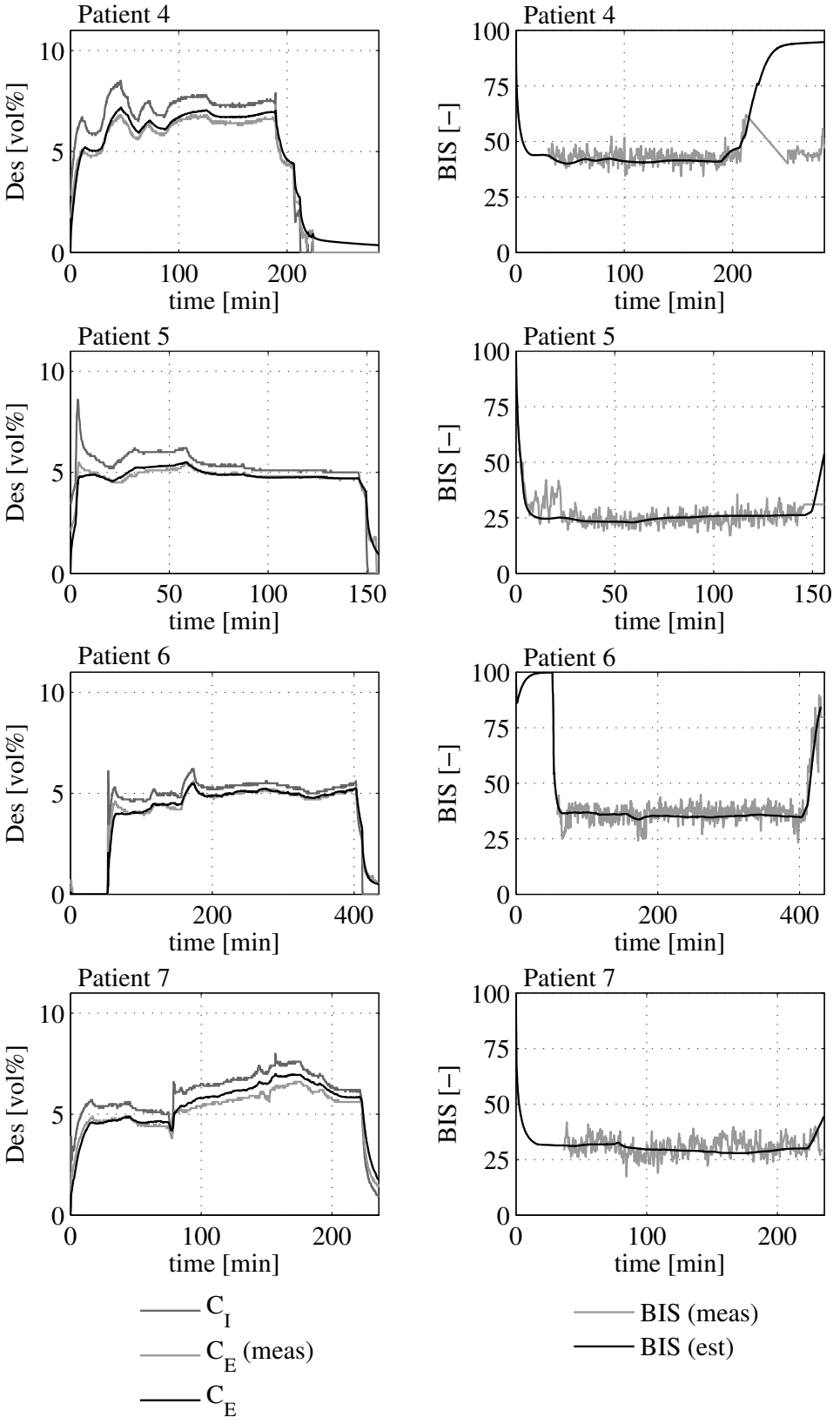

Figure 5.2.: Inspired and expired desflurane concentrations and BIS for Patient 5-7. The measured data points are denoted with (meas), the BIS for individually estimated PD parameters is denoted with (est).

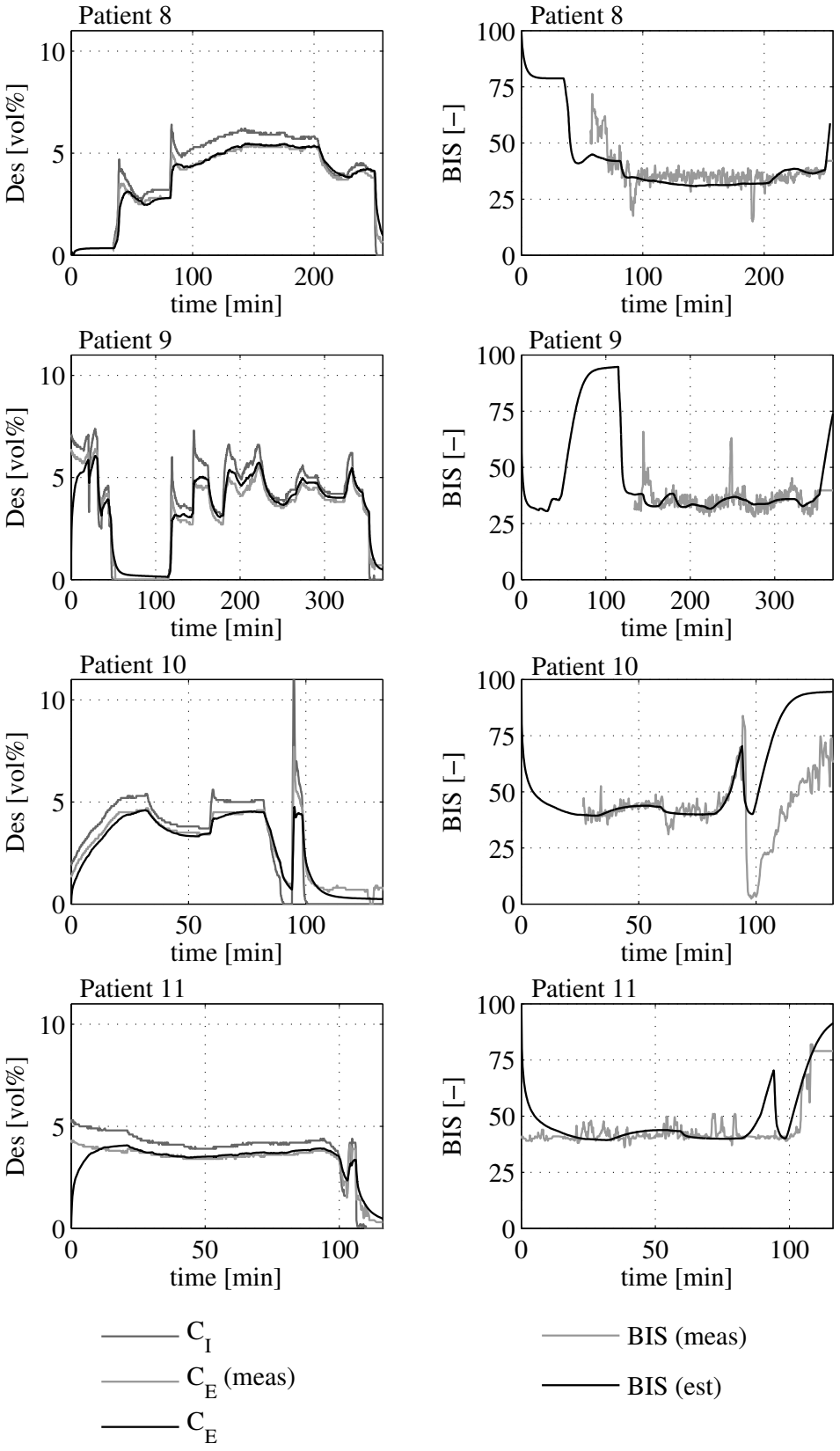

Figure 5.3.: Inspired and expired desflurane concentrations and BIS for Patient 8-11. The measured data points are denoted with (meas), the BIS for individually estimated PD parameters is denoted with (est).

The prediction of the end-tidal concentration C_E by adjusting the PK variables and parameters according to the pharmacokinetic model presented in 3.1 shows very good accordance with the measurements of the end-tidal concentration measurements C_E (meas) for Patient 5, Patient 6, Patient 8 and Patient 11. Also the simulation results of the other patients show a correct tendency of the measured data. The prediction of the BIS is in good accordance for individually estimating the PD parameters even though the estimated values lie at the boundary of the estimation problem, Table 5.4. This study confirms that C_{50} is the parameter with the highest influence, not at the boundary for any patient.

The maintenance of the depth of anaesthesia for Patient 4 in Figure 5.2, even though the administration of desflurane is stopped, is ensured by an extra bolus dose of 500 mg 1% solution propofol.

The mismatch of the prediction of the BIS for Patient 10 in Figure 5.3 is also explained by an extra dose of 150 mg 1% solution of propofol to ensure a safe depth of anaesthesia. This decision was taken by the anaesthetist to ensure a safe anaesthesia as a response to the rising BIS measurement.

5.3. Concluding Remarks

The high inter-patient variability of the PD parameters, already observed in this study for three patients undergoing isoflurane based anaesthesia, is further confirmed. This shows the need for on-line estimation of the PD parameters.

The PD parameters γ and k_{e0} do not seem to be essential for the parameter estimation problem, as they are at their respective bounds, primarily for the desflurane study. This might be due to the lack of data during induction of anaesthesia. However, the estimation of C_{50} is sufficient to obtain a good match with the clinical data. Therefore, C_{50} is further recommended to be estimated on-line.

The strategy of choice to ensure sufficient and correct prediction of the depth of anaesthesia through the mathematical model is an on-line parameter estimation (Parker and Doyle, 2001) and is investigated in Chapter 10.

6. Simulation Results

In this chapter the capabilities of using the model presented in Chapter 3 as a teaching tool for the distribution and uptake of volatile anaesthetics are demonstrated. By applying the model, additional in-sights of drug concentrations in tissues and blood pools that are not accessible by measurement are possible.

In Figure 6.1 all tissue and blood concentrations for Patient 1 in Table 5.1, Figure 5.1 are depicted.

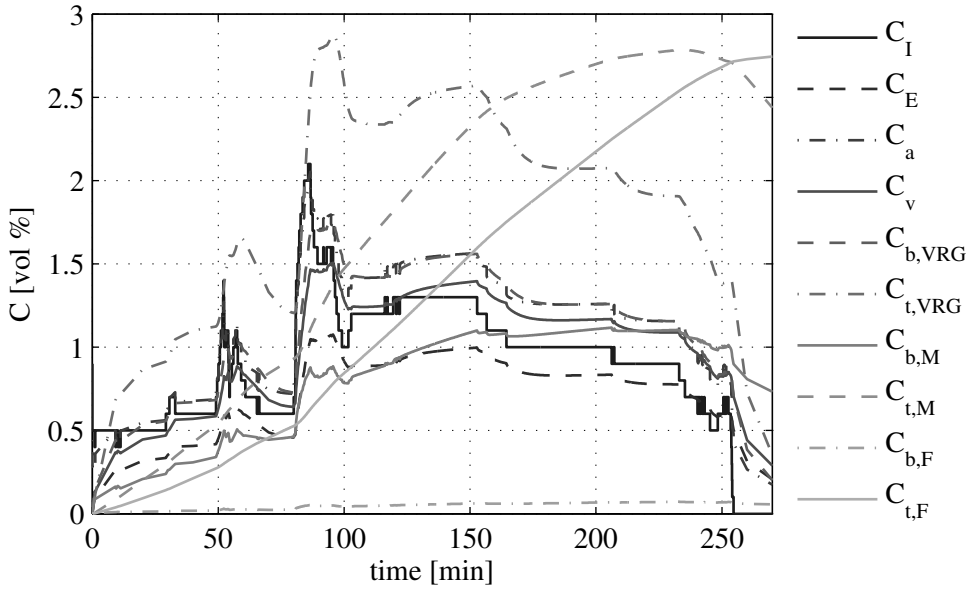

Figure 6.1.: Isoflurane tissue and blood concentrations for Patient 1, Table 5.1, Figure 5.1.

Figure 6.1 shows that the concentrations in the tissues are considerably higher than the concentrations in the blood pools, due to the higher capacity of accumulation and a higher solubility of the volatile anaesthetic agent, (Miller *et al.*, 2010).

In Figures 6.2 - 6.4 the blood and tissue concentrations of the desflurane study of Patient 4 in Table 5.4, Figure 5.2 are shown. Figure 6.2 shows that the concentrations of desflurane are much lower compared to the inspired concentrations. This is related to the lower solubilities of desflurane in the

tissues and blood, Table 5.2.

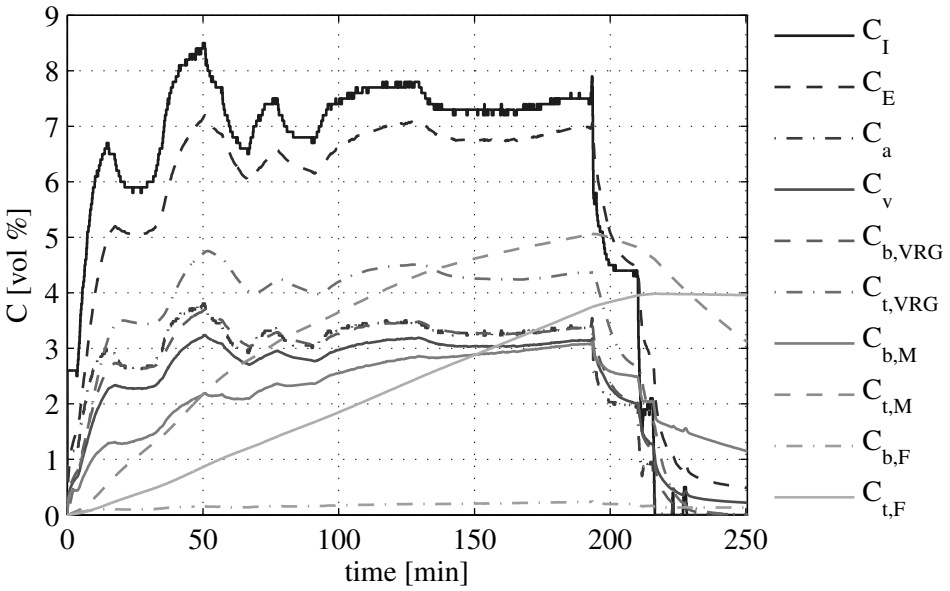

Figure 6.2.: Desflurane tissue and blood concentrations for Patient 4, Table 5.4, Figure 5.2.

Further a simulation is performed to investigate the influence of body weight on the induction and wake-up times. As an example a simulation is performed where Patient 4 is assumed to be obese, 180kg, and underweight, 55kg and the influence of this change in body weight distribution is shown in Figure 6.3 and Figure 6.4 respectively.

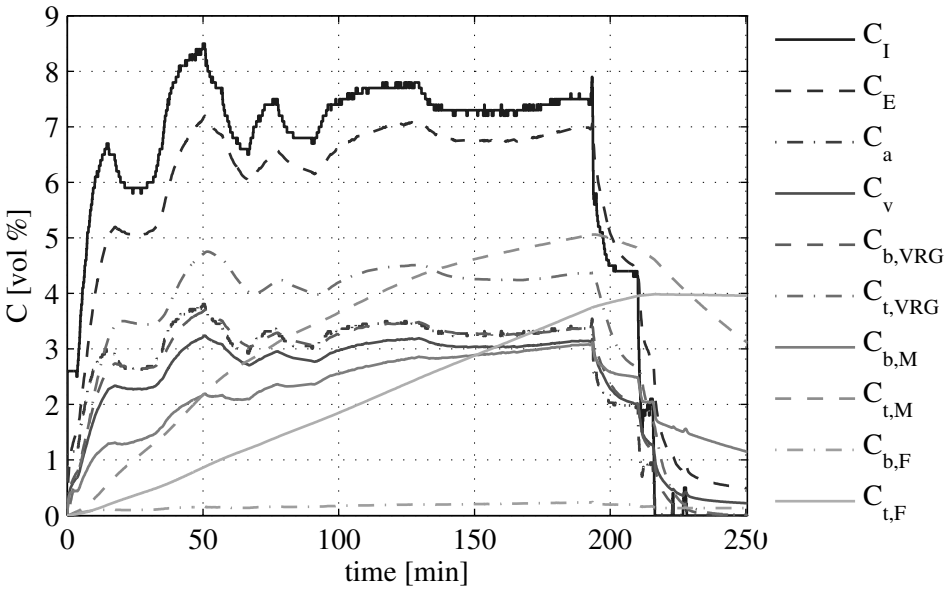

Figure 6.3.: Desflurane tissue and blood concentrations for obese Patient 4, Table 5.4, Figure 5.2.

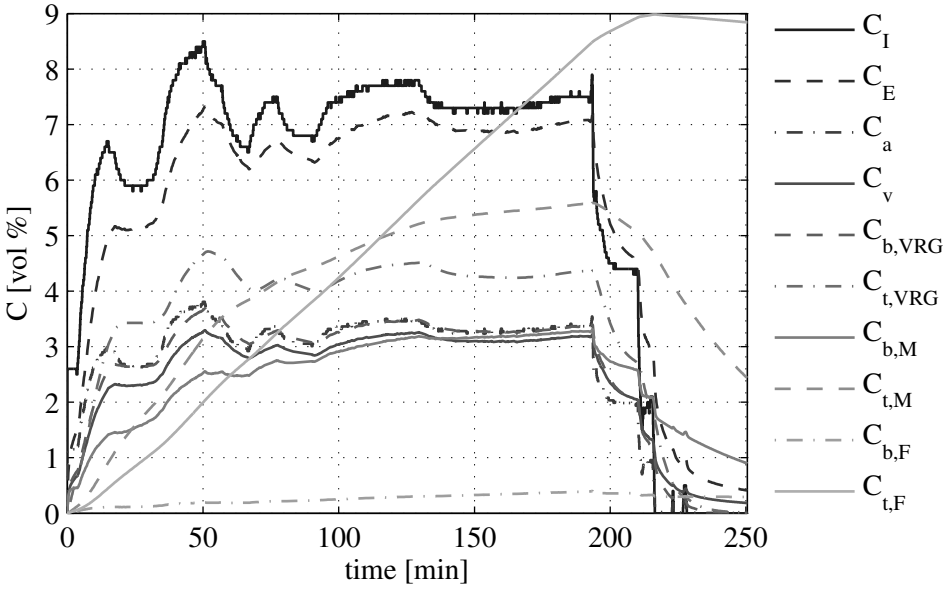

Figure 6.4.: Desflurane tissue and blood concentrations for underweight Patient 4, Table 5.4, Figure 5.2.

A comparison of Figure 6.3 and Figure 6.4 shows that the concentration in the adipose tissue $C_{t,F}$ in Figure 6.3 is increasing rapidly. This is explained by the high solubility of desflurane in fat and the comparatively small volume of the compartment.

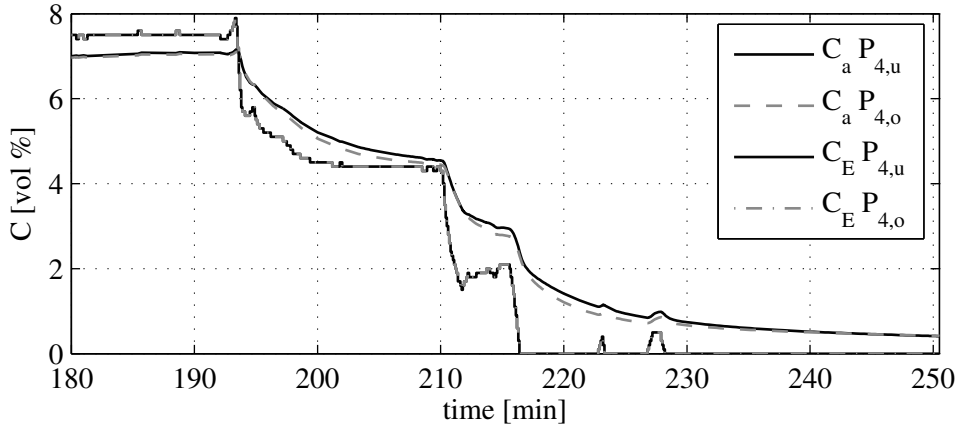

Figure 6.5.: Wake up phase of anaesthesia, u - underweight, o - obese, C_a arterial concentration, C_E end-tidal concentration.

After administration of desflurane the arterial concentration, C_a, and the end-tidal concentration, C_E, of both patients are similar. This is illustrated in Figure 6.5. This results contradicts the assumption of longer wake-up times in obese patients, because of anaesthetic accumulation in the fatty tissue and reintroduction into the circulatory system, when the arterial concentration of the anaesthetic drops after anaesthetic administration. Clinical studies by Cork *et al.* (1981) confirm the simulation results. Cork *et al.* also found similar wake-up times for normal and obese patients. This is further confirmed by the global sensitivity analysis, Section 4.2 Table 4.2. The low SI of $V_{t,F}$ indicates that the volume of the fatty tissue has a relatively low impact on the BIS and C_E.

6.1. Concluding Remarks

The derived model shows additional features to existing teaching and simulation tools to contribute to better understanding of anaesthesia and enables predictions of the drug concentrations in the various tissue parts of the patient.

Part II:
Optimisation and Model Predictive Control

Objective and Summary

The objective of Part II is to design a control strategy based on the system model derived in Part I, which is able to handle the uncertainty through inter-patient variability identified in Part I.

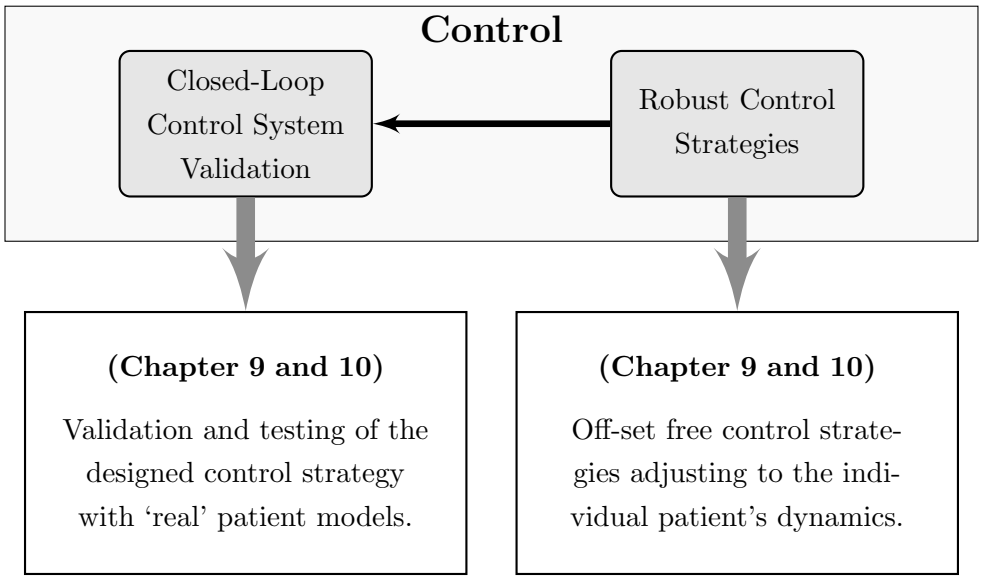

Figure 6.6.: Control framework and contributions presented in Part II.

The extensive review and analysis of the system model in Part I, Figure 1.4, help to thoroughly design and validate a control strategy for optimal and safe closed-loop control under uncertainty. The contributions of this part are illustrated in Figure 6.6 and are summarised as follows:

I) Design of a closed-loop control strategy for robust off-set free control of the hypnotic depth of volatile anaesthesia.
   - ▶ Model linearisation.
     - ▷ Algebraic compensation of the non-linear Hill equation.
     - ▷ Piece-wise affine linearisation of the non-linear Hill equation.
   - ▶ State estimation by the 'perfect' observer and the Kalman filter.
   - ▶ Model predictive control under uncertainty.
     - ▷ Control strategy able to adjust to the patient's dynamics.
     - ▷ On-line parameter estimation of the parameter with the highest sensitivity: C_{50} as identified in Part I.

- ▷ Disturbance rejection for an intravenous anaesthesia linear parameter varying (LPV) system[1].

II) Validated closed-loop control strategy for patients undergoing isoflurane based anaesthesia presented in Part I - Chapter 5.

- ▶ Testing of nominal, open-loop, mp-MPC control strategies for 'real' patients.
- ▶ Testing and validation of the control strategies with robust set-point tracking for 'real' patients.
- ▶ Testing of on-line parameter estimation for 'real' patients.

[1] This work, in collaboration with Chang *et al.* (2013b), was submitted for publication and is summarised in Appendix D.

7. Model Predictive Control of Anaesthesia

In the operating theatre the anaesthetist faces the task of providing sufficient hypnosis, analgesia and muscle relaxation, while maintaining the vital functions of the patient. The idea of supporting the anaesthetist with decisions on drug infusion rates and/or to directly automate the amount of infused drug has been an active research topic since the 1950s, (Chilcoat, 1980). Particularly in critical situations, model predictive control design is believed to contribute to safe and optimal anaesthesia, (Hemmerling, 2009).

Before surgery the reference point and the constraints are individually adjusted by the anaesthetist to the patient and type of surgery. Given this information, the control action can be modified according to the patient's characteristics and the duration and requirements of surgery. Here the states of the patient are determined via monitoring devices, whereas non-measurable states are estimated based on the available measurements. Foreseen and unforeseen disturbances such as surgical stimulation might occur during surgery, which the control strategy has to cope with and reject successfully. During anaesthesia a combination of drugs is administered to assure anaesthesia, amnesia, muscle relaxation, analgesia and maintain the vital functions. The combinations of different drugs, e.g. anaesthetics, analgesics and muscle relaxants, is big and often a personal choice of the anaesthetists based on their experience and preference.

The automation of intravenous control of anaesthesia is more advanced, because the plasma concentration of the intravenous anaesthetic is not directly measurable and hence drove the search for (i) a measurement device for the hypnotic depth and (ii) a reliable model to predict the plasma concentration.

An open-loop control example, which is common in clinical practise, for intravenous anaesthesia, usually using propofol, is target controlled infusion (TCI). Here, the drug infusion is based on model predictions of the plasma concentration in the patient's blood. The hypnotic depth is measured by the BIS or other measurement devices. Recent advances in total intravenous anaesthesia (TIVA) are listed in Table 7.1. TIVA is not as common as volatile

anaesthesia.

Volatile anaesthesia is preferred by most anaesthetists, because of the standardly available measurement of the end-tidal concentration, which is directly linked to the arterial drug concentration and the drug concentration in the brain. Therefore the end-tidal concentration is commonly used as a guideline to determine the hypnotic depth of the patient, cp. Section 2.2 Figure 2.2.

The automatic drug administration of volatile anaesthetic agents was first considered by Westenskow *et al.* (1986) and tested in a dog by Zbinden *et al.* (1986). Advances on the control of volatile anaesthesia are given in Table 7.2. Mansour and Linkens (1989), Behbehani and Cross (1991) and Yu *et al.* (1992) used automatic drug infusion devices to maintain the hemodynamic state of the patient, e.g. the cardiac output or the blood pressure. Since then researchers understood the benefit of automatic control of anaesthesia. In Table 7.3 studies that report a better performance of automatic control compared to manual control are summarised. Due to the multiple-input multiple-output character of the system, where the inputs are the various drug infusions and the outputs are the anaesthetic states of the patient and/or the vital functions, different model predictive control (MPC) methods such as explicit MPC, general predictive control or fuzzy logic control were applied to the system.

The control of the end-tidal concentration is commercially available in the Zeus® anaesthesia machine. Here the research interest is motivated by patient safety, reduction of the pollution of the operating theatre with the anaesthetic agent and reduction of consumption of the anaesthetic agents. A summary is given in Table 7.4.

Table 7.1.: Closed-loop intravenous anaesthesia in the operating theatre.

Reference	Summary
Hemmerling *et al.* (2013)	McSleepy platform: propofol, remifentanil, rocuronium.
West *et al.* (2013)	closed-loop propofol anaesthesia in children.
Hemmerling *et al.* (2010)	Significantly better control for the closed-loop propofol administration for 40 patients compared to manual control, measured by BIS.

Table 7.2.: Closed-loop control of depth of volatile anaesthesia in the operating theatre.

Reference	Summary
Reboso *et al.* (2012)	PI controller for closed-loop propofol infusion measured by BIS, feasible and safe for a clinical study of 12 patients.
Liu *et al.* (2006)	closed-loop control with propofol outperforms manual control, assessment of depth of hypnosis by BIS, 163 patients.
Gentilini *et al.* (2001)	Isoflurane based anaesthesia feedback by BIS for 20 patients.
Lockwood (1998)	Closed-loop PID control with isoflurane and enflurane.

Table 7.3.: Manual vs. closed-loop control.

Reference	Summary
Locher *et al.* (2004), Stadler (2003)	Performance for closed-loop isoflurane control in favour for automatic control (23 patients).
Morley *et al.* (2000)	No significant difference between closed-loop and manual control of (i) propofol/alfentanil and of (ii) isoflurane anaesthesia.

Table 7.4.: Closed-loop control of end-tidal volatile anaesthetic concentration.

Reference	Summary
Singaravelu and Barclay (2013)	Improved anaesthetic consumption for desflurane and sevoflurane for closed-loop control of end-tidal concentration.
Lortat-Jacob *et al.* (2009)	Desflurane and oxygen end-tidal concentration control resulting in economical more beneficial anaesthesia with Zeus® anaesthesia machine.
Struys *et al.* (2005)	Good performance of desflurane and sevoflurane target end-tidal concentration in a test lung with Zeus® anaesthesia machine.
Sieber *et al.* (2000)	closed-loop control of end-tidal concentration, performing better than manual control for isoflurane anaesthesia.

8. Closed-loop Explicit Model Predictive Control

8.1. Model Predictive Control

Model predictive control (MPC) uses a process model to compute the optimal input sequence by minimising an objective function, while respecting constraints on the control inputs, the outputs and the states of the system. The control of volatile anaesthesia system is described as a reference tracking problem. Here, the objective is to find the optimal input trajectory to steer the BIS, measuring the anaesthetic depth, to a target reference point. At each time step the optimal control input u corresponding to the inhaled concentration C_I for the patient is calculated. An illustrative figure of the control objective is given in Figure 8.1. Further notation is given in the nomenclature in the beginning of this thesis.

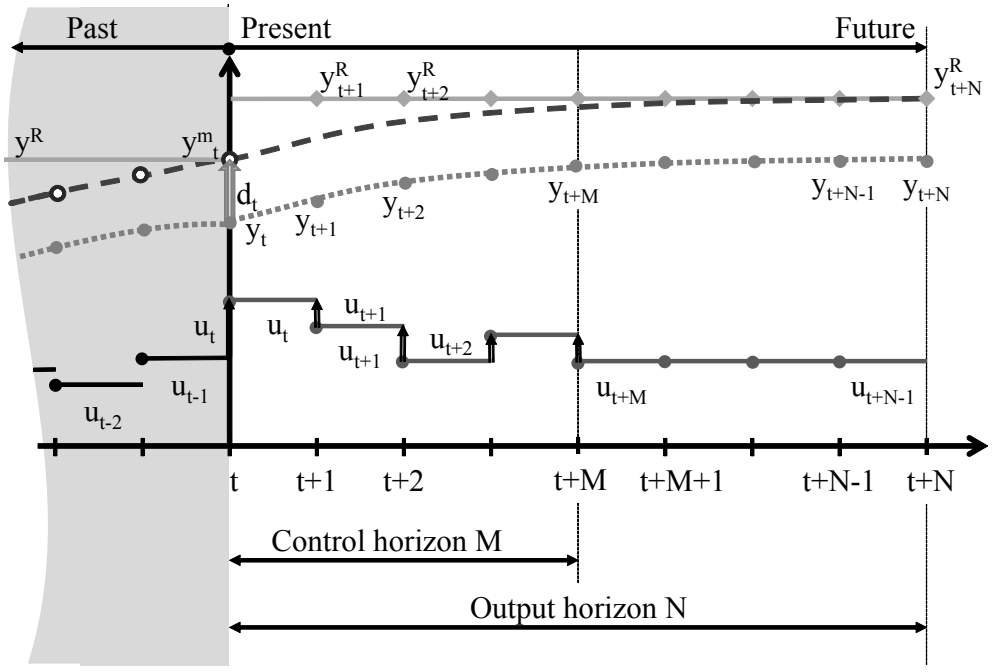

Figure 8.1.: Illustration of MPC, dotted line: MPC system output (y), dashed line: real system output (y^m), light grey solid line: output reference point (y^R), grey solid line: control input (u).

The optimal control trajectory u at each point is calculated as the optimal solution of an objective function. Although the optimal sequence of u for the entire prediction horizon N is computed, only the control input u_0 at the current time point is implemented and at the next time point the objective function (8.1) is solved repeatedly.

$$
\begin{aligned}
\min_{u} J = {} & x_N' P x_N + \sum_{k=1}^{N-1} x_k' Q x_k + \sum_{k=1}^{N} (y_k - y_k^R)' Q_R (y_k - y_k^R) \\
& + \sum_{k=0}^{M-1} u_k' R u_k + \sum_{k=0}^{M-1} \Delta u_k' R_1 \Delta u_k \\
s.t. \quad & x_{k+1} = A x_k + B u_k \\
& y_k = C x_k \\
& x_{\min} \le x_1, \dots x_N \le x_{\max} \\
& u_{\min} \le u_0, \dots, u_{M-1} \le u_{\max} \\
& y_{\min} \le y_1, \dots, y_N \le y_{\max} \\
& \Delta u_{\min} \le u_{-1} - u_0, \dots, u_{M-2} - u_{M-1} \le \Delta u_{\max}
\end{aligned}
\tag{8.1}
$$

N	output horizon
M	control horizon, with $M \le N$
P	weight matrix on the final states
Q	weight matrix on the states
Q_R	weight matrix on reference tracking error
R	weight matrix on control input u
R_1	weight matrix on change in control input
A, B, C	linear state space system matrices
x	states of the system, $(C_{b,i},\ C_{t,i})$
y	system output, $(C_E,\ BIS)$
y^R	reference point
y_k^m	measured system output
u	control input, (C_I)
Δu	step change in control input, (ΔC_I)

The application of MPC is restricted by an on-line optimisation step required to obtain the optimal control inputs at every time point for the given states and reference trajectory, (Mayne *et al.*, 2006; Sui *et al.*, 2008). For a complex model with multiple inputs and outputs, and constraints, a fast and expensive on-line computer is required. In the worst case the optimisation can-

not be solved in the available time. Explicit MPC overcomes this drawback of the need for a real-time optimiser, (Bemporad *et al.*, 2002), and furthermore allows extensive testing of the control action for different scenarios, because all possible control trajectories are pre-computed off-line.

To obtain an explicit MPC solution, the objective function is formulated as a multi-parametric quadratic programming (mp-QP) problem, where the objective function in (8.1) is formulated as a function of the parameters θ and the optimisation variables $U = [u_0, u_1, \ldots, u_{M-1}]$, which are the control inputs for the entire control horizon. In the parameter vector all dependent variables of the objective function are included $\theta = [x_0, u_{-1}, y^R]$, where x_0 are the states of the system at the start of the horizons, u_{t-1} is the previous control input, to obtain Δu_0, and y^R is the constant reference trajectory for the entire prediction horizon N.

This results in the following formulation of the objective function (8.1) as an mp-QP:

$$\min_U J(\theta) = \frac{1}{2}U'HU + \theta'FU + \frac{1}{2}\theta'Y\theta \tag{8.2a}$$

$$\text{s.t.} \quad GU \leq W + E\theta \tag{8.2b}$$

with $\theta = [x_0, u_{t-1}, y^R]$ and $U_t = [u_t, u_{t+1}, \ldots, u_{t+M-1}]$. A detailed description of the reformulation of the MPC objective function as an mp-QP problem with equality and inequality constraints is given in Appendix A.

The mp-QP problem in (8.2) can now be solved with multi-parametric programming techniques, which are implemented in the POP toolbox for MATLAB, (Bemporad *et al.*, 2002; ParOS, 2004). The optimal solution of the mp-QP problem (8.2) U_t is obtained as a set of continuous piece-wise affine functions of the parameters θ_t which are known or measured at the current time point t and therefore are fixed in the objective function.

$$U_t = \begin{cases} K_1\theta_t + c_1 & \text{if} \quad H_1\theta_t \leq b_1, \\ \vdots & \\ K_{n_C}\theta_t + c_{n_C} & \text{if} \quad H_{n_{CR}}\theta_t \leq b_{n_{CR}}, \end{cases} \tag{8.3}$$

where $U_t = K_i\theta_t + c_i$ for $i \in \{1, \ldots, n_{CR}\}$ is the optimal solution in the critical region $H_i\theta_t \leq b_i$. Here n_{CR} denotes the number of critical regions of the solution of the mp-QP problem (8.2).

Applying multi-parametric MPC, the expensive on-line computation of the optimal control function is bypassed (on-line optimisation via off-line optimisation) and the previously computed control law can be implemented low-cost

on a chip (MPC-on-a-chip), citepPistikopoulos2009. Hence, the optimal control law is retrievable immediately through simple function evaluations.

Advantages of mp-MPC for drug delivery systems for anaesthesia are:

- Hard constraints on states (drug concentrations) and inputs (drug infusion).
- Advance testing with respect to high safety standards.

8.2. Robust Control

One of the key challenges for the design of drug delivery systems for anaesthesia is the high inter-patient and intra-patient variability, which introduces a high degree of uncertainty into the system. Therefore the control design should be robust against implying uncertainty and tested for the uncertain system.

In brief, robust control can be defined as the solution of an optimal trajectory of the system under the presence of uncertainty and/or disturbances, which guarantees constraint satisfaction for all admissible values of uncertainty, and optimally steers the system to the target reference point, (Bemporad and Morari, 1999; Rawlings and Mayne, 2009).

The uncertainty can originate from model-mismatch, non-captured hidden process dynamics and/or input or output disturbances, (Muske and Badgwell, 2002).

The uncertain system can be described by the linear time invariant (LTI) system where w_k represents the bounded disturbance analogously to noise entering the system, (Bemporad and Morari, 1999):

$$\begin{aligned} x_{k+1} &= Ax_k + Bu_k + Gw_k \\ y_k &= Cx_k + Fw_k \end{aligned} \tag{8.4}$$

The bounded disturbance w_k belongs to a compact polyhedral set $w_k \in \mathcal{W} \Leftrightarrow \{w_k^L \leq w_k \leq w_k^U\}$, $i = 1, \ldots, w$, (Sakizlis *et al.*, 2004a). In an alternative approach, uncertainty is included by considering polyhedral uncertainty on the system matrices described as follows:

$$\begin{aligned} x_{k+1} &= A_k x_k + B_k u_k \\ y_k &= Cx_k \end{aligned} \tag{8.5}$$

where $[A_k \;\; B_k] \in \Omega$ and $\Omega = \text{conv}\{[A_1 \;\; B_1], \ldots, [A_M \;\; B_M]\}$ is the convex hull of $[A_i \;\; B_i]$, (Bemporad and Morari, 1999).

Robust control strategies obtain a feasible and optimal solution with respect to bounded uncertainty of the types described in (8.4) and (8.5).

An open-loop solution is the formulation of a min max optimisation problem, where the optimal value for u is obtained under the assumption of maximal uncertainty in w_k. This solution is equivalent to the optimisation of the worst-case scenario, which is often not realistic for the actual system and might lead to an over-conservative controller, (Kouramas *et al.*, 2008; Sakizlis *et al.*, 2004a,b).

An extended approach is a closed-loop parametric controller, where the past uncertainty is included at each step in the computation of the optimal control law, (Bemporad *et al.*, 2003; Kerrigan and Maciejowski, 2004; Kouramas *et al.*, 2008; Manthanwar *et al.*, 2005; Pistikopoulos *et al.*, 2009; Sakizlis *et al.*, 2004a).

In the algorithm presented by Kouramas *et al.* feasibility and constraint satisfaction is assured for bounded polytopic uncertainty in the system matrices A and B (8.5) and the objective function is derived based on the nominal values of the state space system A_0 and B_0, (Kouramas *et al.*, 2011, 2013; Panos *et al.*, 2010; Pistikopoulos *et al.*, 2009). These algorithms guarantee feasibility and constraint satisfaction under the given polytopic or additive uncertainty.

Robust reference tracking algorithms are required for systems with steady state disturbances that might otherwise lead to a persisting off-set. Sakizlis *et al.* presented an mp-MPC controller with integral action for off-set free control by adding an integral state defined as follows, (Sakizlis *et al.*, 2002, 2004a),

$$x_{q,k+1} = x_{q,k} + \underbrace{(y^R - y_k)}_{error}, \quad \forall k = 1, \ldots, N \tag{8.6}$$

and added penalties in the objective function (8.1)

$$\min_u J = x'_{q,N} P_q x_{q,N} + \sum_{k=1}^{N-1} x'_{q,k} Q_q x_{q,k}. \tag{8.7}$$

To incorporate the disturbance model explicitly in the controller's dynamics the input and state disturbance can be determined by a Kalman filter, (Badgwell and Muske, 2002; Maeder and Morari, 2010; Maeder *et al.*, 2009; Muske and Badgwell, 2002; Sakizlis *et al.*, 2004b). In this approach the system is

augmented with an integrating disturbance d

$$\begin{bmatrix} x_{k+1} \\ d_{k+1} \end{bmatrix} = \begin{bmatrix} A & B_d \\ 0 & I \end{bmatrix} \begin{bmatrix} x_k \\ d_k \end{bmatrix} + \begin{bmatrix} B \\ 0 \end{bmatrix} u_k + w_k$$
$$y_k = \begin{bmatrix} C & C_d \end{bmatrix} \begin{bmatrix} x_k \\ d_k \end{bmatrix} + v_k \tag{8.8}$$

and a Kalman filter is applied to estimate the states and the disturbances of the augmented system (8.8). The choice of the matrices B_d and C_d determines whether the augmented system is observable and depends on the known process and the disturbance model. The most common choice is $B_d \in \mathbb{R}^{n \times n_d} = 0$ and $C_d = I \in \mathbb{R}^{n_d \times n_d}$, where n is the dimension of the state vector and n_d the dimension of added disturbance vector, (Pannocchia and Bemporad, 2007).

An additional condition is that the state space system can reach the target reference point. For an LTI system of the form in (8.4) the system can reach a target reference point under any disturbance when $\bar{A}$, defined in (8.9), has full rank, (Pannocchia and Bemporad, 2007; Pannocchia and Rawlings, 2003):

$$\operatorname{rank} \underbrace{\begin{bmatrix} I - A & -B \\ HC & 0 \end{bmatrix}}_{\bar{A}} = n + n_d, \tag{8.9}$$

If condition (8.9) holds and the system is detectable, off-set free tracking can be obtained, (Rawlings and Mayne, 2009, p.49), and the closed-loop augmented system, under the condition that no constraints are active, reaches the reference point without off-set

$$Hy_s = y^R, \tag{8.10}$$

where y_s denotes the system output at steady state, (Rawlings and Mayne, 2009, p.49).

For the system of anaesthesia, a control strategy considering polytopic uncertainty on the system matrices A and B (8.5) or assuming the maximum possible disturbance (8.4) will result in an off-set, when the optimal control trajectory is computed based on the nominal system. Hence, robust, off-set free tracking algorithms should be applied for the control design of anaesthesia.

An alternative for a robust control strategy, describing the system as a linear time varying system (LPV), is evaluated in Appendix D, (Chang *et al.*, 2013a,b).

8.3. State Estimation

State feedback control strategies are relying on full state information. For the anaesthesia system not all states, which are the drug concentrations in the compartmental model, can be measured directly. Therefore a state estimator is required to determine the unmeasured states based on the input, the system model and the available measurements.

8.3.1. 'Perfect' Observer

A straightforward and obvious open-loop control approach to determine the system's states is via a copy of the system, where the input of the system u_k is known.

$$\begin{aligned} \hat{x}_{k+1} &= A\hat{x}_k + Bu_k \\ \hat{y}_k &= C\hat{x}_k \end{aligned} \tag{8.11}$$

However, this is only applicable if the system matrices are known with a high accuracy, the initial states are known and no disturbances are present or the system is fully observable, hence all states can be measured.
On the contrary, one has to consider that the state feedback controller is derived based on these system dynamics.

The advantages and disadvantages of the 'perfect' observer are summarised as follows:

- ✔ Simple implementation.
  MPC is based on the same model, therefore there is no risk of infeasibility.
- ✘ No compensation for model uncertainty and/or external disturbances.

8.3.2. Kalman Filter

The state estimation of the linear Kalman filter gives the unconstrained state estimation by minimising the error covariance. This is the optimal solution for linear stochastic systems with independent zero mean Gaussian process noise v_k and measurement noise w_k, (Kalman, 1960; Rawlings and Mayne, 2009).

$$\begin{aligned} x_{k+1} &= Ax_k + Bu_k + w_k \\ y_k &= Cx_k + v_k, \end{aligned} \tag{8.12}$$

where w_k represents the process noise and v_k the measurement noise with covariance matrix $\hat{Q}$ and $\hat{R}$ respectively. The solution of the state estimation

problem is obtained in a predictor-corrector algorithm, (Rawlings and Mayne, 2009):

1) Time update:

State prediction:

$$\hat{x}_k^- = A\hat{x}_{k-1} + Bu_{k-1} \tag{8.13}$$

Projection of the error covariance:

$$P_k^- = AP_{k-1}A^T + \hat{Q} \tag{8.14}$$

2) Measurement update:

Computation of the Kalman gain :

$$K_k = P_k^- C^T (CP_k^- C^T + \hat{R})^{-1} \tag{8.15}$$

State estimate update:

$$\hat{x}_k = \hat{x}_k^- + K_k(y_k - C\hat{x}_k^-) \tag{8.16}$$

Update of the error covariance:

$$P_k = (I - K_k C)P_k^- \tag{8.17}$$

The advantages and disadvantages of the Kalman filter are summarised as follows:

✔ Simple implementation, stable and optimal.

✘ Not optimal for non-zero mean.
Unconstrained.

8.4. Concluding Remarks

Multi-parametric model predictive control (mp-MPC) techniques and formulations will now be further investigated in the context of drug delivery systems for anaesthesia. In the next section the control and state estimation strategies, presented in this section, are combined to design and evaluate a control strategy for volatile anaesthesia.

9. Control Design for Volatile Anaesthesia

In this chapter the design and evaluation of the closed-loop control strategy for volatile anaesthesia is presented. A schematic of the closed-loop control structure is depicted in Figure 9.1.

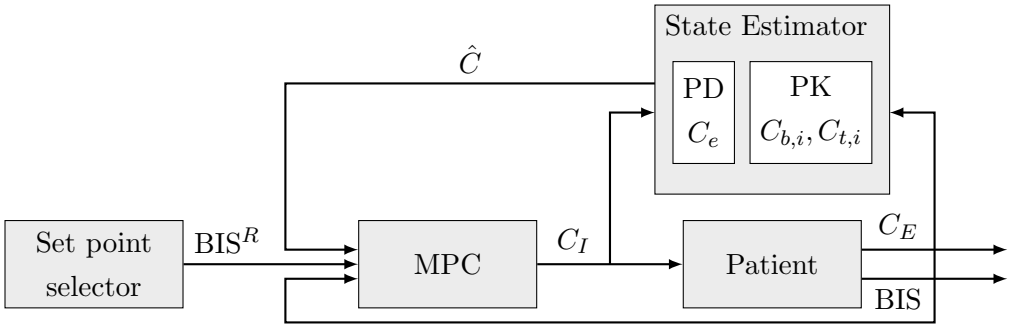

Figure 9.1.: Closed-loop control design for volatile anaesthesia.

The control objective is a fast onset and stable maintenance of the desired depth of hypnosis measured by the BIS. In order to achieve this objective the MPC manipulates the control input, the inspired concentration C_I. The feedback MPC calculates the optimal control strategy as a function of the states of the system and the measured outputs.

The available measurements are the BIS and the end-tidal concentration C_E. Given these measurements and the control input C_I, the state estimator obtains the predicted states $\hat{C}$ of the system that are not measurable.

For control validation the patient model is simulated with different PK and PD variables and parameters compared to the nominal values.

9.1. State Estimator

For the applied state feedback MPC design the optimal control law is obtained as a function of the system's states. This is indicated by the state estimator block in Figure 9.1. For the control of volatile anaesthesia the two measurable outputs are the end-tidal concentration, C_E, and the BIS.

For constant inputs, f_R and V_T, the system results in a linear state space system, where the end-tidal concentration is the output,

$$\begin{aligned} C_{k+1} &= \mathbf{A}\, C_k + \mathbf{B}\, C_{I,k} \\ C_{E,k} &= \mathbf{C}\, C_k. \end{aligned} \tag{9.1}$$

The state vector C is of dimension $n = 7$:

$$C = [C_e \;\; C^{\mathrm{PK}}]' = [C_e \;\; C_{b,VRG} \;\; C_{t,VRG} \;\; C_{b,M} \;\; C_{t,M} \;\; C_{b,F} \;\; C_{t,F}]' \tag{9.2}$$

The state space vector C, (9.2), contains 6 pharmacokinetic states (C^{PK}), i.e. the concentrations in the blood and tissue compartments in the respective compartments of the PK model and the effect site concentration, C_e, of the PD model.

Because of the identified higher uncertainty in the pharmacodynamics than in the pharmacokinetics the strategy of choice is to estimate the states based on the measurement of the end-tidal concentration, C_E, which is a PK variable. The effect site concentration, C_e, cannot be estimated from the measurement of the end-tidal concentration, C_E, because the output related to the effect site concentration is the BIS and not C_E, see (3.20) and (3.21). This can be concluded from the physiological understanding of the system and the observability matrix $\mathcal{O}$, (Rawlings and Mayne, 2009). The analysis of the observability matrix for the state space system (9.1) further confirms that an estimation of the effect site concentration by the end-tidal concentration is not possible, i.e.

$$\mathcal{O} = \begin{bmatrix} \mathbf{C} \\ \mathbf{CA} \\ \vdots \\ \mathbf{CA}^{n-1} \end{bmatrix} \tag{9.3}$$

with the state space system matrices $\mathbf{A}$ and $\mathbf{C}$, (9.1). Here n denotes the rank of $\mathbf{A}$ in (9.5) for the system including all $n = 7$ states in (3.8)-(3.10), (3.20), which are the 6 PK states, C^{PK} and C_e. The rank of $\mathcal{O}$ is lower than n, i.e.

$$\mathrm{rank}(\mathcal{O}) = 6 < n = 7 \tag{9.4}$$

Hence, only 6 states of the 7 states are observable based on the measurement of C_E. These are the 6 PK states: the blood and tissue concentrations in the lumped body compartments, (3.8)-(3.10).

As a result the 6 states of the PK model, C^{PK}, are estimated based on

the end-tidal concentration, C_E, with the linear state space model given as follows:

$$\hat{C}^{\mathrm{PK}}_{k+1} = \mathbf{A}\,\hat{C}^{\mathrm{PK}}_{k} + \mathbf{B}\,C_{I,k} + w_k \tag{9.5}$$

$$\hat{C}_{E,k} = \mathbf{C}\,\hat{C}^{\mathrm{PK}}_{k} + v_k, \tag{9.6}$$

The 6 PK states, C^{PK}, are estimated by a Kalman filter, described in section 8.3.2, with measurement noise covariance matrix $\hat{R}$ and process noise covariance matrix $\hat{Q}$.

The effect site concentration, C_e, is estimated as a function of the estimated arterial concentration, $\hat{C}_a$, see Chapter 3, and given by combination of (3.1)-(3.7) and (3.20):

$$\hat{C}_{a,k} = \left(1 - \frac{\dot{Q}_s}{\dot{Q}}\right)\left(\frac{\lambda(C_I V_T + \hat{C}_{E,k} V_A)}{V_A + V_T}\right) - \frac{\dot{Q}_s}{\dot{Q}}\,\hat{C}_{E,k}\,\lambda, \tag{9.7}$$

$$\hat{C}_{e,k+1} = \mathbf{A}_e \hat{C}_{e,k} + \mathbf{B}_e \hat{C}_{a,k} \tag{9.8}$$

where $\hat{C_E}$ refers to the estimated end-tidal concentration obtained from (9.6) and $\mathbf{A}_e$ and $\mathbf{B}_e$ denote the discrete state space system matrices resulting from (3.20).

An estimation of $\hat{C}_e$ based on the BIS measurement and all PD parameters of the Hill equation, which would include, all three PD parameters, γ, C_{50} and k_{e0}, is not performed due to the high uncertainty in the PD parameters by inter- and intra-patient variability and the possibility of an inaccurate estimation. Hence the estimation of C_e is predicted to be more accurate based on the PK concentration and only one of the PD parameters, i.e. k_{e0}, by the combination of (9.7) and (9.8).

9.2. Model Linearisation

Under the assumption of constant inputs for the respiratory frequency f_R and the tidal volume V_T such as constant PK variables, the model equations presented in Chapter 3 result in a linear system with the 7 states (9.2).

The only static non-linearity is introduced by the Hill equation (3.21), which relates the linear PK model to the effect measured by the BIS. In this work we only consider linear mp-MPC algorithms. The Hill equation is an algebraic equation and therefore introduces a static non-linearity into the system. Two options to compensate for the non-linearity are considered in this work.

I) Algebraic inverse of the Hill equation

II) Linearised Hill equation

i) Linearisation at BIS reference point

ii) Set of piecewise affine functions

Both options and their advantages and disadvantages are discussed in this section.

I) Algebraic Hill equation

The reference effect site concentration C_e^R is calculated by the inverse of the Hill equation for the reference BIS^R, (Gentilini *et al.*, 2001; Ionescu *et al.*, 2008; Nascu *et al.*, 2012)

$$C_e^R = C_{50} \left(\frac{\text{BIS}^R - \text{BIS}_0}{\text{BIS}_{max} - \text{BIS}^R} \right)^{1/\gamma} . \tag{9.9}$$

The control design consisting of the mp-MPC controller, a state estimator, the patient and the inverse Hill equation is depicted in Figure 9.2.

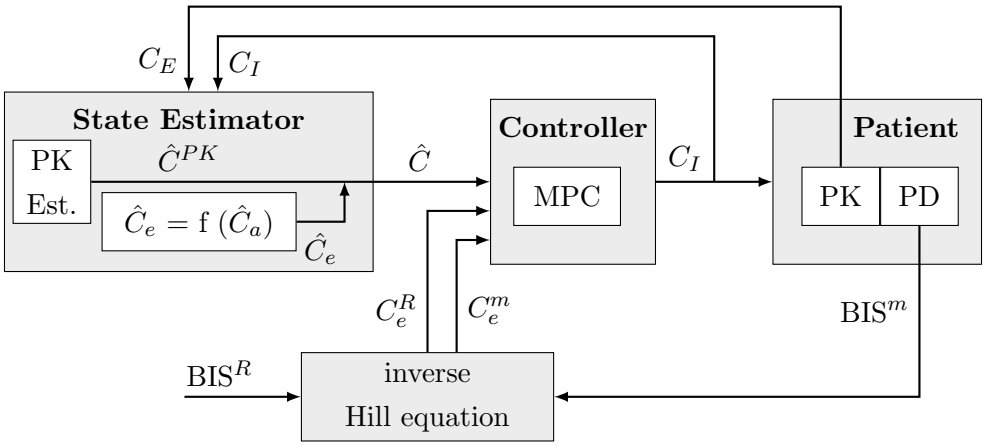

Figure 9.2.: Control design for algebraic inverse of the Hill equation.

This design requires robustification against the uncertainty in the PD parameters C_{50} and γ, which are parameters of the Hill equation (3.21) and (9.9). For the proposed design of compensating the non-linearity by the inverse of the Hill equation these parameters are not included in the control design where they can be compensated by the disturbance rejection formulation in (8.8). Hence, this design can only compensate uncertainty in the PD parameter k_{e0}.

The advantages and disadvantages of the algebraic inverse of the Hill equation are summarised as follows:

✔ Exact approximation of the Hill equation.

✘ Robustification strategy for inter-patient variability in C_{50} and γ.

II) Linearised Hill equation

The second design is a linearisation of the Hill equation at the desired reference point. This control design is depicted in Figure 9.3.

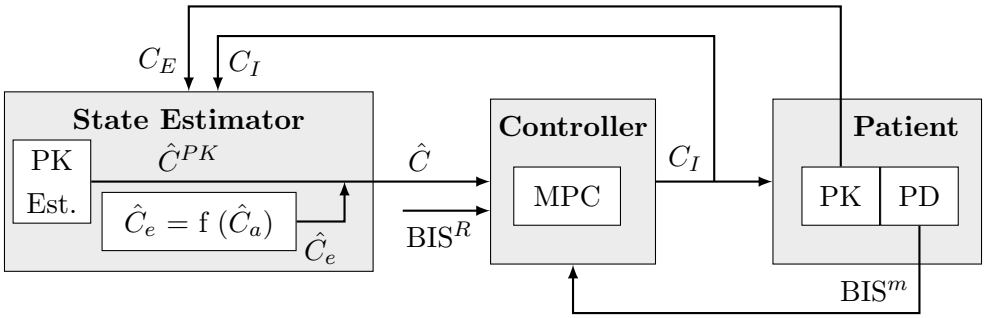

Figure 9.3.: Control design for linearised Hill equation.

The linearised Hill equation is given by

$$\mathrm{BIS}|_{\mathrm{BIS}_{lin}} = a_{\mathrm{BIS}_{lin}}\, C_e + b_{\mathrm{BIS}_{lin}}, \tag{9.10}$$

where *lin* denotes the linearisation point. The linearisation constants for a linearisation at $\mathrm{BIS} = 50$ are:

$$a_{\mathrm{BIS}_{50}} = (\mathrm{BIS}_{max} - \mathrm{BIS}_0)\left(\frac{\gamma}{4\,C_{50}}\right) \tag{9.11a}$$

$$b_{\mathrm{BIS}_{50}} = \mathrm{BIS}_0 + \frac{(\mathrm{BIS}_{max} + \mathrm{BIS}_0)}{2} - a_{\mathrm{BIS}_{50}}\, C_{50} \tag{9.11b}$$

i) Linearisation at reference point

The linearised Hill equation at the operating point of $\mathrm{BIS} = 50$ was applied by Gentilini *et al.* (2001) and Yelneedi *et al.* (2009). The visualised linearisation is shown in Figure 9.4 for nominal isoflurane PD parameters.

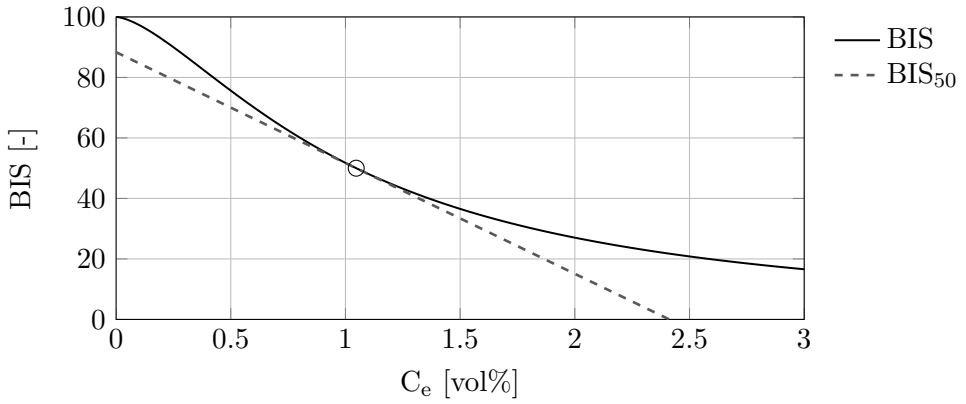

Figure 9.4.: Linearised Hill equation at BIS = 50. The dot marks the linearisation point.

However, this approach might not be accurate when the anaesthetist decides another operating point e.g. BIS = 40 or BIS = 25 as in the case study for desflurane in Section 5.2. Furthermore the intersection of the linearised Hill equation and the y-axis does not coincide with the initial condition of the patient during induction, where BIS = 100. Hence this strategy results in a large off-set during induction of anaesthesia.

The advantages and disadvantages of the linearisation at a single reference point are summarised as follows:

✔ Good approximation at reference point.
Straight-forward implementation.

✘ Large linearisation error outside of the linearisation region.

ii) Set of piecewise affine functions

A safer and more accurate linearisation procedure to achieve a smooth transition of the non-linearity for the full Hill equation is a set of piecewise linear approximations, where the Hill equation is linearised at BIS = 60 and BIS = 30 and the controller is switching at the intersection points. The linearisation for induction is obtained by a line through the points (BIS = 100, $C_e = 0$) and (BIS = 60, $C_e = C_{e,BIS=60}$), Figure 9.5.

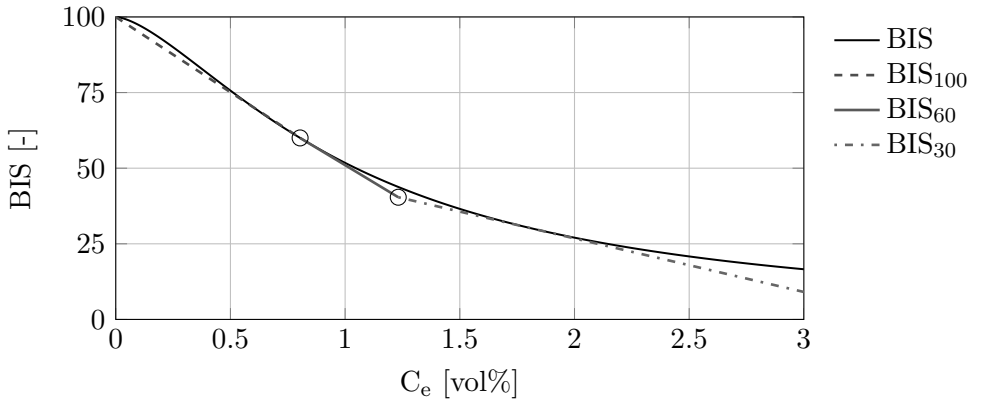

Figure 9.5.: Piece-wise linearisation of the Hill equation. The dots mark the intersection of the linearisation functions and the switching points of the controllers respectively.

The advantages and disadvantages of the piecewise affine linearisation of the Hill equation are summarised as follows:

✔ Linearisation of the full parameter space.
Compensation of uncertainty in C_{50} and γ.

✘ Implementation of controller switching to guarantee stability.

9.3. MPC

The MPC block in Figure 9.1 is based on the derived PK-PD in Chapter 3 for nominal patient parameters. The formulation of the linear MPC objective function is given as follows, (8.1):

$$
\begin{aligned}
\min_{u} J = & \sum_{k=1}^{N} (y_k - y_k^R)' Q_R (y_k - y_k^R) + \sum_{k=0}^{M-1} \left(u_k' R\, u_k + \Delta u_k' R_1\, \Delta u_k \right) \\
s.t. \quad & x_{k+1} = A x_k + B u_k \\
& y_k = C x_k \\
& x_{\min} \leq x_k \leq x_{\max} \\
& y_{\min} \leq y_k \leq y_{\max} \\
& u_{\min} \leq u_k \leq u_{\max} \\
& \Delta u_{\min} \leq u_{k-1} - u_k \leq \Delta u_{\max}
\end{aligned}
\tag{9.12}
$$

The main objective of this reference tracking control problem is a fast onset and a stable maintenance of the anaesthetic depth specified by the anaesthetist. Therefore the term with the highest weight in the objective function

(9.12) is the weight matrix Q_R penalising the error between system output and reference point. The inlet concentration $u = C_I$ is penalised with R, to minimise the amount of anaesthetic used. The change in the input $\Delta u := u_{t-1} - u_t$ is penalised with R_1. The states x, outputs y, inputs u and the change in input Δu are restricted by hard constraints, (9.12).

9.4. Case study: Controller Evaluation for Isoflurane Based Anaesthesia

In this section the control designs described in the previous chapter are evaluated. To motivate for the need of an output feedback controller an open-loop control design is included in the case study. The control strategies are presented and compared regarding their performance for a reference point change for a 60 min isoflurane based anaesthesia. The initial reference point is BIS = 40 during the initial 30 min and BIS = 60 for the last 30 min. The MPC is derived based on the model for the nominal patient described in Section 5.1, MPC block in Figure 9.1.

The linear mp-MPC is evaluated applying

I) the algebraic inverse of the Hill equation or

II) a piecewise affine linear approximation of the Hill equation

in combination with either

i) the 'perfect' observer or

ii) the Kalman filter.

Performance measure

The performance error of the controller during induction and maintenance is assessed by the root mean squared error (RSME) defined as follows:

$$E = \frac{1}{n}\sum_{i=1}^{n}\sqrt{\left(\frac{\mathrm{y}_i^m - \mathrm{y}_i^R}{\mathrm{y}_i^R}\right)^2}, \tag{9.13}$$

where y^R refers to the reference output value and y^m to the measured value. This measure for the evaluation of the control strategy was chosen to include a measure for oscillations.

9.4.1. Motivational Example: Nominal mp-MPC

In this section the nominal controller, for both control designs, the algebraic compensation of the Hill equation and the piecewise linear approximation of the Hill equation, is evaluated. The perfect observer and the Kalman filter are applied to obtain the state information of the system. Here, the implementation with the 'perfect' observer is equivalent to an open-loop control design. The control designs are summarised in Table 9.1 and the MPC design parameters in (9.12) are summarised in Table 9.2:

Table 9.1.: Control design (*CD*) set-up.

	MPC	State Est	PD
CD 1	mp-MPC	'Perfect' observer	algebraic
CD 2	mp-MPC	Kalman filter	algebraic
CD 3	mp-MPC	'Perfect' observer	linearised
CD 4	mp-MPC	Kalman filter	linearised

Table 9.2.: mp-MPC tuning parameters and specifications.

Variable	Value	Variable	Value	Unit
t_s	0.1667 ≙ 10 sec	$\Delta u_{\max}$	0.5	vol %
N	6 ≙ 1 min	$\Delta u_{\min}$	-0.5	vol %
M	3 ≙ 30 sec	$u_{\max}$	4	vol %
Q_R	1000	$u_{\min}$	0	vol %
R	1	$C_{e,\max}$	3.08	vol %
R_1	1	$C_{e,\min}$	0	vol %
$\hat{Q}$	0.3	$\text{BIS}_{\max}$	100	-
$\hat{R}$	0.03	$\text{BIS}_{\min}$	0	-

The mp-MPC (9.12) is evaluated for the patients undergoing isoflurane based anaesthesia. The designs *CD 1*-*CD 4* are evaluated for the nominal patient and the three other patients of the clinical study for isoflurane. The patient block in Figure 9.1 comprises of the model with individualised PK and PD parameters and variables reported in Table 3.2 and Table 5.1. As a motivational example for the need of a more advanced than open-loop control strategy, the control performance for the nominal controller in line with the 'perfect' observer (*CD 1*) is shown for all patients in Figures 9.6 - 9.9. The explicit solution C_I by simple function evaluations of the first 6 critical regions passed is given in Appendix B.

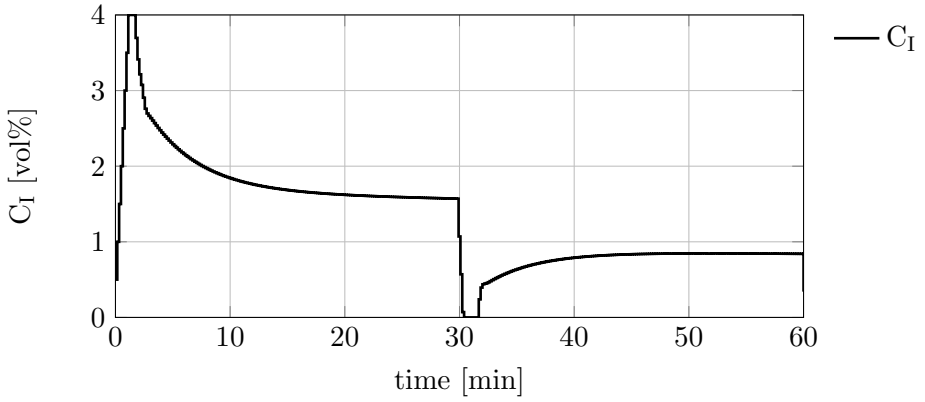

Figure 9.6.: C_I all patients.

The open-loop controller computes the optimal control law entirely based on the obtained states by the state estimator. There is no output feedback loop of the actual measurement of the patient. Therefore, an identical control input for all four patients is computed, Figure 9.6.

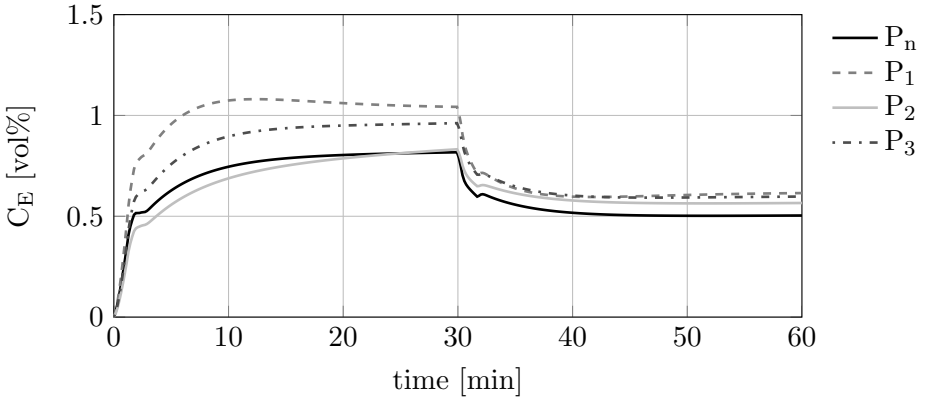

Figure 9.7.: C_E all patients.

Figure 9.7 shows a significantly different end-tidal concentration C_E for the same inhaled concentration C_I in Figure 9.6 for the four patients. This is a result of different PK parameters of each patient, which determine a different uptake and C_E of the anaesthetic agent, cp. Table 4.3.

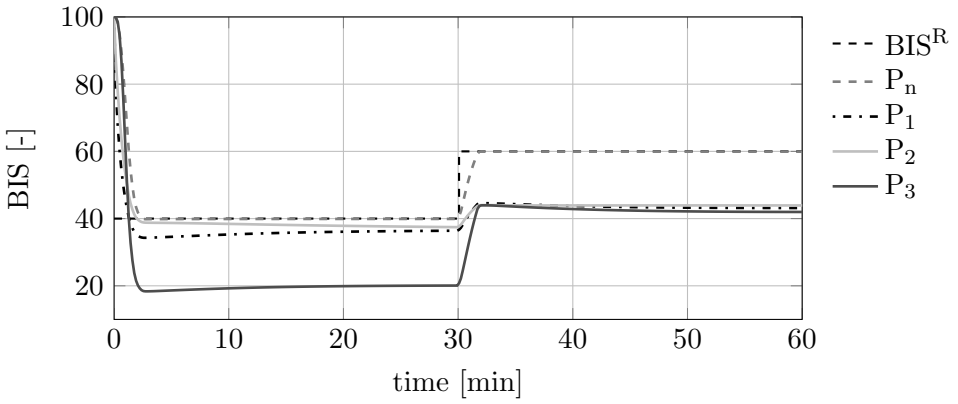

Figure 9.8.: Measured BIS of all patients.

Figure 9.8 shows the BIS of all four patients. The open-loop, nominal MPC obtains a good control performance for the nominal patient (P_n) only. The other patients, in particular Patient 3 (P_3), show a significant off-set from the target BIS.

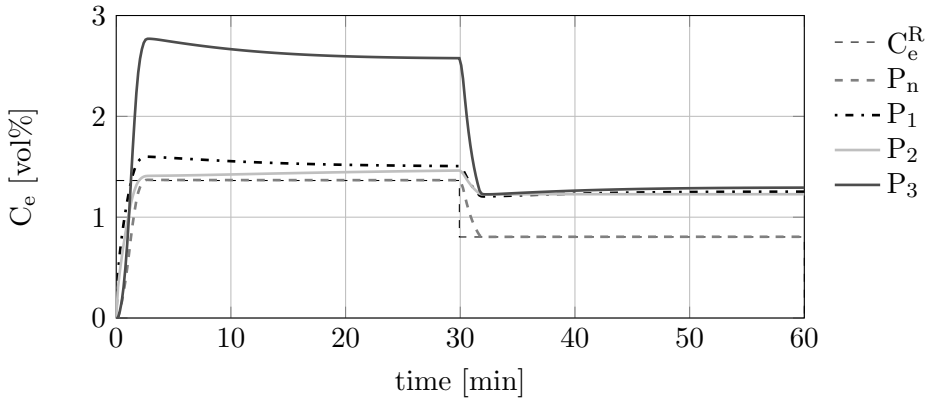

Figure 9.9.: C_e all patients.

The results in Figure 9.9 show a satisfactory performance of *CD 1* only for the nominal patient (P_n). The results of the other patients (P_1-P_3) indicate the significant off-set from the BIS reference point directly linked to the effect site concentration in (9.9). Both the off-set from the target BIS and the off-set from the target effect-site concentration is originated from the high inter-patient variability especially in the PD parameters, Chapter 4, and motivates the need for a more advanced control strategy.

Performance analysis of control designs CD 1 - CD 4

The RMSE (9.13) is calculated for all control designs *CD 1* - *CD 4* during induction (0 min-5 min), $\text{BIS}^R = 40$ (20 min - 40 min) and $\text{BIS}^R = 60$ (50 min -

60 min), to further analyse the presented control strategies. The results are shown for all patients and all control designs in Figures 9.10 - 9.11.

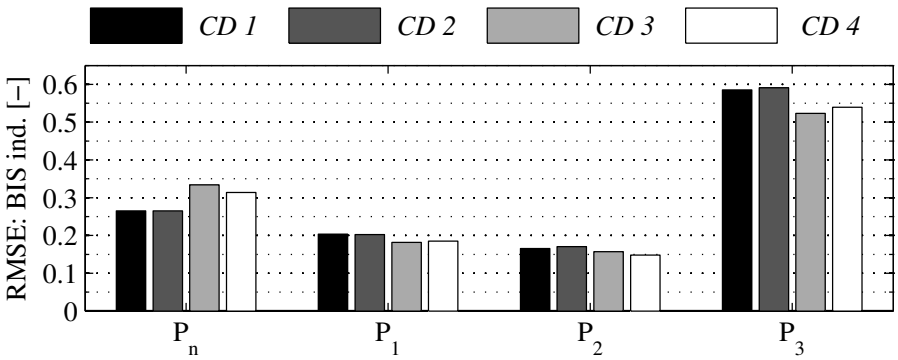

Figure 9.10.: RSME for induction (ind.) of anaesthesia, t = 0-5 min.

During induction all control designs seem to perform better for P_1 and P_2 even compared to the nominal patient, P_n. However, this is related to the faster response of the patient given by a different sensitivity to the drug. The significantly worse performance of all controllers for P_3 can be explained by very different dynamics of the system already observed in Figure 9.8.

An accurate comparison the algebraic compensation of the Hill equation and the piecewise affine linearisation of the Hill equation can only be obtained for the performance of P_n, as both controllers are designed with identical dynamics with the patient. Here the algebraic controller *CD 1* and *CD 2* performs better, because of the exact approximation of the Hill equation, whereas *CD 3* and *CD 4* suffer from a linearisation error, see Figure 9.5.

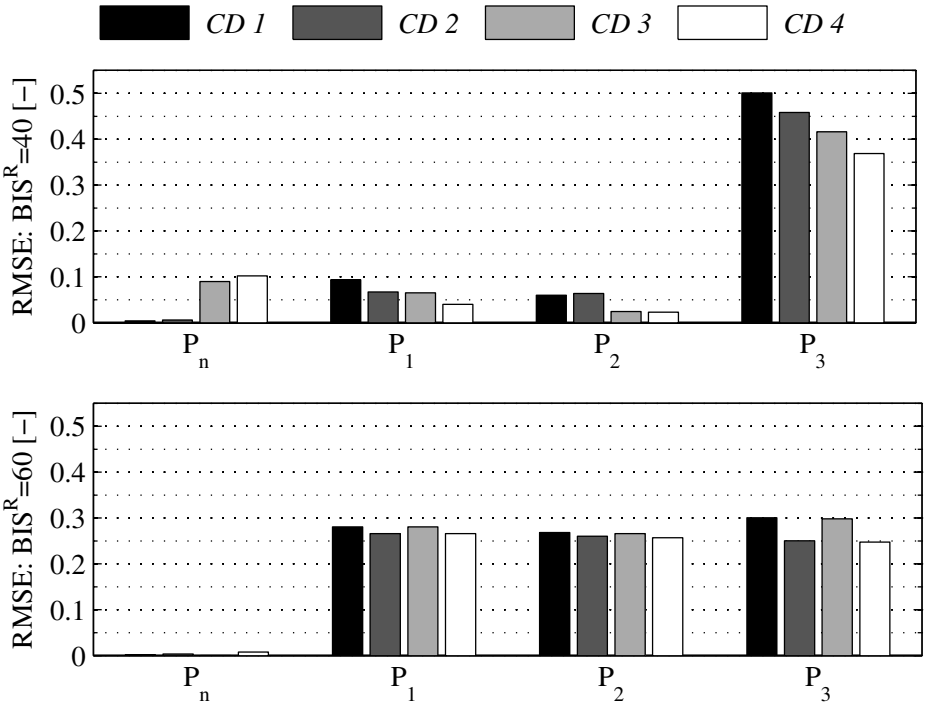

Figure 9.11.: RSME during maintenance at BIS = 40 (20 - 30 min) and BIS = 60 (50 - 60 min) for *CD 1*-*CD 4* and all patients.

The comparison of the control designs during the maintenance phase gives further insights in the dynamics of the system. Here, the control design based on the algebraic inverse of the Hill equation shows an excellent performance (*CD 1, CD 2*) for the nominal patient P_n. Also during induction of anaesthesia, the piecewise affine linearisation of the Hill equation suffers form the linearisation error, which is minimal at BIS = 60, but more significant at BIS = 40 for the nominal patient, see Figure 9.5. The state estimation by the Kalman filter in *CD 2* and *CD 4* improves the performance of the nominal MPC for all patients, P_1 - P_3. This is because of a better mapping of the real system's states to the measured end-tidal concentration C_E, which also is varying considerably depending on the patient's individual uptake, Figure 9.7. The state estimation with the Kalman filter can reduce the maintenance off-set. However, this control strategy is not satisfactory to compensate for the uncertainty introduced by inter-patient variability in the PD parameters.

The different off-set for the four patients at the two different reference points BIS = 40 and BIS = 60 is originated from the individual Hill equation (3.21), which describes the BIS as a function of the effect site concentration. All three patients show a deviation from the nominal Hill equation depending on the reference point. This should be considered for the algebraic inverse of

the Hill equation as well as for the piecewise affine linearisation of the Hill equation. The individual Hill equations of the three patients, the nominal and the piecewise affine linear Hill equation are depicted in Figure 9.12.

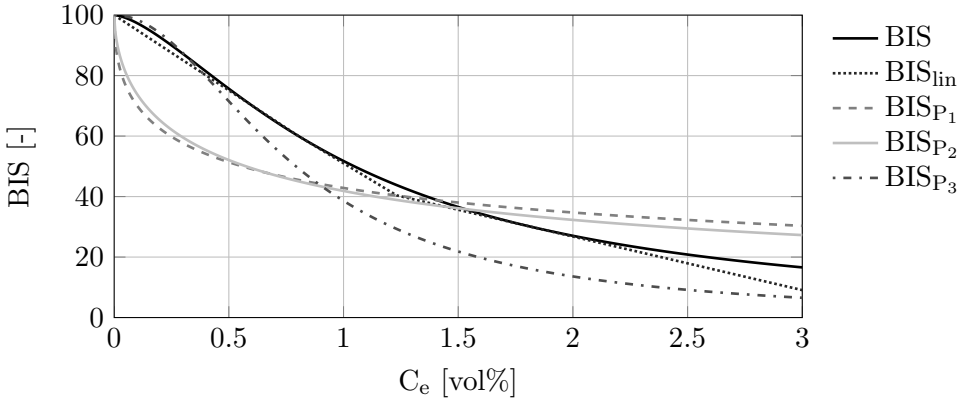

Figure 9.12.: Algebraic and piecewise affine Hill equation of the nominal patient and Hill equations of the three patients for isoflurane based anaesthesia.

Furthermore one has to consider that the effect site concentration is changing with individual patient variables and parameters as a function of the PD parameter k_{e0} and the arterial concentration C_a, which is determined by the possibly uncertain PK parameters.

As a conclusion, control designs (*CD 1* - *CD 4*) only lead to satisfactory results when the patient's parameters are very well known and model uncertainty can be reduced to a minimum as shown for the results of the nominal patient P_n. This is further motivated by the performance of all controllers for Patient 3 in Figures 9.13 - 9.14.

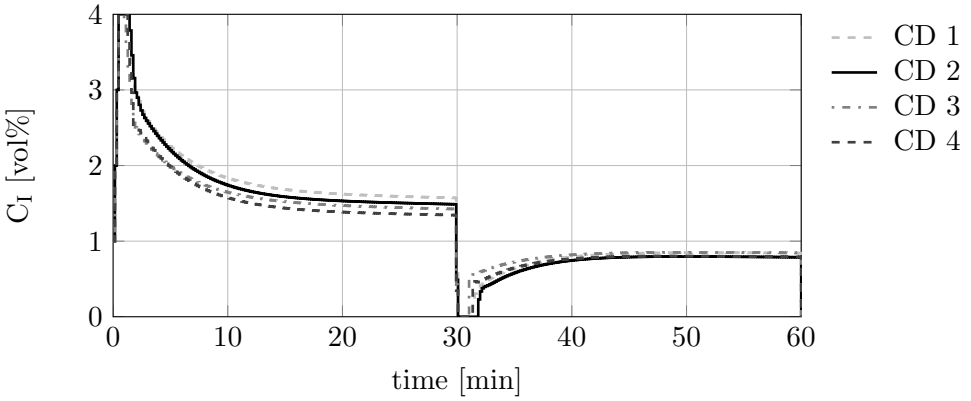

Figure 9.13.: Inlet concentration all CD patient 3.

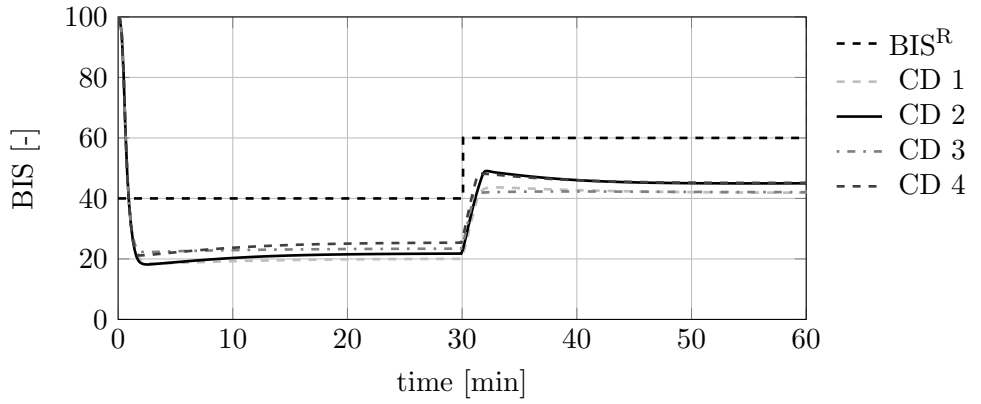

Figure 9.14.: BIS patient 3.

9.4.2. MPC with Output Disturbance

In this section an off-set free output feedback design is presented. The dynamics of the controller are adjusted to the system via an output disturbance d in the system model, (8.1).

Given the derived state space matrices for the piecewise affine system all matrix pairs (**A**,**C**) (9.1) are observable. However, the augmented system with the choice of $B_d = 0, \in \mathbb{R}^{7\times 1}$ and $C_d = 1$ with $n_x = 7$ and $n_d = n_y = 1$, is not observable, see (8.8). An alternative choice for B_d is challenging and difficult to define, because the entries are suffering from uncertainties due to inter-patient variability in the PK and PD variables and parameters that might not be linearly related. To test the off-set free method via including an output disturbance, the disturbance estimation is circumvented by assuming a constant output disturbance d_k for the entire horizon given by the difference of measured output y_k^m and predicted output y_k of the system model.

$$\begin{aligned} d_k &= y_k^m - y_k \\ d_{k+1} &= d_k \end{aligned} \tag{9.14}$$

This disturbance is then incorporated in the formulation of the objective function in (8.1) and the mp-QP problem, Appendix A, as an output disturbance to adjust the controller to the patient's dynamics, (Rawlings and Mayne, 2009, p. 49):

$$\min_{x,y,u} J = \sum_{k=1}^{N} (y_k + d_k - y_k^R)' Q_R (y_k + d_k - y_k^R) \tag{9.15}$$

The system matrices of all three piece-wise affine systems were evaluated and they satisfy the condition for the rejection of all disturbances and off-set

free control (9.14). The design of the controllers is given in Table 9.3.

Table 9.3.: Control design (*CD*) for output disturbance MPC.

	MPC	State Est	PD
CD 5	output feedback MPC	'Perfect' observer	linearised
CD 6	output feedback MPC	Kalman filter	linearised

To obtain a stable control performance the sampling time was decreased to $t_s = 3$ seconds and the control horizon and output horizon were increased accordingly, Table 9.4. All other parameters were set identical to the specification in Table 9.2. Because of the high control and output horizon, no explicit solution was obtained. Therefore the on-line version of the controller, solving a QP problem, was applied to obtain the simulation results. The derivations of the explicit and on-line/conventional controller are given in Appendix A.

Table 9.4.: Control design for *CD 5*-*CD 6*.

Variable	Value
t_s	0.05 ≙3 sec
N	20 ≙ 1 min
M	8 ≙ 24 sec

Performance analysis of control designs CD 5 - CD 6

The output feedback design shows a considerably better performance than designs *CD 1*-*CD 4*. The RSME during induction, Figure 9.15, and maintenance for both reference points is reduced, Figure 9.16. Note the different scale in comparison to Figures 9.10 - 9.11.

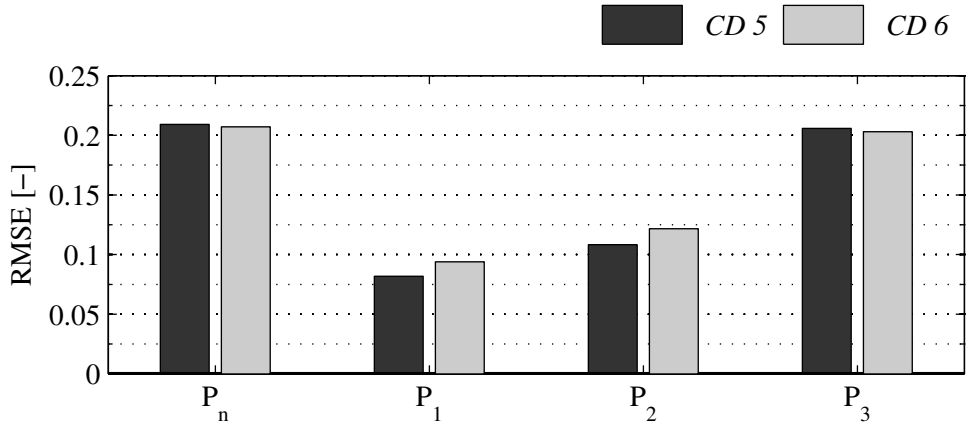

Figure 9.15.: RSME for induction of anaesthesia from t = 0-5 min *CD 5* and *CD 6*.

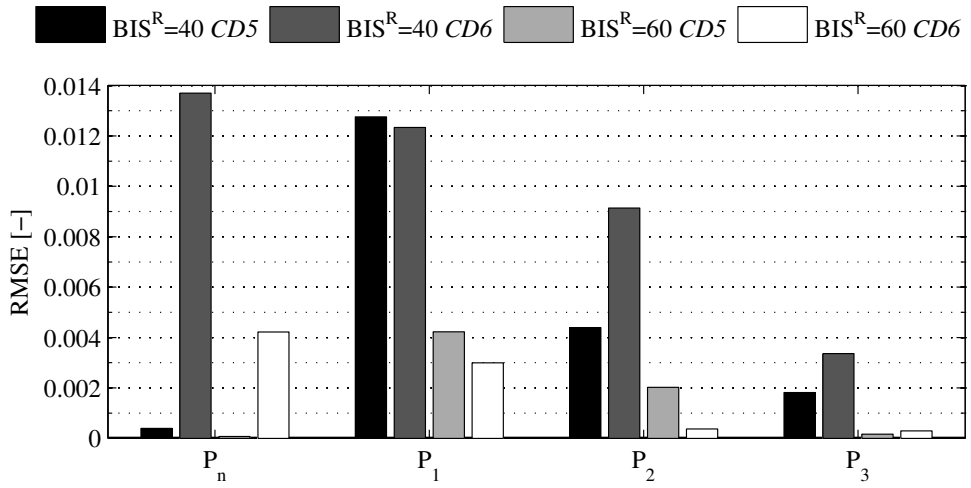

Figure 9.16.: RSME in the maintenance phase for *CD 5* and *CD 6* BIS=40 from 20-30 min, BIS=60 from 50-60min of anaesthesia.

The simulation results of the closed-loop control performance are shown in Figures 9.17 - 9.19. The on-line MPC is adjusting the required input to the patient's dynamics, based on the measured BIS and maintains a stable reference point change for all patients.

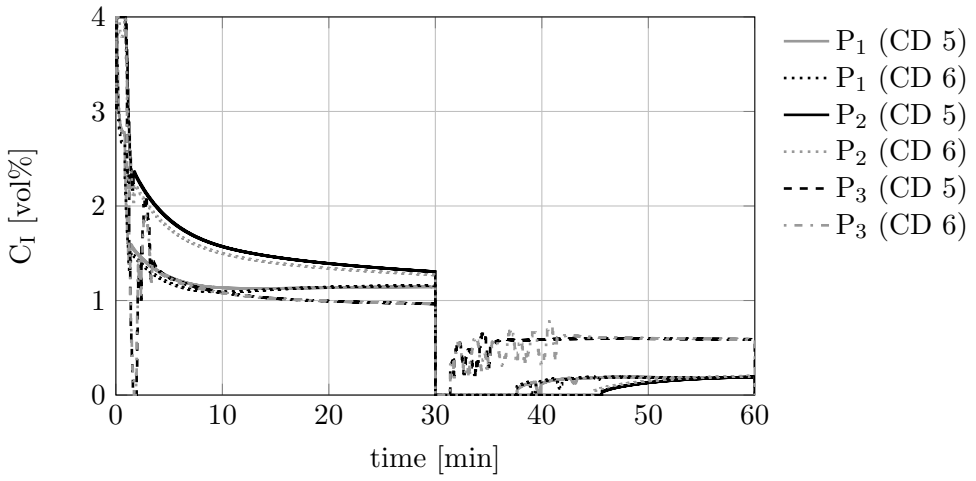

Figure 9.17.: Inlet concentration of all patients for *CD 5* and *CD 6*.

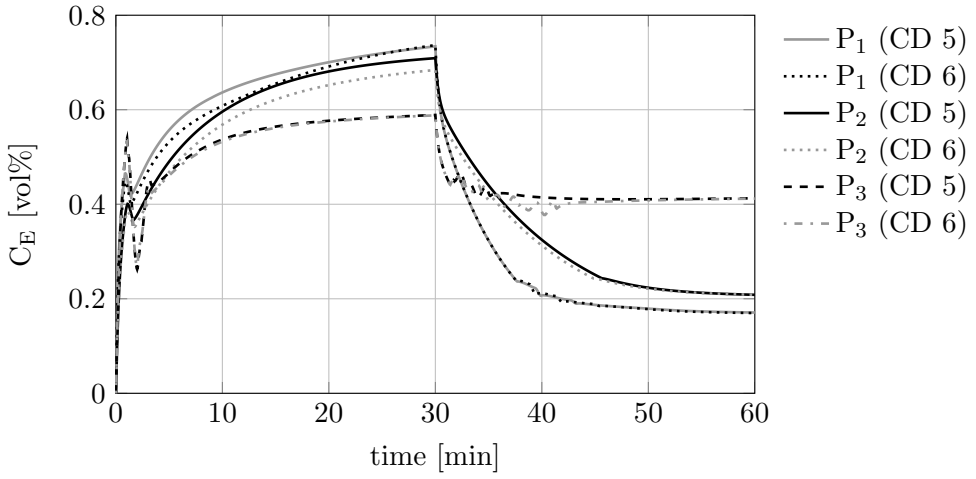

Figure 9.18.: End-tidal concentration of all patients for *CD 5* and *CD 6*.

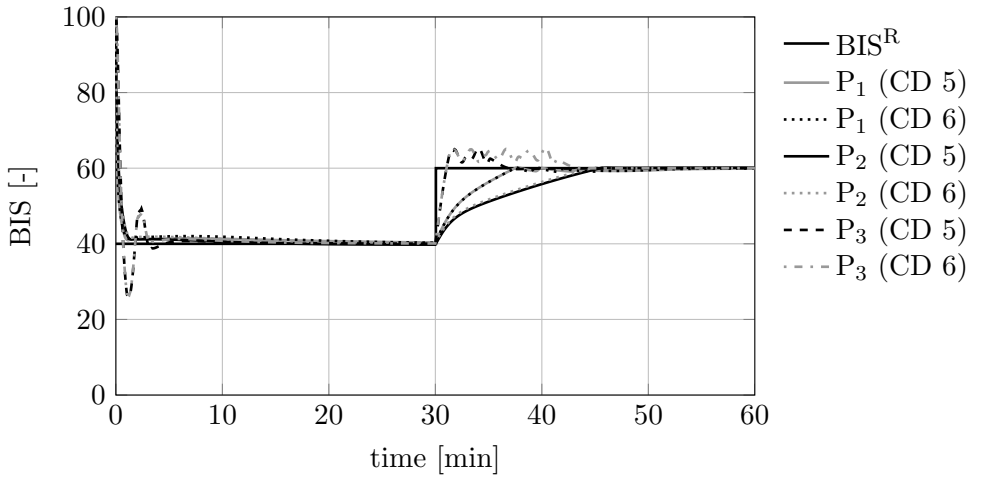

Figure 9.19.: Measured BIS of all patients for *CD 5* and *CD 6*.

9.5. Concluding Remarks

The results clearly confirm the need for a robust control method to adjust the controller's dynamics to the patient based on an output feedback strategy. The presented control strategy, including an output disturbance, shows a good performance for all patients and is able to reduce the off-set of the controller to an acceptable limit compared to the nominal mp-MPC.

In the next chapter advances towards on-line estimation of the PD parameter with the highest sensitivity C_{50} will be investigated.

10. On-line Parameter Estimation

This chapter presents an on-line estimation of the PD parameter C_{50} as an alternative method to cope with the high model uncertainty. The intensive analysis of the model variables and parameters in Chapter 4 led to the conclusion that C_{50} is the parameter with the highest sensitivity and influence on the BIS. Furthermore due to correlation with the other PD parameters an estimation of C_{50} can compensate for a model mismatch resulting from uncertainty in the other PD parameters and the PK parameters, Table 4.5 and Table 4.4. Hence, it is believed that an on-line estimation of C_{50} can compensate model mismatch and provide off-set free reference tracking of the BIS. This statement is further investigated and an algorithm to estimate C_{50} on-line is presented in this Chapter.

The strategy of on-line parameter estimation for anaesthesia control was performed for Propofol by Sartori *et al.* (2005) and Robayo *et al.* (2010). In Robayo *et al.* (2010) the authors estimated the slope of the linearised Hill equation at BIS = 50 as a function of the cross correlation between measurement in the intensive care unit and prediction of the BIS. Sartori *et al.* (2005) formulated the non-linear PK-PD system and added the parameters C_{50} and k_{e0} as system states. The resulting system was linearised at every step and the states and parameters were estimated by a Kalman filter. In Sreenivas *et al.* (2009) the authors mention an improved prediction of the BIS, when estimating C_{50} for isoflurane based anaesthesia, based on the measurement during induction. However, no method for the estimation of C_{50} is described in Sreenivas *et al.* (2009).

10.1. Control and Algorithm Design

The proposed control design is based on the control design previously presented in Figure 9.2. An additional block for the on-line estimation of C_{50} is added and the resulting control structure is depicted Figure 10.1. The non-linearity of the Hill equation is compensated by its inverse (9.9) analogously to the design in Figure 9.2. Hence the reference point of the effect site concentration C_e^R is calculated as a function of the reference point on the hypnotic depth

BIS^{R} and the PD parameters C_{50} and γ in (9.9).

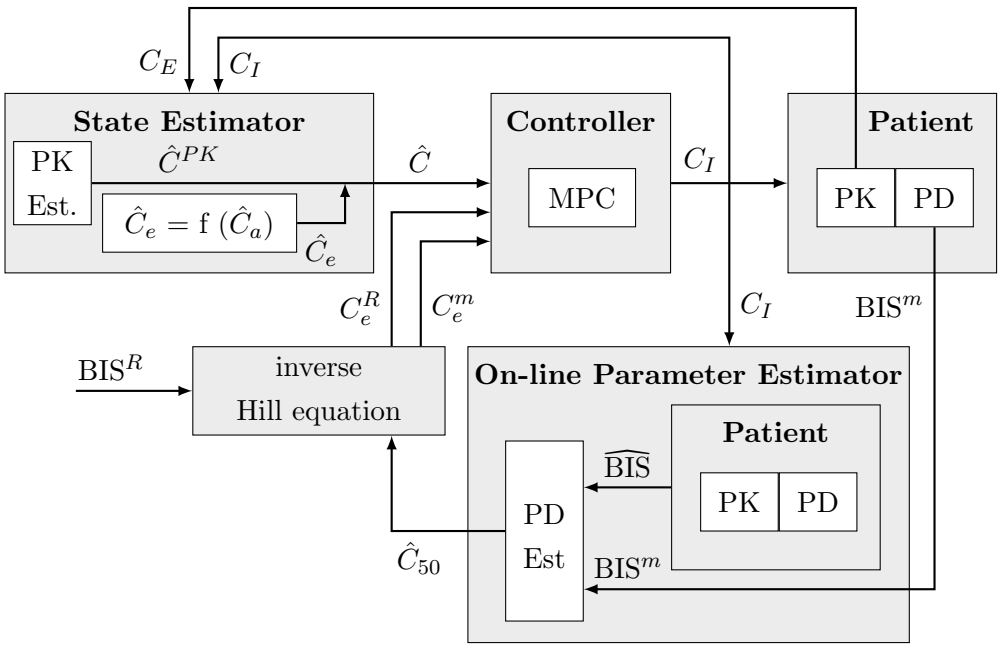

Figure 10.1.: Closed-loop control design for on-line parameter estimation of C_{50}.

The decision process of the on-line estimator block in Figure 10.1 is illustrated in Figure 10.2. The on-line parameter estimator can be switched *on* or *off*. If active, C_{50} is estimated and updated under the conditions depicted in the flow chart in Figure 10.2.

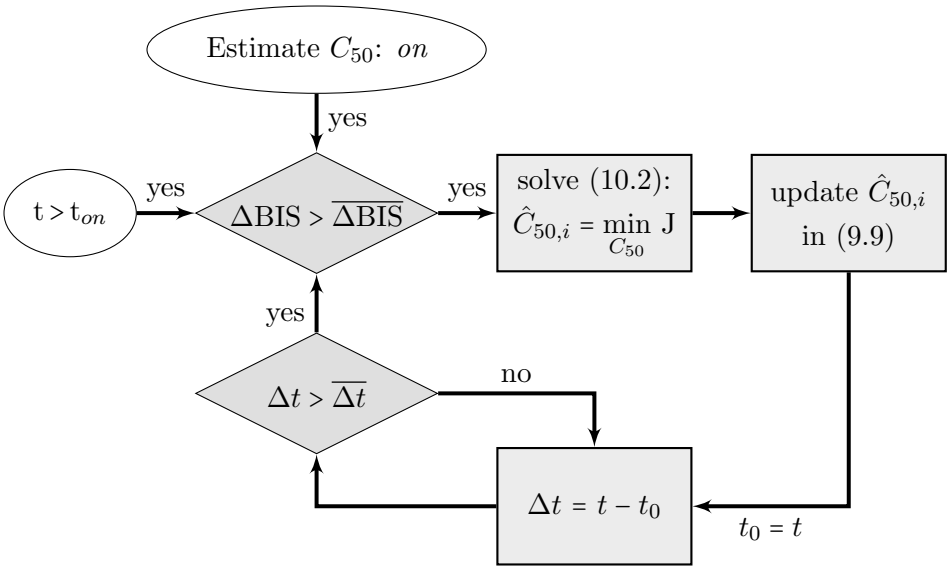

Figure 10.2.: Decision process of the on-line parameter estimator block.

The first estimation and update of C_{50} occurs at least t_{on} min after induction of anaesthesia, $(t > t_{on})$. If the on-line parameter estimation is switched *on*, the parameter estimation block becomes active, when an error between the measured BIS, BIS^m, and the predicted BIS, $\widehat{\text{BIS}}$, by the Hill equation with the current parameters is detected. A mismatch is defined as a deviation of prediction and measurement of more than $\overline{\Delta\text{BIS}}$ during in the last $\overline{\Delta t}$ min, i.e. $\Delta\text{BIS} > \overline{\Delta\text{BIS}}$.

$$\Delta\text{BIS} = \frac{1}{n} \sum_{i=t-\overline{\Delta t}}^{t} \left(\left(\frac{\text{BIS}_i^m - \widehat{\text{BIS}}_i}{\text{BIS}_i^m} \right)^2 \right)^{\frac{1}{2}} \tag{10.1}$$

This triggers the on-line estimation by solving a constrained non-linear least squares problem. The solution of C_{50} is obtained by minimising the error between $\widehat{\text{BIS}}$ and BIS^m:

$$\begin{aligned} \min_{C_{50}} J &= \sum_{i=t-t_\Delta}^{t} (\text{BIS}_i^m - \widehat{\text{BIS}}_i)^2 \\ s.t.\ \widehat{\text{BIS}}_i &= \text{BIS}_0 + (\text{BIS}_{max} - \text{BIS}_0) \frac{C_{e,i}^\gamma}{C_{50}^\gamma + C_{e,i}^\gamma} \\ & (1 - \overline{\Delta C_{50}})\ C_{50,t-1} \le C_{50,t} \le (1 + \overline{\Delta C_{50}})\ C_{50,t-1} \\ & C_{50,\min} \le C_{50,t} \le C_{50,\max} \end{aligned} \tag{10.2}$$

Constraints on the change of the estimated value of $C_{50,t}$ aim for a smooth transition of the parameter to the real value and secure stability against short term disturbances and/or measurement errors. Before anaesthesia $C_{50,t-1}$ is set to its nominal value. Throughout the simulation $C_{50,t}$ is initialised with its previous estimate $C_{50,t-1}$. The solution of the estimation problem is constrained by $\pm\overline{\Delta C_{50}}$ of its previous value $C_{50,t-1}$ and a lower and upper bound, $C_{50,\min}$ and $C_{50,\max}$, given in Table 3.2. When a feasible and optimal solution for $C_{50,t}$ of the estimation problem is obtained, the inverse Hill equation (9.9) is updated with this value after each on-line estimation step. An additional parameter to enhance a smooth transition of C_{50} to its real value is the time interval t_Δ. Only the measurements and predictions in this interval are included in the on-line parameter estimation problem, (10.2). The least squares estimation problem is solved using GAMS and the global solver BARON (GAMS, 2013). The estimated parameter is send to MATLAB via GDXMRW, (Ferris *et al.*, 2011).

The design parameters of the presented on-line parameter estimation algorithm and the tuning parameters are summarised in Table 10.1.

Table 10.1.: On-line parameter estimation tuning parameters and design.

Parameter	Value	Unit	
t_{on}	5	min	Minimum time after anesthesia induction to trigger parameter estimation.
$\overline{\Delta BIS}$	5	%	Error to initiate a parameter estimation.
$\overline{\Delta t}$	3	min	Time since the last update of the Hill equation.
t_{Δ}	3	min	Past measurements included in the parameter estimation problem.
$\overline{\Delta C_{50}}$	20	% vol %	Deviation of old and newly estimated value of C_{50}.

10.2. Evaluation of the On-line Estimation Algorithm

This strategy is now investigated for Patient 3, because Patient 3 is showing the highest off-set for all control strategies presented in Chapter 9, Figure 9.8. The MPC is designed according to the control design *CD 1* in Table 9.1. Analogously to the closed-loop control validation in Section 9.4 the state estimator and mp-MPC are both based on the derived PK-PD model with nominal patient values, whereas the patient model is based on individualised variables and parameters. The control strategy with on-line parameter estimation ($\widehat{CD}$) is tested for a constant reference point of $\text{BIS}^R = 40$ for 100 min. The simulation results are shown in Figures 10.3 - 10.6 for control design *CD* and $\widehat{CD\,1}$.

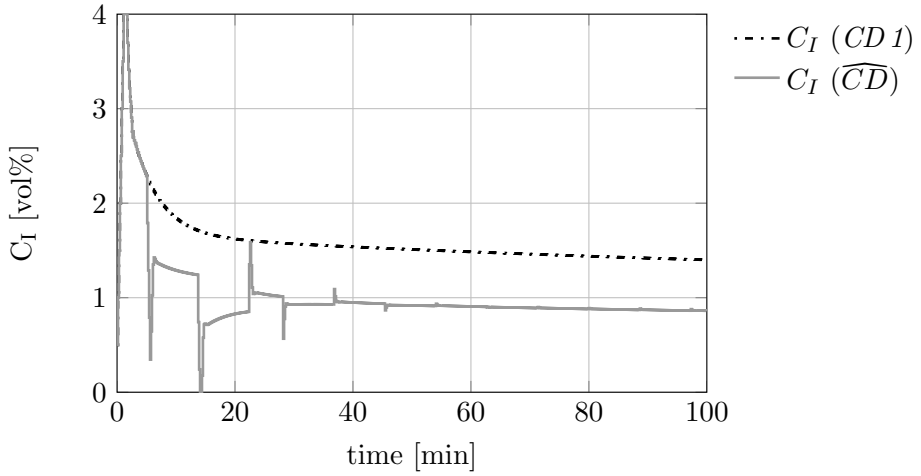

Figure 10.3.: Control input for Patient 3 of *CD 1* and $\widehat{CD}$.

During the initial 5 minutes, $t < t_{on}$, both controllers give an identical input, while after 5 min the input of $\widehat{CD}$ is adjusted according to the update of C_{50} in Figure 10.6. This update triggers a reference point change on the effect site concentration C_e^R as a result of the updated value of C_{50} in the inverse Hill equation and a more accurate knowledge of the patient's individual parameters. Figure 10.3 shows the changing inlet concentration of the controller as a consequence of this reference point change of C_e^R depicted in Figure 10.4. The reference concentration C_e^R is updated with every new estimate of C_{50}.

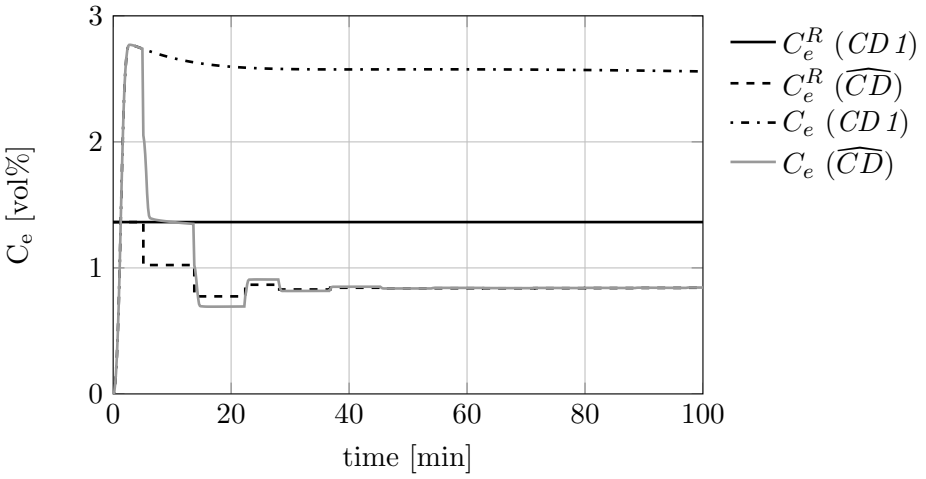

Figure 10.4.: C_e^R and actual C_e for Patient 3 of *CD 1* and $\widehat{CD}$.

Figure 10.4 shows a large off-set, which was also reported in Chapter 9 for control design *CD 1* and emphasises the need of an off-set free control design. This off-set in the effect site concentration originates from different PK and PD variables and parameters of the nominal patient and Patient 3 and causes a further off-set in the BIS shown in Figure 10.5.

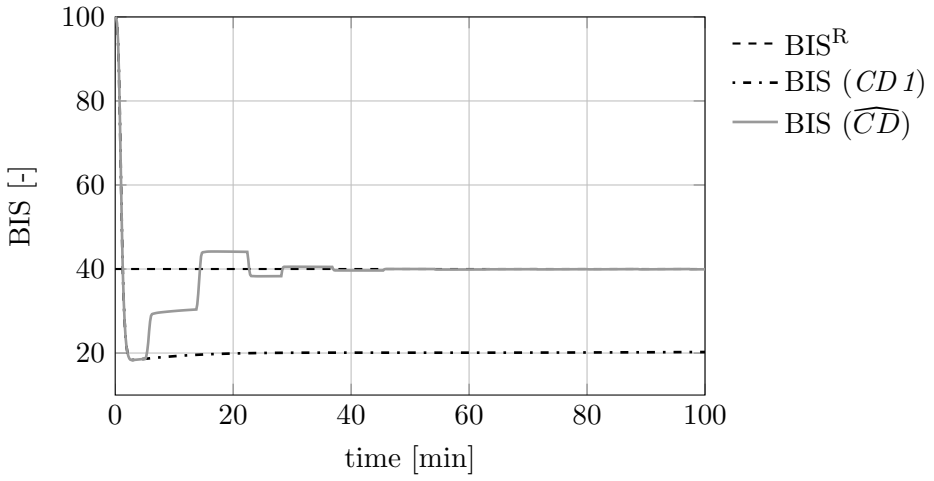

Figure 10.5.: BIS^R and actual BIS for Patient 3 of *CD 1* and $\widehat{CD}$.

By the estimation of C_{50}, $\widehat{CD}$ converges to the reference point BIS = 40, Figure 10.5. Likewise the estimated value of C_{50} converges to a final value of $\hat{C}_{50}$= 0.647 [vol%].

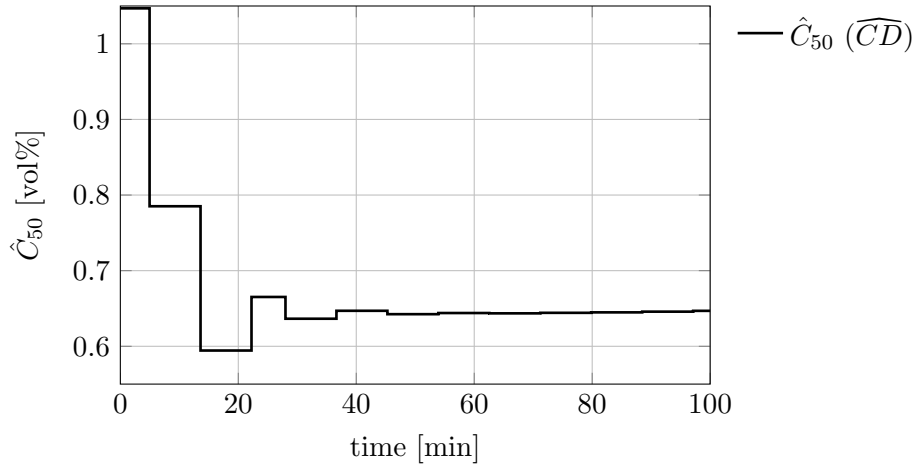

Figure 10.6.: Estimated $\hat{C}_{50}$ of $\widehat{CD}$ for Patient 3.

To confirm and validate this result of the least squares parameter estimation (10.2) with GAMS, (GAMS, 2013), a maximum likelihood parameter estimation for nominal values of all the PK and PD variables and initialised with the nominal value of C_{50} was performed with gPROMS (PSE, 2011). The obtained estimated value was C_{50} = 0.612 [vol%]. This result is reasonably close to the result obtained by the solution of the least squares problem and confirms the accuracy of the parameter estimation result with GAMS (2013).

10.3. Case study: Controller Evaluation for Isoflurane Based Anaesthesia

The control design of $\widehat{CD}$ is now investigated for all three patients undergoing isoflurane based anaesthesia and described in Section 5.1 for a reference point change from BIS = 40 to BIS = 60 after 60 min of anaesthesia. The simulation results of all three patients are shown in Figures 10.7 - 10.10.

During the initial 5 minutes the MPC computes an identical input for all three patients. After this short induction time C_{50} of each patient is estimated individually based on the obtained measurements of the BIS during the last 3 minutes (10.2). This is depicted in Figure 10.9. The estimation of C_{50} results in an update of the reference effect site concentration C_e^R in Figure 10.8. The

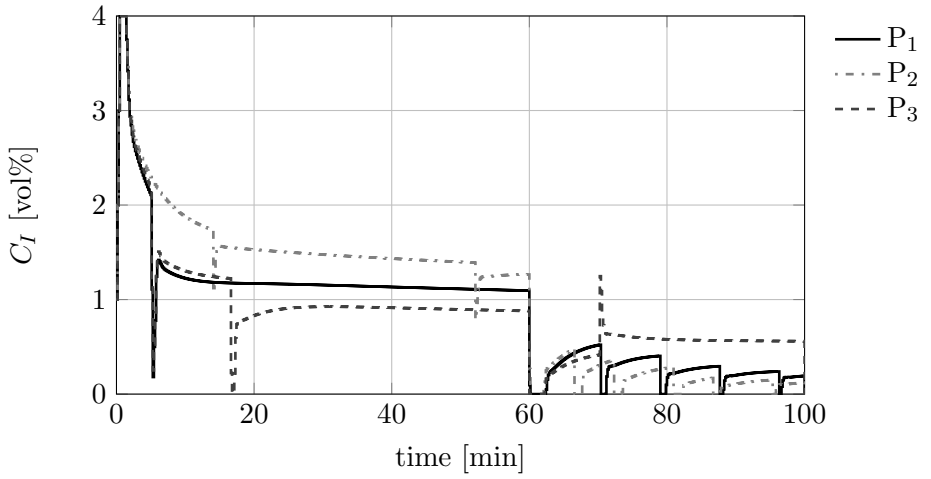

Figure 10.7.: Control input for Patient 1-3 of $\widehat{CD}$.

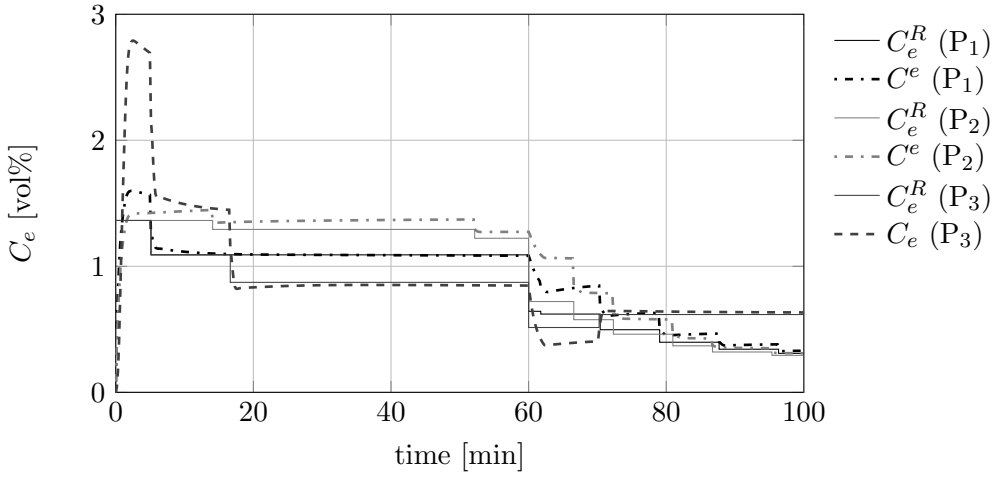

Figure 10.8.: C_e^R and actual C_e for Patient 1-3 of $\widehat{CD}$.

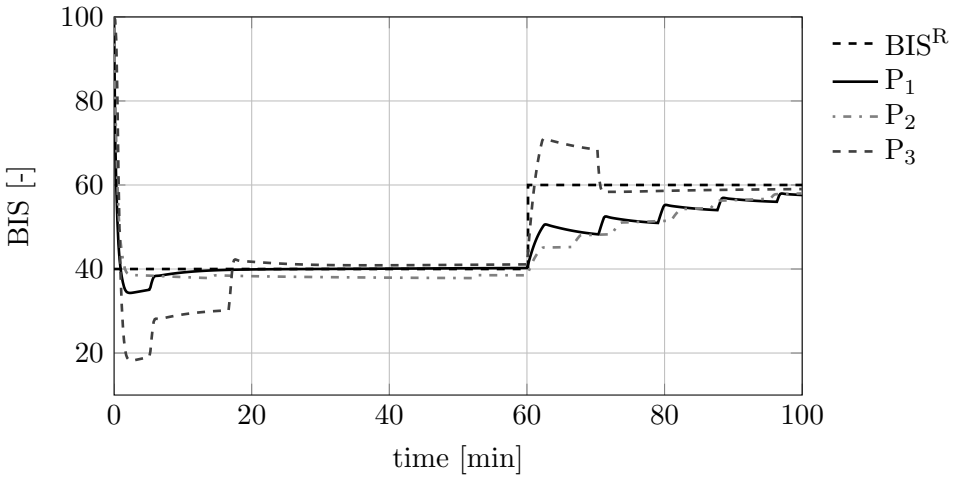

Figure 10.9.: BIS^R and actual BIS for Patient 1-3 of $\widehat{CD}$.

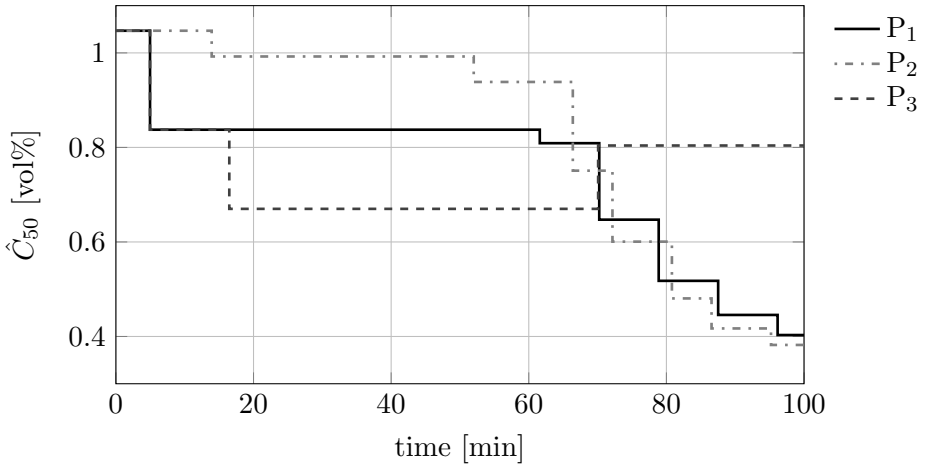

Figure 10.10.: Estimated $\hat{C}_{50}$ of $\widehat{CD}$ for Patient 1-3.

measured BIS of all three patients converges to the reference point BIS^R in Figure 10.9. The required target effect site concentration to obtain BIS^R is varying significantly between patients due to large inter-patient variability, discussed in detail in Chapter 4. Figure 10.7 shows the individual control inputs obtained correctly through the individualised parameter estimation of C_{50} shown in Figure 10.10.

The estimated values of C_{50} converge to a constant value in less than 20 min of anaesthesia. Due to the change in BIS^R the estimation of C_{50} is triggered repeatedly, Figure 10.10. Here the updated parameter, C_{50}, for Patient 3 converges faster to a steady value. C_{50} of Patient 1 and Patient 2 is repeatedly updated every 3 minutes and at the constraint at the lower bound $C_{50,t} \geq 0.8\, C_{50,t-1}$ is active. This is originated from the different slope of the

individual Hill equations in Figure 9.12 and the distinct deviation from the nominal value at BIS = 40 and BIS = 60.

10.4. Concluding Remarks

The on-line estimation of C_{50} shows promising results towards an individualised control strategy of anaesthesia. This strategy allows to adjust the controller to the individual sensitivity of the patient towards the anaesthetic agent. Furthermore the anaesthetist gains understanding of the patient's sensitivity, which could be advantageous for future surgeries of the same patient. The presented strategy is believed to be safe for the patient ensured by constraints in the controller configuration and constraints in the parameter estimation problem.

The tuning parameters of this strategy are (i) the permitted deviation from the initial value for C_{50} in the parameter estimation problem, which was set to $\widehat{\Delta C_{50}}$ = ±20% in this study, (ii) the percentage of deviation from the measured BIS, which triggers an estimation of C_{50}, set to $\widehat{\Delta BIS}$=5% in this study, and (iii) Δt the sampling time between each parameter estimation, which was set to Δt=3 min.

A first study to investigate the capabilities of the on-line parameter estimation algorithm to reject disturbances is presented in Appendix C.

11. Conclusions and Future Directions

The framework presented in this thesis and illustrated anew in Figure 11.1 provided a valuable guideline for model development and analysis when aiming for a robust control strategy and the design of a safe drug delivery system for anaesthesia.

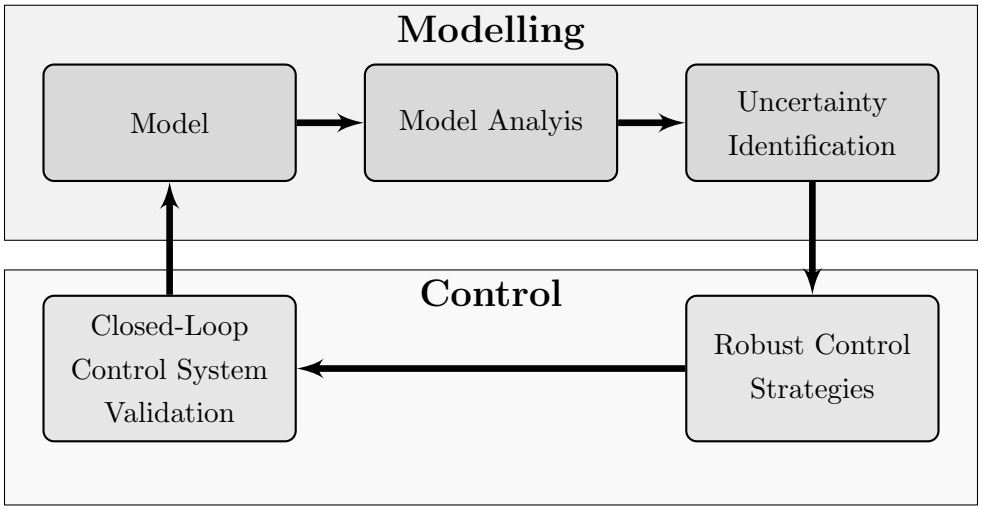

Figure 11.1.: Framework presented in this thesis for volatile anaesthesia.

11.1. Publications from this Thesis

Journal Articles

Krieger, A., Panoskaltsis, N., Mantalaris, A., Georgiadis, M., Pistikopoulos, E.N., 2013. Modelling and Analysis of Individualized Pharmacokinetics and Pharmacodynamics for Volatile Anaesthesia. IEEE Transactions on Biomedical Engineering. Vol. 61, pp. 25-34.

Krieger, A., Pistikopoulos, E. N., 2013. Model predictive control of anaesthesia under uncertainty. submitted to Special Issue in Bio-systems Modeling and Engineering, Computers and Chemical Engineering.

Chang, H., **Krieger, A.**, Astolfi, A., Pistikopoulos, E. N., 2013. Robust Multi-parametric Model Predictive Control for LPV systems with Application to Anaesthesia. submitted to Journal of Process Control.

Nascu, I., **Krieger, A.**, Ionescu, C. M., Pistikopoulos, E. N., 2013. Multi-Parametric Model Predictive Control for the Induction and Maintenance of Intravenous Anaesthesia. to be submitted to Medical & Biological Engineering & Computing.

Conference Proceedings

Krieger, A., Panoskaltsis, N., Mantalaris, A., Georgiadis, M. C., Pistikopoulos, E. N., 2011. A Novel Physiologically Based Compartmental Model for Volatile Anaesthesia. In Computer Aided Process Engineering. Vol. 29. Elsevier, pp. 1495 – 1499.

Krieger, A., Panoskaltsis, N., Mantalaris, A., Georgiadis, M. C., Pistikopoulos, E. N., 2012. Analysis of an Individualized Physiologically Based Model for Anesthesia Control. In: IFAC Proceedings Volumes (IFAC-PapersOnline), pp. 385–390.

Oral Presentations

Krieger, A., Panoskaltsis, N., Mantalaris, A., Georgiadis, M. C., Pistikopoulos, E. N., 2012. Individualized Physiologically Based Modeling and Model Predictive Control of Volatile Anesthesia. (312f) 2012 AIChE Annual Meeting. Pittsburgh, PA, US. 28 October - 2 November 2012.

Krieger, A., Pistikopoulos, E. N., 2012. Individualised Physiologically Based Modelling and Control of Anaesthesia, Chemical Engineering PhD Research Symposium, Imperial College London, 30 March 2012.

Krieger, A., Panoskaltsis, N., Mantalaris, A., Georgiadis, M. C., Pistikopoulos, E. N., 2012. Analysis of an Individualized Physiologically Based Model for Anesthesia Control. 8th IFAC Symposium on Biological and Medical Systems (2012), Budapest Hungary, 29 - 31 August 2012.

Poster Presentations

Krieger, A., Pistikopoulos, E. N., 2013. Modelling, Analysis and Explicit Multi-parametric Model Predictive Control of Volatile Anaesthesia. 126th International Summer Course, BASF SE, Ludwigshafen, Germany, 20 - 29 August 2013.

Krieger, A., Panoskaltsis, N., Mantalaris, A., Georgiadis, M. C., Pistikopoulos, E. N., 2011. A Novel Physiologically Based Compartmental Model for Volatile Anaesthesia. 21st European Symposium on Computer Aided Process Engineering (ESCAPE 21), Chalkidiki, Greece, 29 May - 01 June 2011.

11.2. Key Contributions from this Thesis

Part I: Modelling[1]

- Individualised physiologically based pharmacokinetic-pharmacodynamic model for volatile anaesthesia.
- Insights in the model dynamics via analysis of the individualised parameters and variables of the derived model.
  - Envelope of model uncertainty.
  - Global sensitivity analysis.
  - Variability analysis.
  - Correlation analysis.
- Validation of the pharmacokinetic part of the model with clinical data for isoflurane and desflurane based anaesthesia.
- Individual estimation of the pharmacodynamic parameters for isoflurane and desflurane of the Hill equation for each patient.
- Capabilities of the model to be applied as teaching tool of drug distribution and drug effect modelling for anaesthesia.

Part II: Model Predictive Control

- Testing of the consequence of inter- and intra-patient variability for open-loop nominal mp-MPC.

[1]The work presented in Part I has been partly published in Krieger *et al.* (2013).

- Design of an explicit control strategy, which adjusts to the patient's dynamics and enables off-set free control for drug delivery systems for volatile anaesthesia.
- Design of a control strategy which adjusts to the patient's dynamics by on-line parameter estimation of the parameter with the highest sensitivity: C_{50}.
- Contribution towards personalised health care by taking into account the individual patient characteristics.

11.3. Summary of this Thesis

The presented model for volatile anaesthesia combined existing ideas of compartmental and physiologically based models for the uptake and distribution of anaesthesia originated from the work of Mapleson (1963) and Eger (1974). In the derived model the PK variables and parameters where described as a function of age, weight, height and gender of the patients to account for individual patient characteristics. This strategy was validated by the comparison of the simulation results with clinical studies for 11 patients and 2 different anaesthetic agents, 3 patients undergoing isoflurane based anaesthesia and 8 patients undergoing desflurane anaesthesia.

The sequential analysis and grouping of the variables and parameters of the model in their related PK and PD group led to a good understanding of the model's dynamics and the influence of the specific parameters on the measurable outputs, BIS and C_E. (i) The lung volume and the cardiac output mainly determine the uptake of the drug. (ii) The concentration at 50% drug effect C_{50} defines the sensitivity of the patient and therefore the resulting effect for a fixed effect site concentration. The results for tissue concentrations are in accordance with the literature, (Eger, 1974, p.89).

The considerably more profound uncertainty in the PD parameters in comparison with the PK parameters and variables found in this thesis was previously reported in the literature (Mertens and Vuyk, 1998).

The model showed good capabilities to serve as a teaching tool and examine the influence of a variable and/or parameter on the internal drug concentrations and the uptake.

With respect to robust model predictive control, the extensive modelling process proved to be rewarding, as (i) an underlying model of adequate complexity for control, which is still able to capture the individual patient's characteristics, was found and (ii) the uncertainty the control strategy has to handle

was identified.

Based on the model the risks of using a nominal open-loop explicit MPC for a system that is suffering from such high uncertainty was shown. Consequently, the design of an output feedback controller, including the model mismatch as an output disturbance, was developed that adjusts to the patients' dynamics. The output feedback controller was derived as an on-line controller, which is solving a QP problem at each iteration step.

An alternative on-line solution to adjust the controller to the patients' dynamics was the combination of the mp-MPC with an on-line parameter estimator of C_{50}. This design additionally provides the anaesthetist with information about the patient's sensitivity.

11.4. Ongoing and Future Work

The derived model showed good results for isoflurane and desflurane and can be adapted to other volatile anaesthetic agents by changing the solubility coefficients of the blood and tissue, λ and λ_i. This encourages further testing and validation with clinical data of other volatile anaesthetics or the extension of the model to simultaneous administration more than one anaesthetic agent.

11.4.1. Explicit Model Predictive Control Under Uncertainty

The need for an off-set free and robust control method, because of high inter-patient variability and the probability of changing variables during surgery, due to e.g. surgical stimulation, blood loss, blood transfusion, was clearly shown. The explicit MPC solution provides a excellent testing tool or all possible scenarios that might occur during anaesthesia. Our current work is dealing with deriving the explicit form of the output-feedback controller, for which so far the on-line formulation was tested. Additionally an alternative to estimate the output disturbance is investigated. Further testing will be performed for disturbance rejection of disturbances often occurring during anaesthesia, (Dumont *et al.*, 2009; Struys *et al.*, 2004), and tested in Yelneedi *et al.* (2009) for isoflurane. First results are summarised in Appendix C. The testing and validation of the closed loop control algorithm will be performed with the platform of the derived model for volatile anaesthesia, which also might lead to the development of other robust control strategies, such as including an integral penalty on the reference tracking error.

11.4.2. Model Predictive Control for Hybrid Systems

The piecewise affine linearisation of the Hill equation results in three different controllers, which are switching according to the predicted system output. An alternative is the formulation of the objective function as a hybrid system, where the optimal control trajectory can be obtained by dynamic programming, (Rivotti *et al.*, 2012a).

11.4.3. Moving Horizon Estimation

Concerning the state estimation, the application of the 'perfect' observer inherits the advantage that no infeasibilities of the controller can occur, as controller and estimator are based on the same model. The Kalman filter, however, showed to improve the performance of the mp-MPC because the states were estimated based on the measured output and, naturally, closer to the real states, the internal blood and tissue concentrations. The application of a moving horizon estimator (MHE) for state estimation combines both advantages, because of constraint handling on the states, at the cost of a more difficult implementation, i.e.

$$\begin{aligned} \min_{\hat{x}_{t-\hat{N}},\{\hat{w}\}_{t-\hat{N}}^{t-1}} \; & J = \left\|\hat{x}_{t-\hat{N}} - \bar{x}_{t-\hat{N}}\right\|_{P_{t-\hat{N}}^{-1}} + \sum_{k=t-\hat{N}}^{t-1} \|\hat{w}_k\|_{Q_k^{-1}}^2 + \sum_{k=t-\hat{N}}^{t} \|\hat{v}_k\|_{R_k^{-1}}^2 \\ \text{s.t. } & x_{t-\hat{N}+k+1} = Ax_{t-\hat{N}+k} + Bu_{t-\hat{N}+k} + Gw_{t-\hat{N}+k}, \\ & y_{t-\hat{N}+k} = Cx_{t-\hat{N}+k} + Du_{t-\hat{N}+k} + v_{t-\hat{N}+k}, \end{aligned} \tag{11.1}$$

where $\hat{N}$ denotes the estimation horizon. Here the computation of the disturbance matrix G involves the highest challenge, because it maps coloured noise on the states, (Findeisen, 1997). As the system itself is uncertain, the choice of G is more challenging and the influence of a nominal choice of G on the closed control loop might lead to an unstable system and needs to be further investigated. The task of finding G is similar to the challenge of determining B_d in Section 8.2 (8.8) and estimate the output disturbance's impact on the system states.

The simultaneous design of the explicit solution of the MHE and the MPC Voelker *et al.* (2010, 2013) offers a full explicit solution of the closed control loop for anaesthesia control that accomplishes the high safety measures for testing required for the control of a biomedical system such as anaesthesia.

11.4.4. Model Reduction

An alternative strategy in order to obtain an explicit mp-MPC, while maintaining the system's dynamics of a complex model, is via model reduction techniques, (Lambert *et al.*, 2013; Rivotti *et al.*, 2012b).

11.4.5. Linear Parameter Varying Systems

The approach presented in Chang *et al.* (2013a,b) shows promising results for LPV systems, while maintaining the explicit solution of the nominal mp-MPC. The extension of the presented method to a time-varying system matrix A_k and a time varying system matrix B_k,

$$\begin{aligned} x_{k+1} &= A_k x_k + B_k u_k \\ y_k &= C x_k, \end{aligned} \tag{11.2}$$

allows to adjust the controller in advance to the varying or knowingly different PK parameters without the need of deriving an new explicit solution of the mp-MPC.

11.5. Anaesthesia Automation

Closing the loop of the anaesthetic system implies automatic drug infusion based on the model predictions and the feedback through the measured patient variables. Apart from hypnotic depth, anaesthesia is defined by amnesia, analgesia, muscle relaxation and the maintenance of the vital functions. A multiple-input multiple-output (MIMO) controller could regulate all of these variables (Biro, 2013).

11.5.1. Main Challenges

The main challenges to fully automate anaesthesia are, (Absalom *et al.*, 2011; Struys *et al.*, 2006):

(i) Development of new sensors to measure adequately all variables of interest to the anaesthetist, where challenge is the measurement of amnesia and analgesia.

(ii) Further evaluation and testing of robust control strategies with respect to patient safety.

(iii) New development of multiple drug effect interaction models for the design of MIMO control strategies.

The lack of reliable sensors is probably the most profound problem. An adequate measurable signal is essential for the successful design of a process model; besides the control strategy relies heavily on an accurate feedback of the patient's current state. Apart from the BIS, used for most closed loop applications, the Narcotrend Monitor or auditory evoked potentials are available. This variety of possible feedback signals and design of models increases the difficulty of model and control design, because the parameters cannot be easily projected from one measurement to another, (Bibian *et al.*, 2011; Bruhn *et al.*, 2006; Kent and Domino, 2009).

The interactions of various drugs administered simultaneously are very complex, anaesthetics e.g suppress awareness and likewise act as a weak analgesic agent, (Miller *et al.*, 2010). Most simultaneously administered drugs show synergetic effects, (Hendrickx *et al.*, 2008). These interactions are very different to distinguish without adequate sensors. Therefore often the desired plasma concentration is targeted for the control or modelling strategy, (Kennedy, 2013). Developed interaction models of two or more drugs, response surface models, account for synergetic, additive or antagonistic effects, (Minto *et al.*, 2000).

As a natural consequence of the previously mentioned challenges, there are legitimate safety concerns regarding stability, robustness and disturbance rejection with respect to control algorithms designed for anaesthesia, (Luginbühl *et al.*, 2006).

Nevertheless, Hemmerling *et al.* (2013) performed a clinical trial, where anaesthesia, analgesia and muscle relaxation were maintained by automated simultaneous infusion of propofol, remifentanil and rocuronium, and achieved a better performance compared to manual control.

The way to the fully automated operation theatre is certainly a long way to go, but the realisation of an autopilot for anaesthesia drug delivery is approaching and indeed achievable with a lot of joint research effort in the interdisciplinary areas of sensor development, detailed mathematical modelling and robust control design.

Appendix

A. MPC to mp-QP

A.1. MPC Problem Formulation

The model predictive controller (MPC) is formulated as follows, see also (8.1).

$$\begin{aligned} \min_{x,y,u} J = {} & x_N' P x_N + \sum_{k=1}^{N-1} x_k' Q x_k + \sum_{k=1}^{N} (y_k - y_k^R)' Q_R (y_k - y_k^R) \\ & + \sum_{k=0}^{M-1} u_k' R u_k + \sum_{k=0}^{M-1} \Delta u_k' R_1 \Delta u_k \\ s.t. \quad & x_{k+1} = Ax_k + Bu_k, \quad A \in \mathbb{R}^{n_x \times n_x}, \quad B \in \mathbb{R}^{n_u \times n_x} \\ & y_k = Cx_k, \quad C \in \mathbb{R}^{n_x \times n_y} \end{aligned} \tag{A.1}$$

The MPC problem is formulated as multi-parameteric quadratic programming (mp-QP) problem of the form:

$$\begin{aligned} \min_U J(\theta) = {} & \frac{1}{2} U' H U + \theta' F U + \frac{1}{2} \theta' Y \theta \\ \text{s.t.} \quad & GU \leq W + E\theta \end{aligned} \tag{A.2}$$

Note: The last term is not a function of the optimisation variable U and can therefore be neglected to find the optimal value in U.
Note: The indices in θ are assigned in the following order: $\theta = [x_0, u_{t-1}, y_t^m, y^R]$

x_0 state vector at beginning of the control horizon

u_{t-1} control input at previous time step

y^m measured process output

y^R constant reference point

with $\quad Q, P \in \mathbb{R}^{n_x \times n_x}, \quad Q_R \in \mathbb{R}^{n_y \times n_y}, \quad R \in \mathbb{R}^{n_u \times n_u}$

The states for the output horizon are given as a function of the states at the beginning of the control horizon x_0 and the inputs u.

$$x_n = A^n x_0 + \sum_{k=0}^{n-1} A^{n-1-k} B u_k, \quad \forall n = 1, \dots N-1 \tag{A.3}$$

To reformulate (A.1) as a multi-parametric problem all states are given in the following matrix form as a function of the optimisation variables U and the parameters θ in (A.4).

$$X = \begin{bmatrix} x_1 \\ x_2 \\ \vdots \\ x_N \end{bmatrix}, \quad U = \begin{bmatrix} u_0 \\ u_1 \\ \vdots \\ u_{M-1} \end{bmatrix} \tag{A.4}$$

$$X = \underbrace{\begin{bmatrix} A & \mathbf{0} \\ A^2 & \mathbf{0} \\ A^3 & \mathbf{0} \\ \vdots & \vdots \\ A^{N-2} & \mathbf{0} \\ \dots & \dots \\ A^N & \mathbf{0} \end{bmatrix}}_{:=\tilde{A}\in\mathbb{R}^{Nn_x\times n_\theta}} \theta + \underbrace{\begin{bmatrix} B & 0 & \cdots & 0 & 0 \\ AB & B & \cdots & 0 & 0 \\ A^2B & AB & \cdots & 0 & 0 \\ \vdots & \vdots & \vdots & \vdots & \vdots \\ A^{M-1}B & A^{M-2}A & \cdots & AB & B \\ \dots & \dots & \dots & \dots & \\ A^{M-1}B & A^{M-2}A & \cdots & AB & B \end{bmatrix}}_{:=\tilde{B}\in\mathbb{R}^{Nn_x\times Mn_u}} U \tag{A.5}$$

The matrix $\mathbf{0}$ in $\tilde{A}$ is $\in \mathbb{R}^{(n_\theta - n_x)\times n_x}$. Here the number of tracked outputs is equal to the number of outputs, in any other case n_y is equal to the number of tracked outputs. The control input is constant for all $\mathrm{N} > \mathrm{M}$, therefore the last row in $\tilde{B}$ is repeated for all $\mathrm{N} > \mathrm{M}$, (Goodwin *et al.*, 2005, p. 105).

A.2. Penalty Weights in the Objective Function

The penalty weights on the states x, control inputs u, reference tracking error $(y - y^R)$ and the step change in the input Δu are added and described consecutively.

States x

$$\tilde{Q} = \mathrm{diag}(Q, \dots, Q, P), \in \mathbb{R}^{Nn_x\times Nn_x} \tag{A.6}$$

$$
\begin{aligned}
\min_U J &= X'\tilde{Q}X \\
&= (\tilde{A}\theta + \tilde{B}U)'\tilde{Q}(\tilde{A}\theta + \tilde{B}U) \\
&= \theta'\tilde{A}'\tilde{Q}\tilde{A}\theta + \theta'\tilde{A}'\tilde{Q}\tilde{B}U + U'\tilde{B}'\tilde{Q}\tilde{A}\theta + U'\tilde{B}'\tilde{Q}\tilde{B}U \\
&= \underbrace{\theta'\tilde{A}'\tilde{Q}\tilde{A}\theta}_{\neq f(U)=const} + 2\theta'\tilde{A}'\tilde{Q}\tilde{B}U + U'\tilde{B}'\tilde{Q}\tilde{B}U \\
&= 2\theta'\tilde{A}'\tilde{Q}\tilde{B}U + U'\tilde{B}'\tilde{Q}\tilde{B}U \\
&= U[\tilde{B}'\tilde{Q}\tilde{B}]U + \theta[2\tilde{A}'\tilde{Q}\tilde{B}]U
\end{aligned}
\tag{A.7}
$$

$$H_x = 2\tilde{B}'\tilde{Q}\tilde{B} \tag{A.8}$$

$$F_x = 2\tilde{A}'\tilde{Q}\tilde{B} \tag{A.9}$$

Inputs u

$$\tilde{R} = \mathrm{diag}(R, \ldots, R), \in \mathbb{R}^{Mn_u \times Mn_u} \tag{A.10}$$

$$\min_U J = U'\tilde{R}U \tag{A.11}$$

$$H_u = 2\tilde{R} \tag{A.12}$$

Reference tracking error $(y - y^R)$

$$\tilde{Q_R} = \mathrm{diag}(Q_R, \ldots, Q_R), \in \mathbb{R}^{Nn_y \times Nn_y} \tag{A.13}$$

$$\tilde{C} = \mathrm{diag}(C, \ldots, C), \mathbb{R}^{Nn_y \times Mn_u} \tag{A.14}$$

$$Y = \tilde{C}X \tag{A.15}$$

$$Y^* := Y - Y^R = \tilde{C}[\tilde{A}\theta + \tilde{B}U] - \underbrace{\begin{bmatrix} 0 & \cdots & 1 \\ \vdots & \vdots & \vdots \\ 0 & \cdots & 1 \end{bmatrix}}_{:=\tilde{K}\in\mathbb{R}^{N\times n_\theta}}\theta \tag{A.16}$$

$$Y^* = \underbrace{[\tilde{C}\tilde{A} - \tilde{K}]}_{:=\tilde{L}}\theta + \underbrace{\tilde{C}\tilde{B}}_{:=\tilde{M}}U \tag{A.17}$$

Note: The index of 1 in $\tilde{K}$ corresponds to the index of the reference point y^R in the parameter vector θ.

$$\begin{aligned}\min_U J &= (\tilde{L}\theta + \tilde{M})'\tilde{Q}_R(\tilde{L}\theta + \tilde{M}) \\ &= (\tilde{L}\theta + \tilde{M})'\tilde{Q}_R(\tilde{L}\theta + \tilde{M}) \\ &= \theta'\tilde{L}'\tilde{Q}_R\tilde{L}\theta + \theta'\tilde{L}'\tilde{Q}_R\tilde{M}U + U'\tilde{M}'\tilde{Q}_R\tilde{L}\theta + U'\tilde{M}'\tilde{Q}_R\tilde{M}U \\ &= \underbrace{\theta'\tilde{L}'\tilde{Q}_R\tilde{L}\theta}_{\neq f(U)=const} + 2\theta'\tilde{L}'\tilde{Q}_R\tilde{M}U + U'\tilde{M}'\tilde{Q}_R\tilde{M}U \\ &= 2\theta'\tilde{L}'\tilde{Q}_R\tilde{M}U + U'\tilde{M}'\tilde{Q}_R\tilde{M}U \\ &= U[\tilde{M}\tilde{Q}_R\tilde{M}]U + \theta[2\tilde{L}'\tilde{Q}_R\tilde{M}]U\end{aligned} \tag{A.18}$$

$$H_y = 2[\tilde{M}\tilde{Q}_R\tilde{M}] \tag{A.19}$$

$$F_y = 2[\tilde{L}'\tilde{Q}_R\tilde{M}] \tag{A.20}$$

Input step change Δu

The previous control action u_{-1} is added to the parameter vector in order to respect the constraints on Δu_0 with $\Delta u_k := u_k - u_{k-1}$.

$$\theta = [x_0, y^R, u_{-1}]' \tag{A.21}$$

Therefore an additional line is added to $\tilde{K}$ to account for u_{-1} in θ.

$$\min_u J = \sum_{k=0}^{M-1} \Delta u_k' R_{1,k} \Delta u_k \tag{A.22}$$

$$\tilde{R}_1 = \mathrm{diag}(R_1, \ldots, R_1), \in \mathbb{R}^{Mn_u \times Mn_u} \tag{A.23}$$

$$\Delta U = \begin{bmatrix} \Delta u_0 & \Delta u_1 & \cdots & \Delta u_{M-1} \end{bmatrix}' \tag{A.24}$$

One extra parameter is added to θ: u_{-1} to determine $\Delta u_0 = u_{-1} - u_0$
$\theta = [\ldots, u_{-1}]$

$$\Delta U = \underbrace{\begin{bmatrix} 0 & 1 & \cdots & 0 & 0 \\ 0 & 0 & \cdots & 0 & 0 \\ 0 & 0 & \cdots & 0 & 0 \\ \vdots & \vdots & \vdots & \vdots & \vdots \\ 0 & 0 & \cdots & 0 & 0 \end{bmatrix}}_{:=\tilde{N}} \theta + \underbrace{\begin{bmatrix} 1 & 0 & 0 & \cdots & 0 & 0 \\ -1 & 1 & 0 & \cdots & 0 & 0 \\ 0 & -1 & 1 & \cdots & 0 & 0 \\ \vdots & \vdots & \vdots & \vdots & \vdots & \vdots \\ 0 & 0 & 0 & \cdots & -1 & 1 \end{bmatrix}}_{:=\tilde{O}} U \tag{A.25}$$

The entry of 1 in $\tilde{O}$ corresponds to the index of u_{-1} in the parameter vector θ.

$$H_{\Delta u} = \tilde{N}' \tilde{R}_1 \tilde{N} \tag{A.26}$$

$$F_{\Delta u} = \tilde{N}' \tilde{R}_1 \tilde{O} \tag{A.27}$$

Output Disturbance d

A steady-state target calculation is constructed to remove the effects of estimated output disturbances, (Muske and Badgwell, 2002; Pannocchia and Bemporad, 2007). The output disturbance is defined as the difference between the measurement and the predicted process output and is assumed to be constant for the entire output horizon.

$$\begin{aligned} x_{k+1} &= Ax_k + Bu_k \\ y_k &= Cx_k + d_k, \text{ with } d_k = d_0, \forall k = 0, \ldots, N-1 \\ d_0 &= y_0^m - y_0 \end{aligned} \tag{A.28}$$

The process output at the beginning of the control and output horizon y_0^m is added to the parameter vector θ. Equation (A.15) is updated as follows:

$$\textbf{Note: } D := (Y_0^m - Y_0) \tag{A.29}$$

$$Y = \tilde{C}X, \quad \tilde{C} \in \mathbb{R}^{Nn_y \times Mn_u} \tag{A.30}$$

$$
\begin{aligned}
Y^* &:= (Y - Y^R) + \underbrace{\begin{bmatrix} d \\ \vdots \\ d \end{bmatrix}}_{:=D} = (Y - Y^R) + (Y_0^m - Y_0) \\
&= (\tilde{C}[\tilde{A}\theta + \tilde{B}U] - Y^R) + \left(\underbrace{\begin{bmatrix} 0 & \cdots & 1 & 0 \\ \vdots & \vdots & \vdots & \vdots \\ 0 & \cdots & 1 & 0 \end{bmatrix}}_{:= Y_0^m} \theta - \underbrace{\begin{bmatrix} C & \cdots & 0 \\ \vdots & \vdots & \vdots \\ C & \cdots & 0 \end{bmatrix}}_{:= Y_0} \theta \right) \\
&= \tilde{C}[\tilde{A}\theta + \tilde{B}U] - \underbrace{\begin{bmatrix} C & \cdots & -1 & 1 \\ \vdots & \vdots & \vdots & \vdots \\ C & \cdots & -1 & 1 \end{bmatrix}}_{:=\tilde{K} \in \mathbb{R}^{N \times n_\theta}} \theta \\
Y^* &= \underbrace{[\tilde{C}\tilde{A} - \tilde{K}]}_{:=\tilde{L}} \theta + \underbrace{\tilde{C}\tilde{B}}_{:=\tilde{M}} U
\end{aligned}
\tag{A.31}
$$

$$H_y = 2[\tilde{M}\tilde{Q}_R\tilde{M}] \tag{A.32}$$

$$F_y = 2[\tilde{L}'\tilde{Q}_R\tilde{M}] \tag{A.33}$$

A.3. Constraints

The generic form of the constraints is

$$GU \leq W + E\theta. \tag{A.34}$$

The constraints on the states x, control inputs u, the output y and the step change in the input Δu are added and described consecutively.

Constraints on x

$$
\begin{aligned}
&x_{\min} \leq x_1, \ldots x_N \leq x_{\max} \\
&x_{\max} \geq \tilde{A}\theta + \tilde{B} \\
&x_{\min} \leq \tilde{A}\theta + \tilde{B}
\end{aligned}
\tag{A.35}
$$

$$G_x = \begin{bmatrix} \tilde{B} \\ -\tilde{B} \end{bmatrix}, \quad \in \mathbb{R}^{[2Nn_x]\times Mn_u} \tag{A.36}$$

$$W_x = \begin{bmatrix} x_{\max} \\ -x_{\min} \end{bmatrix}, \quad \in \mathbb{R}^{[2Nn_x]\times 1} \tag{A.37}$$

$$E_x = \begin{bmatrix} -\tilde{A} \\ \tilde{A} \end{bmatrix}, \quad \in \mathbb{R}^{[2Nn_x]\times[n_x+n_y]} \tag{A.38}$$

Constraints on u

$$\begin{aligned} &u_{\min} \leq u_0, \ldots, u_{M-1} \leq u_{\max} \\ &u_{\max} \geq U \\ &u_{\min} \leq U \end{aligned} \tag{A.39}$$

$$G_u = \begin{bmatrix} I \\ -I \end{bmatrix}, \quad \in \mathbb{R}^{[2Mn_u]\times Mn_u} \tag{A.40}$$

$$W_u = \begin{bmatrix} u_{\max} \\ -u_{\min} \end{bmatrix}, \quad \in \mathbb{R}^{[2Mn_u]\times 1} \tag{A.41}$$

$$E_u = \begin{bmatrix} 0 \\ 0 \end{bmatrix}, \quad \in \mathbb{R}^{[2Mn_u]\times[n_x+n_y]} \tag{A.42}$$

Constraints on y

$$\begin{aligned} &y_{\min} \leq y_1, \ldots, y_N \leq y_{\max} \\ &y_{\max} \geq \tilde{C}X = \tilde{C}[\tilde{A}\theta + \tilde{B}U] = \tilde{C}\tilde{A}\theta + \tilde{C}\tilde{B}U \\ &y_{\min} \leq \tilde{C}X = \tilde{C}[\tilde{A}\theta + \tilde{B}U] = \tilde{C}\tilde{A}\theta + \tilde{C}\tilde{B}U \end{aligned} \tag{A.43}$$

$$G_y = \begin{bmatrix} \tilde{C}\tilde{B} \\ -\tilde{C}\tilde{B} \end{bmatrix}, \quad \in \mathbb{R}^{[2Nn_y]\times Mn_u} \tag{A.44}$$

$$W_y = \begin{bmatrix} y_{\max} \\ -y_{\min} \end{bmatrix}, \quad \in \mathbb{R}^{[2Nn_y]\times 1} \tag{A.45}$$

$$E_y = \begin{bmatrix} -\tilde{C}\tilde{A} \\ \tilde{C}\tilde{A} \end{bmatrix}, \quad \in \mathbb{R}^{[2Nn_y]\times[n_x+n_y]} \tag{A.46}$$

Constraints on Δu_k

$$\begin{aligned} &\Delta u_{\min} \leq \Delta u_0, \ldots, \Delta u_{M-1} \leq \Delta u_{\max} \\ &\Delta u_{\max} \geq \Delta U \\ &\Delta u_{\min} \leq \Delta U \end{aligned} \tag{A.47}$$

$$G_{\Delta u_k} = \begin{bmatrix} \tilde{N} \\ -\tilde{N} \end{bmatrix}, \quad \in \mathbb{R}^{[2Mn_u] \times Mn_u} \tag{A.48}$$

$$W_{\Delta u_k} = \begin{bmatrix} \Delta u_{\max} \\ -\Delta u_{\min} \end{bmatrix}, \quad \in \mathbb{R}^{[2Mn_u] \times 1} \tag{A.49}$$

$$E_{\Delta u_k} = \begin{bmatrix} \tilde{O} \\ -\tilde{O} \end{bmatrix}, \quad \in \mathbb{R}^{[2Mn_u] \times [n_x + n_y]} \tag{A.50}$$

A.4. Formulation of the Multi-parametric QP Problem

The optimisation function A.2 is now formulated as follows

$$\begin{aligned} H &= H_x + H_y + H_{\Delta u} \\ F &= F_x + F_y + F_u + H_{\Delta u} \end{aligned} \tag{A.51}$$

with the constraints matrices

$$\begin{aligned} G &= G_x + G_u + G_y + G_{\Delta u} \\ W &= W_x + W_u + W_y + W_{\Delta u} \\ E &= E_x + E_u + E_y + E_{\Delta u} \end{aligned} \tag{A.52}$$

and can be solved by applying the POP toolbox for MATLAB, (ParOS, 2004).

B. Explicit solution of the mp-MPC

For control design *CD 1*-*CD 2* in Table 9.1 the parameters θ of the mp-QP problem are defined as follows:

$$\theta = [C_{e,0}\ C_{b,VRG,0}\ C_{t,VRG,0}\ C_{b,M,0}\ C_{t,M,0}\ C_{b,F,0}\ C_{t,F,0}\ C_{I,-1}\ C_e^R], \tag{B.1}$$

where the subscript 0 denotes the start of the control horizon and the subscript -1 the previous time point $t = 0 - 1$. The optimisation variables, for a control horizon $\mathrm{M} = 3$, are given by

$$U = [C_{I,0}\ C_{I,1}\ C_{I,2}]. \tag{B.2}$$

The solution of the mp-QP problem in (8.1) results in n_{CR}=650 such critical regions. The function evaluation to obtain the inhaled anesthetic concentration which is applied, i.e. $C_{I,0}$, for the initial critical regions passed and a set point of $\mathrm{BIS}^R = 40$ are summarised in (B.3), see Figures 9.6, 9.13. All numbers are rounded to the third decimal place.

$$\begin{aligned}
&\mathrm{CR}_1, \mathrm{CR}_9 : C_{I,0} = C_{I,-1} + 0.5 \\
&\mathrm{CR}_{178}, \mathrm{CR}_{215}, \mathrm{CR}_{293} : C_{I,0} = 4 \\
&\mathrm{CR}_{211} : C_{I,0} = -13.325C_{e,0} - 0.557C_{b,VRG,0} - 0.364C_{t,VRG,0} \\
&\qquad\qquad - 0.111C_{b,M,0} - 0.075C_{t,M,0} - 0.003C_{b,F,0} \\
&\qquad\qquad - 0.002C_{t,F,0} + 0.224C_{I,-1} + 15.441C_e^R
\end{aligned} \tag{B.3}$$

The critical region CR_1 in the 9 dimensional parameter space, θ (B.1), is given by the polyhedron in (B.4). All numbers are rounded to the third decimal place.

$$
\begin{aligned}
&0.001C_{b,VRG,0} + 0.007C_{b,M,0} + C_{t,M,0} \leq 9.10\\
&0.001C_{b,VRG,0} + 0.009C_{b,M,0} + C_{t,M,0} + 0.001C_{I,-1} \leq 9.12\\
&0.002C_{b,VRG,0} + 0.001C_{t,VRG,0} + 0.009C_{b,M,0} + C_{t,M,0} + 0.002C_{I,-1} \leq 9.13\\
&0.002C_{b,VRG,0} + 0.002C_{t,VRG,0} + 0.009C_{b,M,0} + C_{t,M,0} + 0.004C_{I,-1} \leq 9.14\\
&0.003C_{b,VRG,0} + 0.003C_{t,VRG,0} + 0.009C_{b,M,0} + C_{t,M,0} + 0.005C_{I,-1} \leq 9.14\\
&0.003C_{b,VRG,0} + 0.004C_{t,VRG,0} + 0.009C_{b,M,0} + C_{t,M,0} + 0.006C_{I,-1} \leq 9.15\\
&0.003C_{b,VRG,0} + 0.004C_{t,VRG,0} + 0.001C_{t,M,0} + 0.011C_{b,F,0} + C_{t,F,0} + 0.007C_{I,-1}\\
&\leq 10.22\\
&C_{e,0} + 0.027C_{b,VRG,0} + 0.006C_{t,VRG,0} + 0.006C_{b,M,0} + 0.001C_{t,M,0} + 0.021C_{I,-1}\\
&\quad \leq 2.329\\
&C_{e,0} + 0.041C_{b,VRG,0} + 0.019C_{t,VRG,0} + 0.008C_{b,M,0} + 0.004C_{t,M,0}\\
&\quad + 0.045C_{I,-1} \leq 2.453\\
&C_{e,0} + 0.062C_{b,VRG,0} + 0.077C_{t,VRG,0} + 0.011C_{b,M,0} + 0.016C_{t,M,0} + 0.137C_{I,-1}\\
&\quad \leq 2.824\\
&0.801C_{e,0} + 0.042C_{b,VRG,0} + 0.039C_{t,VRG,0} + 0.008C_{b,M,0} + 0.008C_{t,M,0}\\
&\quad + 0.094C_{I,-1} - C_e^R \leq -0.108\\
&0.767C_{e,0} + 0.044C_{b,VRG,0} + 0.048C_{t,VRG,0} + 0.008C_{b,M,0} + 0.010C_{t,M,0}\\
&\quad + 0.121C_{I,-1} - C_e^R \leq -0.156\\
&-C_{e,0} \leq 0\\
&C_e^R \leq 2.2\\
&-C_{b,VRG,0} \leq 0\\
&C_{b,VRG,0} \leq 10.717\\
&-C_{t,VRG,0} \leq 0\\
&C_{t,VRG,0} \leq 17.617\\
&-C_{b,M,0} \leq 0\\
&C_{b,M,0} \leq 5.559\\
&-C_{t,M,0} \leq 0\\
&C_{t,M,0} \leq 9.076\\
&-C_{b,F,0} \leq 0\\
&C_{b,F,0} \leq 5.207\\
&-C_{t,F,0} \leq 0\\
&-C_{I,-1} \leq 0\\
&C_{I,-1} \leq 2.50
\end{aligned}
\tag{B.4}
$$

C. Disturbance Rejection during Maintenance of Anaesthesia

During maintenance of anesthesia the aim is stable and constant reference tracking of the target BIS, BIS^R, set by the anesthetist. The ability of the control strategies *CD 2* in Chapter 9 and $\widehat{CD}$ in Chapter 10 to reject typical disturbances on the BIS occurring during the course of surgery is presented in this appendix. These disturbance profiles were published by Dumont *et al.* (2009) and Struys *et al.* (2004) and are shown in Figures C.1 - C.2.

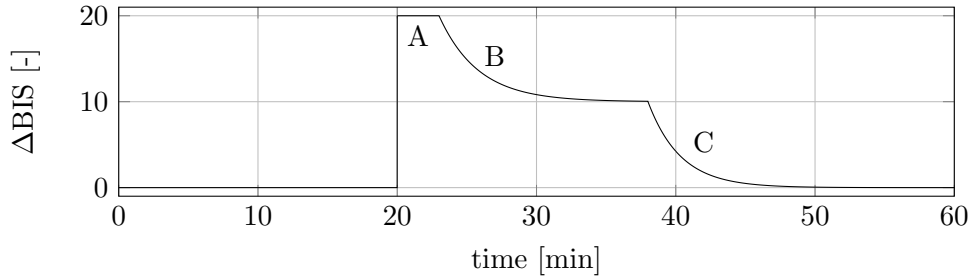

Figure C.1.: Disturbance profile (Dumont *et al.*, 2009; Hahn *et al.*, 2012): A arousal reflex due to the first surgical incision; B offset slowly decreases but settles at an onset of 10% due to continuous normal surgical stimulations; C withdrawal of stimulations during skin-closing.

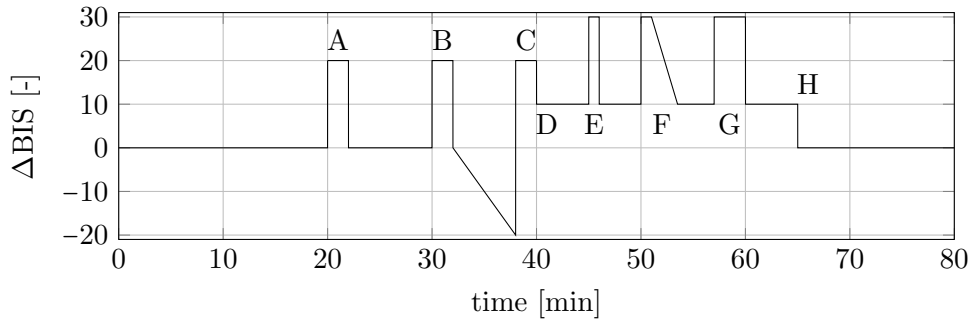

Figure C.2.: Disturbance profile (Struys *et al.*, 2004): A laryngoscopy/intubation; B surgical incision followed by no surgical stimulation; C abrupt stimulus after a period of low stimulation; D onset of a continuous normal surgical stimulation; E, F, and G simulate short-lasting, larger stimulations; H withdrawal of stimulation during closing.

The tuning parameters of the on-line parameter estimator are summarised in Table C.1. To enable a faster adjustment of the controller's dynamics to the measurement $\overline{\Delta t}$ and t_Δ were decreased.

Table C.1.: On-line parameter estimation tuning parameters and design.

Parameter	Value	Unit	
t_{on}	1	min	Minimum time after anesthesia induction to trigger parameter estimation.
$\overline{\Delta BIS}$	2	%	Error to initiate a parameter estimation.
$\overline{\Delta t}$	1	min	Time since the last update of the Hill equation.
t_Δ	30	sec	Past measurements included in the parameter estimation problem.
$\overline{\Delta C_{50}}$	20	% vol %	Deviation of old and newly estimated value of C_{50}.

The simulated BIS, optimal control input, C_I, and estimated C_{50} for *CD 2* and $\widehat{CD}$ and the nominal patient $\mathrm{P_n}$ during maintenance of anesthesia under disturbances in Figures C.1 - C.2 are shown in Figures C.3 - C.8.

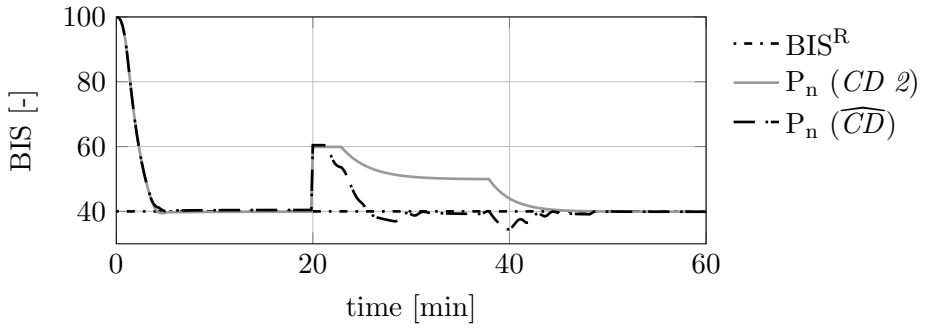

Figure C.3.: BIS for disturbance profile in Figure C.1.

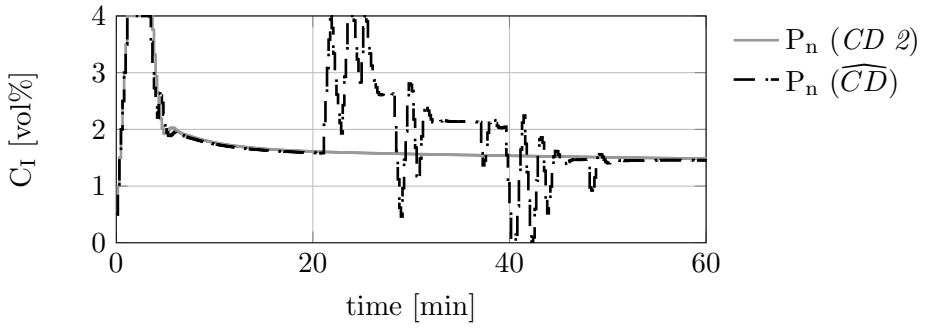

Figure C.4.: C_I for disturbance profile in Figure C.1.

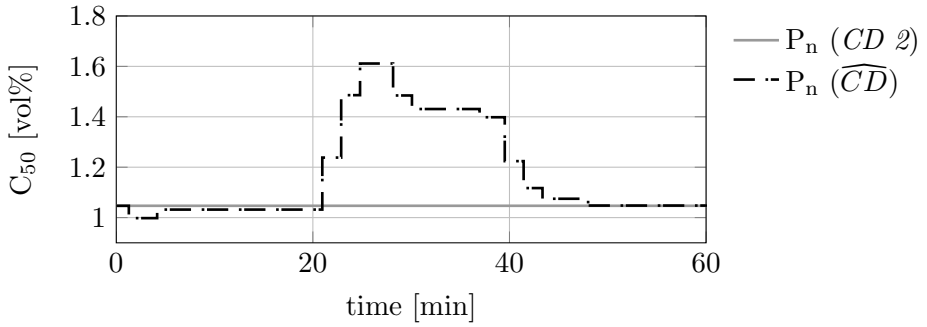

Figure C.5.: Nominal and estimated C_{50} for P_n for disturbance profile Figure C.1.

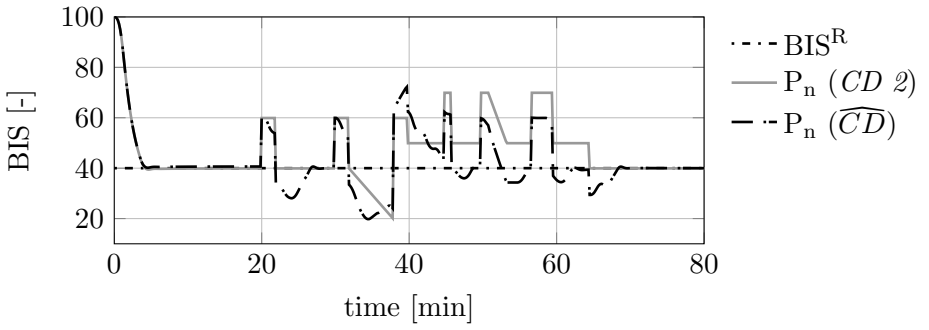

Figure C.6.: BIS for disturbance profile in Figure C.2.

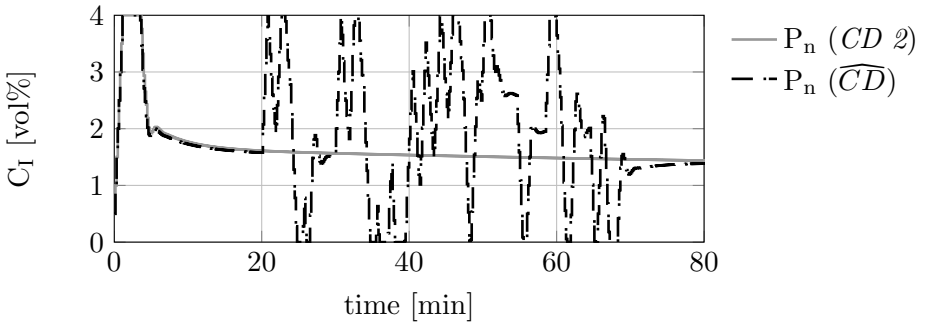

Figure C.7.: C_I for disturbance profile in Figure C.2.

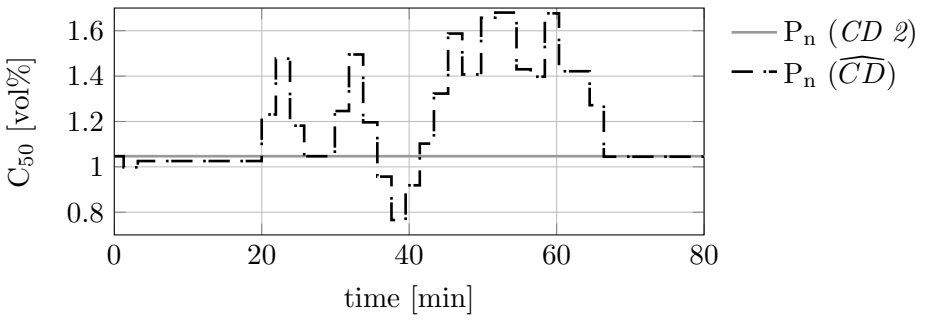

Figure C.8.: Nominal and estimated C_{50} for P_n for disturbance profile in Figure C.2.

Figure C.3 and Figure C.6 show an improved tracking of the BIS for control design $\widehat{CD}$ compared to the nominal controller *CD 2* under external disturbances. The control input, C_I, is shown in Figure C.4 and Figure C.7. The varying C_I is initiated by estimated value of C_{50} in Figure C.5 and Figure C.8 and an updated set point.

$\widehat{CD}$ shows a better performance for the rejection of both disturbance profiles compared to the nominal controller, *CD 2*. For a slowly changing disturbance $\widehat{CD}$ is able to reject the disturbance successfully and steer the system to

the target reference value, shown in Figure C.3 and Figure C.6. After the sequences of different disturbances the estimated value of C_{50} is converging to its nominal value Figure C.5 and Figure C.8, which further affirms the accuracy of the on-line parameter estimator.

C.1. Concluding Remarks

The control strategy $\widehat{CD}$ combines mp-MPC and on-line parameter estimation of C_{50} to address control of anesthesia under uncertainty.
The control strategy was evaluated in this appendix for disturbance rejection of commonly occurring disturbances during the course of surgery. Here, the on-line estimation of C_{50} showed promising results for slowly varying disturbances. However, further investigation is needed to guarantee safe and robust control also during fast acting disturbances.

D. Application of Robust mp-MPC for LPV systems to Anaesthesia

The work presented in this appendix was submitted for publication in Chang *et al.* (2013b). The solution of a multi-parametric model predictive control (mp-MPC) problem for linear time-invariant (LTI) systems is extended to discrete-time linear parameter-varying (LPV) systems, (Chang *et al.*, 2013a).

The method presented in Chang *et al.* (2013a) and in Chang *et al.* (2013b) yields a controller that takes parameter changes into account. This work addresses a robust performance of mp-MPC applied to LPV systems. This method can be implemented conveniently as an add-on to the mp-MPC design. No modification of the established mp-MPC algorithm for LTI systems is required and the simple computational steps can be implemented on-line.

The presented approach for LPV systems is applied to the biomedical application of anaesthesia control. The control objective during anaesthesia is to provide adequate hypnosis for the individual patient undergoing surgery. This objective is obtained by continuous intravenous infusion of the anaesthetic agent propofol, while the hypnotic depth is monitored by the Bispectral Index (BIS). In the presented example for the control of intravenous anaesthesia, the time varying system matrix mimics an external disturbance on the output.

D.1. Intravenous Anaesthesia Model

The first step in order to derive a model predictive controller is the choice of an adequate model of the system. The depth of anaesthesia is monitored by the Bispectral Index (BIS) calculated as a function of the patient's electroencephalogram. The objective of the model is to link the BIS to the propofol infusion. The model predictive control strategy optimises the optimal propofol infusion in order to obtain the desired BIS for a safe depth of anaesthesia. The equation most commonly used to calculate the BIS is the Hill equation:

$$\mathrm{BIS} = \mathrm{BIS}_0 + (\mathrm{BIS}_{max} - \mathrm{BIS}_0)\,\frac{(x_e)^\gamma}{(C_{50})^\gamma + (x_e)^\gamma}, \tag{D.1}$$

here C_{50} is the concentration triggering 50% of the total effect and γ the slope of the Hill equation. $\mathrm{BIS}_0 = 100$ describes a fully awake patient at zero drug concentration and BIS_{max} describes the maximum possible effect, $\mathrm{BIS}_{max} = 0$, (Schnider *et al.*, 1999). x_e denotes the effect-site concentration, which is mimicking the delay of the drug effect and determined as follows:

$$\frac{dx_e}{dt} = k_{e0}(x_1 - x_e), \tag{D.2}$$

where the rate constant k_{e0} describes the time delay between plasma x_1 and effect-site concentration x_e. The link of the intravenous propofol infusion to the plasma concentration x_1 is described by a commonly used and validated pharmacokinetic model for propofol distribution. The individualised model for the specific patient's characteristics is adapted from Schüttler and Ihmsen (2000).

For the presented case study the three compartmental pharmacokinetic model in Schüttler and Ihmsen (2000) for propofol distribution (PK_3) was reduced to a two compartmental pharmacokinetic model (PK_2).

$$\begin{aligned} \frac{dx_1}{dt} &= -(k_{01} + k_{12})x_1 + k_{21}x_2 + \frac{m}{V_1}u, \\ \frac{dx_2}{dt} &= k_{12}x_1 - k_{21}x_2, \end{aligned} \tag{D.3}$$

where the concentration in the plasma is denoted with x_1 and the concentration in the peripheral tissue with x_2. The metabolism of propofol in the plasma is denoted by k_{10} and the distribution from plasma 1 to peripheral tissue 2 and vice versa is denoted by k_{12} and k_{21}, respectively. The volume of the plasma compartment is denoted by V_1 and m is the body weight of the patient, (Schüttler and Ihmsen, 2000). The parameters k_{10}, k_{12} and k_{21} (D.3) were estimated in order to fit the dynamics of the PK_3 model by Schüttler and Ihmsen (2000). All values of the here presented model for a standard male patient and the estimated parameter values of the PK_2 and the original parameter values of the PK_3 model are summarised in Table D.1.

Table D.1.: Parameter list of the intravenous anaesthesia model for propofol.

Parameter	PK_2	PK_3	Units	Ref.
V_1	8840		mL	
m	68		kg	
age	30		years	
k_{10}	0.232	0.162	min^{-1}	Schüttler and Ihmsen (2000)
k_{12}	0.282	0.246	min^{-1}	Schüttler and Ihmsen (2000)
k_{21}	0.041	0.053	min^{-1}	Schüttler and Ihmsen (2000)
k_{e0}	0.456		min^{-1}	Schnider *et al.* (1999)
γ	3.19		-	Schnider *et al.* (1999)
C_{50}	1.68		μg mL	Schnider *et al.* (1999)
BIS_0	100		-	Schnider *et al.* (1999)
BIS_{max}	0		-	Schnider *et al.* (1999)

The output of interest is the effect site concentration x_e (D.2), as it is directly linked to the hypnotic effect and the BIS (D.1); the effect site concentration x_e of the original PK_3 model and the reduced PK_2 model is shown in Figure D.1.

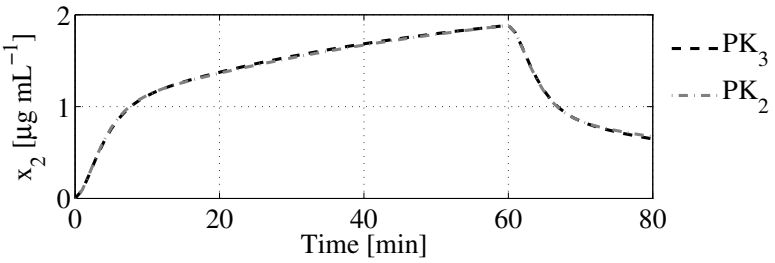

Figure D.1.: Effect site concentration x_e of the PK_3 and PK_2 used in this study. The input profile of u for the shown simulation is $u = 50\,\mu$g min^{-1} for $0\,\text{min} \leq t \leq 60\,\text{min}$ and $u = 0$ for $60\,\text{min} < t \leq 80\,\text{min}$.

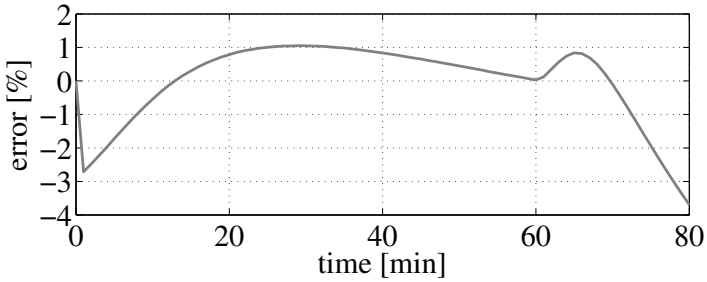

Figure D.2.: The error of Figure D.1 (i.e. PK_3 – PK_2) in percentage.

The continuous state space model for propofol distribution and effect, which is described by (D.2) and (D.3), is formulated as follows:

$$\begin{aligned} \dot{x} &= \mathcal{A}x + \mathcal{B}u \\ y &= \mathcal{C}x, \end{aligned} \tag{D.4}$$

where the matrices of the continuous state space system are:

$$\mathcal{A} = \begin{bmatrix} -(k_{10}+k_{12}) & k_{21} & 0 \\ k_{12} & -k_{21} & 0 \\ k_{e0} & 0 & -k_{e0} \end{bmatrix},$$

$$\mathcal{B} = \begin{bmatrix} \frac{m}{V_1} & 0 & 0 \end{bmatrix}', \quad \mathcal{C} = [0 \;\; 0 \;\; 1].$$

The states of the system x are $x = [x_1 \;\; x_2 \;\; x_e]$, where x_1, the concentration of the plasma compartment 1, x_2, is the concentration of the peripheral compartment 2 and x_e is the effect site concentration. All concentrations are given in $[\mu\text{g mL}^{-1}]$. The propofol infusion u is given in $[\mu\text{g min}^{-1}]$.

In order to bypass for the non-linearity of (D.1), the target effect site concentration x_e, which leads to the desired BIS, is calculated by the inverse Hill equation (D.5) for the control strategy described in the next section,

$$x_e = C_{50}\left(\frac{BIS - BIS_0}{BIS_{max} - BIS}\right)^{1/\gamma}. \tag{D.5}$$

D.2. Multi-parametric Model Predictive Controller for the Anaesthesia LTI System

In this section the explicit mp-MPC controller to obtain the desired BIS by targeting the effect-site concentration x_e is derived. The control objective is to achieve a fast onset of anaesthesia and maintain a stable hypnotic level, indicated by BIS = 50. The inverse Hill equation (D.5) with the parameters of the patient in this case study, Table D.1, gives $x_e = 1.68\,[\mu\text{g mL}^{-1}]$ for BIS = 50 as an equivalent set point (y^R).

In order to derive the mp-MPC the continuous-time model (D.4) is first discretised with sampling time $t_s = 30$ seconds. The resulting discrete time state space representation is formulated as follows:

$$\begin{aligned} x(t+1) &= \hat{A}x(t) + Bu(t), \\ y(t) &= Cx(t), \end{aligned} \tag{D.6}$$

$$\hat{A} = \begin{bmatrix} 0.7745 & 0.0179 & 0 \\ 0.1231 & 0.981 & 0 \\ 0.179 & 0.001978 & 0.7961 \end{bmatrix},$$

$$B = \begin{bmatrix} 0.003493 \\ 0.000255 \\ 0.0003847 \end{bmatrix} \text{ and } C = [0 \;\; 0 \;\; 1],$$

where $\hat{A}$ denotes the time invariant discrete system matrix.

This linear MPC reference tracking problem for system (D.6) is formulated as a constrained optimisation problem with constraints on the states x, output y and input u as follows:

$$\min_U J = \min_U \left(x'_{t+N} P x_{t+N} + \sum_{k=0}^{N-1} u'_{t+k} R u_{t+k} + \sum_{k=1}^{N} (y_{t+k} - y^R)' Q_y (y_{t+k} - y^R) \right)$$

s.t.

$$\begin{aligned} & x_{t+k+1} = \hat{A} x_{t+k} + B u_{t+k}, \quad k = 0, \ldots, N-1, \\ & y_{t+k} = C x_{t+k}, \quad k = 1, \ldots, N, \\ & [0 \;\; 0 \;\; 0]' \le x_{t+k} \le [6 \;\; 45 \;\; 6]', \quad k = 1, \ldots, N, \\ & 0 \le y_{t+k} \le 6, \quad k = 1, \ldots, N, \\ & 0 \le u_{t+k} \le 200, \quad k = 0, 1, \ldots, N-1, \end{aligned} \tag{D.7}$$

where $U = \{u(t), u(t+1), \ldots, u(t+N-1)\}$, $N = 6$ (3 min), $Q_y = 10^6$, $R = 1$, and P the solution of the algebraic Riccati equation, $P = \hat{A}'P\hat{A} - (\hat{A}'PB)(B'PB + I)^{-1}(\hat{A}'PB)'$.

The constrained optimisation problem (D.7) is reformulated as an mp-QP problem (8.2). The optimal control law u is obtained as by affine functions of the parameters, the system states and the set-point (y^R), by the POP MATLAB toolbox, (ParOS, 2004). The solution of the mp-QP problem results in 108 polyhedral critical regions, (8.3).

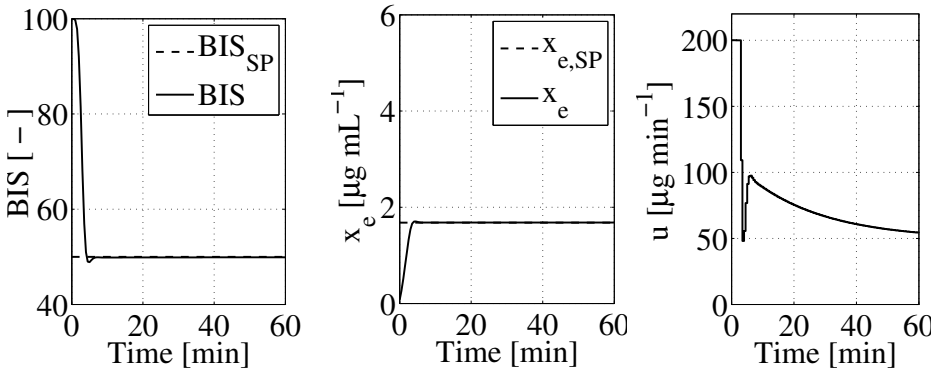

(a) BIS (b) Effect site concentration x_e (c) Measured BIS

Figure D.3.: Closed loop response for the reference tracking linear MPC of the LTI system as a solution of the mp-QP in (D.7).

The closed loop response for the reference tracking linear MPC of the LTI system is shown in Figure D.3. The optimal control trajectory for u is calculated by affine functions of the system states as a solution of the mp-QP (D.7) from initial condition $x(0) = [x_1(0)\ x_2(0)\ x_e(0)]' = [0\ 0\ 0]'$ and set-point BIS $= 50$, Figure D.3(c)). The control objective of a fast induction, low overshoot and stable maintenance of a BIS $= 50$ is successfully achieved by a fast regulation of the effect site-concentration x_e to the calculated set-point $x_{e,SP} = 1.68$ [μg mL^{-1}], Figure D.3(a) and Figure D.3(b)), respectively.

D.3. LPV for Disturbance Rejection During Anaesthesia

During anaesthesia surgical stimulation might act as an external disturbance on the controlled variable, the BIS. For this case study the disturbance is modelled by a slowly time-varying matrix $A(t)$ of the system (D.6), where element $A_{1,1}(t)$ is given as a function of time, i.e.

$$A(t) = \begin{bmatrix} A_{1,1}(t) & 0.0179 & 0 \\ 0.1231 & 0.981 & 0 \\ 0.179 & 0.001978 & 0.7961 \end{bmatrix}. \tag{D.8}$$

The slow change of the system parameter $A_{1,1}$ of up to 50% in magnitude

is given by as follows

$$A_{1,1}(t) = \hat{A}_{1,1}\left(1 - 0.5\sin\left(\frac{\pi t}{30}\right)\right),\ 15 \le t \le 45$$
$$A_{1,1}(t) = \hat{A}_{1,1},\ t < 15, t > 45. \tag{D.9}$$

The change of the value of $A_{1,1}$ in matrix $A(t)$ is shown in Figure D.4.

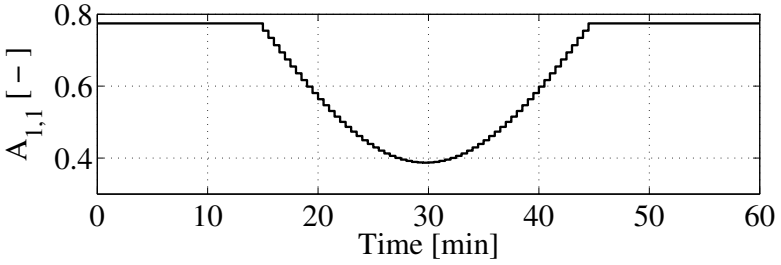

Figure D.4.: Change of $A_{1,1}(t)$ of the LPV system.

The emerging disturbance profile of the BIS which results from (D.9) is shown in Figure D.5(a). The effect of the variation on the states x is shown in Figure D.5(b) and D.5(c).

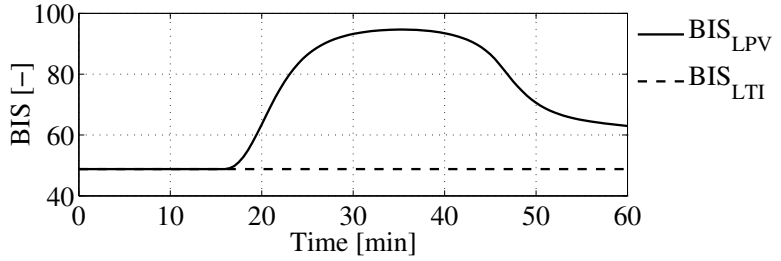

(a) BIS.

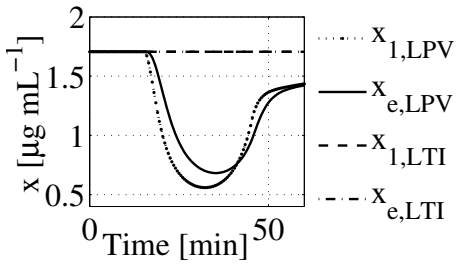

(b) x_1 and x_e.

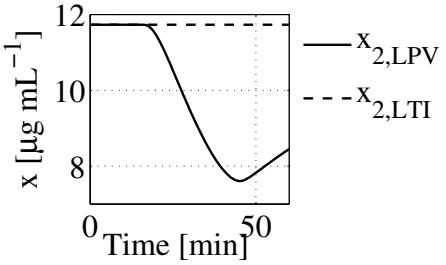

(c) x_2.

Figure D.5.: Disturbance profile of BIS and effect on system states x for the given variation in $A_{1,1}(t)$ (D.9). The system is initialised at steady state for a constant propofol infusion of $u = 50\mu$g min^{-1}.

The error compensation scheme for LPV systems presented in Chang *et al.*

(2013b) is applied to assure safe hypnosis, indicated by a BIS = 50, for this LPV system.

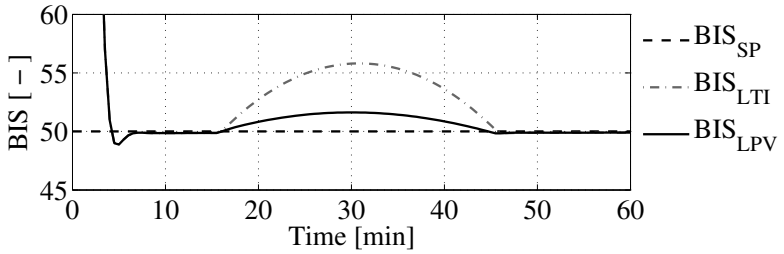

(a) Bispectral Index (BIS).

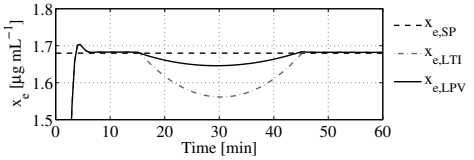

(b) Effect site-concentration x_e.

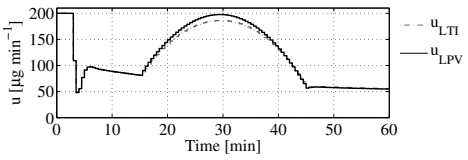

(c) Propofol infusion u.

Figure D.6.: Closed loop response of the mp-MPC for LTI systems ($_{\text{LTI}}$) and the mp-MPC for LPV systems ($_{\text{LPV}}$) for the LPV system (D.6) with $A(t)$ (D.8).

Figure D.6 shows the closed loop response for LPV system with time-varying matrix $A(t)$ for the LTI and LPV mp-MPC. Analogously to the simulation shown Figure D.3, all states are initialised with zero and the set-point is BIS = 50. The proposed error compensation mp-MPC is able to cope with the LPV system and maintains the system closer to the set-points compared to the LTI mp-MPC. Overall the proposed method shows promising results for a 50% reduction in $A_{1,1}$. The application of the mp-MPC for LPV improved the control performance by approximately 60% compared to the LTI mp-MPC.

D.4. Concluding Remarks

The LPV mp-MCP framework was tested for a case study for depth of anaesthesia control by intravenous anaesthesia, where the time variation in the system matrix A described a disturbance due to surgical simulation. The proposed LPV mp-MPC framework showed promising results and steered the system closer to the target set-points compared to the LTI based mp-MPC. The LPV method shows a 60% improvement compared to the mp-MPC for LTI systems.

The presented LPV mp-MPC framework will be further tested in our future

work for a more complex model of anaesthesia, including a wider range of disturbances modelled as variations in the system matrix A that are known to occur during surgery.

Bibliography

Absalom, A. R., De Keyser, R., and Struys, M. M. R. F. (2011). Closed loop anesthesia: Are we getting close to finding the holy grail? *Anesthesia & Analgesia*, **112**(3), 516–8.

Allott, P. R., Steward, A., and Mapleson, W. W. (1976). Pharmacokinetics of halothane in the dog. *British Journal of Anaesthesia*, **48**, 279–295.

Badgwell, T. A. and Muske, K. R. (2002). Disturbance Model Design for Linear Model Predictive Control. In *Proceedings of the American Control Conference*, pages 1621–1626, Anchorage, AK.

Bard, Y. (1974). *Nonlinear Parameter Estimation*. Academic Press, INC. (London) LTD.

Behbehani, K. and Cross, R. R. (1991). A controller for regulation of mean arterial blood pressure using optimum nitroprusside infusion rate. *IEEE Transactions on Biomedical Engineering*, **38**(6), 513–521.

Bemporad, A. and Morari, M. (1999). Robust Model Predictive Control: A Survey. *Robustness in identification and control - Lecture Notes in Control and Information Sciences*, **245**, 207–226.

Bemporad, A., Morari, M., Dua, V., and Pistikopoulos, E. N. (2002). The explicit linear quadratic regulator for constrained systems. *Automatica*, **38**, 3–20.

Bemporad, A., Borrelli, F., and Morari, M. (2003). Min-Max Control of Constrained Uncertain Discrete-Time Linear Systems. *IEEE Transactions on Automatic Control*, **48**(9), 1600–1606.

Bibian, S., Ries, C. R., Huzmezan, M., and Dumont, G. (2005). Introduction to Automated Drug Delivery in Clinical Anesthesia. *European Journal of Control*, **11**(6), 535–557.

Bibian, S., Dumont, G. A., and Zikov, T. (2011). Dynamic behavior of BIS, M-entropy and neuroSENSE brain function monitors. *Journal of Clinical Monitoring and Computing*, **25**(1), 81–7.

Biro, P. (2013). A plea for an independent holistic anaesthesia delivery system. *European Journal of Anaesthesiology*, **30**(3), 97–101.

Bischoff, K. B. (1975). Some fundamental considerations of the applications of pharmacokinetics in cancer chemotherapy. *Cancer Chemotherapy Reports*, **59**, 777–793.

Bischoff, K. B. (1986). Physiological pharmacokinetics. *Bulletin of Mathematical Biology*, **48**(3-4), 309–22.

Bruhn, J., Myles, P. S., Sneyd, R., and Struys, M. M. R. F. (2006). Depth of anaesthesia monitoring: what's available, what's validated and what's next? *British Journal of Anaesthesia*, **97**(1), 85–94.

Brunner, M. D., Braithwaite, P., Jhaveri, R., McEwan, A., Goodman, D. K., Smith, L. R., and Glass, P. S. (1994). MAC reduction of isoflurane by sufentanil. *British Journal of Anaesthesia*, **72**(1), 42–6.

CAE Healthcare (2013). HPS with Müse - The only simulator that truly breathes - for anesthesia, respiratory, emergency and critical care. `http://caehealthcare.com/eng/patient-simulators/hps-human-patient-simulator`.

Carpenter, R. L., Eger, E. I., Johnson, B. H., Unadkat, J. D., and Sheiner, L. B. (1986). Pharmacokinetics of Inhaled Anesthetics in Humans: Measurements during and after the Simultaneous Administration of Enflurane, Halothane, Isoflurane, Methoxyflurane, and Nitrous Oxide. *Anesthesia & Analgesia*, **65**, 575–582.

Chang, H., Pistikopoulos, E. N., and Astolfi, A. (2013a). Robust Multi-parametric Model Predictive Control for Discrete-time LPV Systems. In *2013 American Control Conference (ACC)*, pages 431–436, Washington, DC, USA.

Chang, H., Krieger, A., Astolfi, A., and Pistikopoulos, E. N. (2013b). Robust Multi-parametric Model Predictive Control for LPV systems with Application to Anaesthesia. *submitted to Journal of Process Control*.

Chilcoat, R. (1980). A review of the control of depth of anaesthesia. *Transactions of the Institute of Measurement and Control*, **2**(1), 38–45.

Cork, R. C., Vaughan, R. W., and Bentley, J. B. (1981). General Anesthesia for Morbidly Obese Patients - An Examination of Postoperative Outcomes. *Anesthesiology*, **54**, 310–313.

Cromwell, T. H., Eger, E. I., Stevens, W. C., and Dolan, W. M. (1971). Forane Uptake, Excretion, and Blood Solubility in Man. *Anesthesiology*, **35**(4), 401–8.

Deurenberg, P., Weststrate, J. A., and Seidell, J. C. (1991). Body mass index as a measure of body fatness: age- and sex- specific prediction formulas. *British Journal of Nutrition*, **65**, 105–114.

Dingemanse, J. and Appel-Dingemanse, S. (2007). Integrated Pharmacokinetics and Pharamcodynamics in Drug Development. *Clinical Pharmacokinetics*, **46**, 713–737.

Dumont, G. A., Martinez, A., and Ansermino, J. M. (2009). Robust control of depth of anesthesia. *International Journal of Adaptive Control and Signal Processing*, **23**, 435–454.

Eger, E. I. (1974). *Anesthetic Uptake and Action*. Baltimore: Williams & Wilkins.

Eger, E. I. (2001). Age, minimum alveolar anesthetic concentration, and minimum alveolar anesthetic concentration-awake. *Anesthesia & Analgesia*, **93**(4), 947–53.

Eger, E. I. and Guadagni, N. P. (1963). Halothane Uptake in Man at Constant Alveolar Concentration. *Anesthesiology*, **24**(3), 299–304.

Eger, E. I., Saidman, L. J., and Brandstater, B. (1965). Minimum Alveolar Anesthetic Concentration: A Standard of Anesthetic Potency. *Anesthesiology*, **26**(6), 756–763.

Eger, E. I., Eisenkraft, J. B., and Weiskopf, R. B. (2002). *The Pharmacology of Inhaled Anesthetics*. Dannemiller Memorial Educational Foundation, 1st edition.

Enderle, J. D., Blanchard, S. M., Bronzino, J. D., and Edition, S. (2005). *Introduction to biomedical engineering*. Elsevier Academic Press, 2nd edition.

Ferris, M. C., Jainy, R., and Dirksez, S. (2011). GDXMRW: Interfacing GAMS and MATLAB. `http://www.gams.com/dd/docs/tools/gdxmrw.pdf`.

Findeisen, P. K. (1997). *Moving Horizon State Estimation of Discrete Time Systems*. MSc thesis, University of Wisconsin-Madison.

Fiserova-Bergerova, V. (1992). Inhalation anesthesia using physiologically based pharmacokinetic models. *Drug Metabolism Reviews*, **24**(4), 531–57.

Fiserova-Bergerova, V. and Holaday, D. A. (1979). Uptake and Clearance of Inhalation Anesthetics in Man*. *Drug Metabolism Reviews*, **9**(1), 43–60.

Fiserova-Bergerova, V., Vlach, J., and Singhal, K. (1974). Simulation and prediction of uptake, distribution, and exhalation of organic solvents. *British Journal of Industrial Medicine*, **31**(1), 45–52.

Fiserova-Bergerova, V., Vlach, J., and Cassady, J. C. (1980). Predictable "Individual Differences" in Uptake and Excretion of Gases and Lipid Soluble Vapours Simulation Study. *Brithish Journal of Industrial Medicine*, **37**, 42–49.

GAMS (2013). General Algebraic Modeling System, v 24.1. `http://www.gams.com`.

GE Healthcare (2013). Navigator Applications Suite Software. `http://www3.gehealthcare.co.uk`.

Gentilini, A. L., Rossoni-Gerosa, M., Frei, C. W., Wymann, R., Morari, M., Zbinden, A. M., and Schnider, T. W. (2001). Modeling and closed-loop control of hypnosis by means of bispectral index (BIS) with isoflurane. *IEEE Transactions on Biomedical Engineering*, **48**(8), 874–889.

Ghosh, S., Matsuoka, Y., Asai, Y., Hsin, K.-Y., and Kitano, H. (2011). Software for systems biology: from tools to integrated platforms. *Nature Reviews. Genetics*, **12**(12), 821–32.

Glass, P. S. and Rampil, I. J. (2001). Automated Anesthesia: Fact or Fantasy? *Anesthesiology*, **95**(1), 1–2.

Glass, P. S. A., Gan, T. J., Howell, S., and Ginsberg, B. (1997). Drug Interactions: Volatile Anesthetics and Opioids. *Journal of Clinical Anesthesia*, **9**, 18–22.

Goldberg, I. S., Mostert, J. W., Lanzl, E. F., and Lowe, H. J. (1978). A pharmacokinetic model of closed-circuit inhalation anesthesia. *Annals of Biomedical Engineering*, **6**(3), 231–49.

Goodwin, G. C., Seron, M. M., and De Dona, J. A. (2005). *Constrained control and estimation: an optimisation approach*. Springer, London, UK.

Goutelle, S., Maurin, M., Rougier, F., Barbaut, X., Bourguignon, L., Ducher, M., and Maire, P. (2008). The Hill equation: a review of its capabilities in pharmacological modelling. *Fundamental & Clinical Pharmacology*, **22**(6), 633–48.

Grünberg, F. (2009). Navigating through Anesthesia. Technical Report May, Dräger Review.

Haggard, H. W. (1924a). The absorption, distribution, and elimination of ethyl ether: I. The amount of ether absorbed in relation to the concentration inhaled and its fate in the body. *Journal of Biological Chemistry*, **59**, 737–751.

Haggard, H. W. (1924b). The absorption, distribution, and elimination of ethyl ether: II. Analysis of the mechanism of absorption and elimination of such a gas or vapor as ethyl ether. *Journal of Biological Chemistry*, **59**, 753–770.

Haggard, H. W. (1924c). The absorption, distribution, and elimination of ethyl ether: III. The relation of the concentration of ether, or any similar volatile substance, in the central nervous system to the concentration in the arterial blood, and the buffer action of the body. *Journal of Biological Chemistry*, **59**, 771–781.

Hahn, J.-O., Dumont, G. A., and Ansermino, J. M. (2012). Robust closed-loop control of hypnosis with propofol using WAVCNS index as the controlled variable. *Biomedical Signal Processing and Control*, **7**(5), 517–524.

Hall, C., Lueshen, E., Mosat, A., and Linninger, A. A. (2012). Pharmacokinetics, Pharmacodynamics and Drug Metabolism Interspecies Scaling in Pharmacokinetics: A Novel Whole-Body Physiologically Based Modeling Framework to Discover Drug Biodistribution Mechanisms In Vivo. *Journal of Pharmaceutical Sciences*, **101**(3), 1221–1241.

Hardman, J. G. and Ross, J. J. (2006). Modelling: a core technique in anaesthesia and critical care research. *British Journal of Anaesthesia*, **97**(5), 589–592.

Hemmerling, T. M. (2009). Automated anesthesia. *Current Opinion in Anaesthesiology*, **22**(6), 757–63.

Hemmerling, T. M., Charabati, S., Zaouter, C., Minardi, C., and Mathieu, P. A. (2010). A randomized controlled trial demonstrates that a novel closed-loop propofol system performs better hypnosis control than manual administration. *Canadian Journal of Anaesthesia/Journal canadien d'anesthésie*, **57**(8), 725–35.

Hemmerling, T. M., Arbeid, E., Wehbe, M., Cyr, S., Taddei, R., and Zaouter, C. (2013). Evaluation of a novel closed-loop total intravenous anaesthesia

drug delivery system: a randomized controlled trial. *British Journal of Anaesthesia*, **110**(6), 1031–9.

Hendrickx, J. F. A., Eger, E. I., Sonner, J. M., and Shafer, S. L. (2008). Is synergy the rule? A review of anesthetic interactions producing hypnosis and immobility. *Anesthesia and Analgesia*, **107**(2), 494–506.

Herbst, V. (2010). Anaesthesia Pilot - Dräger Press Release. *Dräger Press Release*, (2), 1–2.

Heymsfield, S., Lohman, T., Wang, Z.-M., and Going, S. (2005). *Human Body Composition*. Human Kinetics, 2nd edition.

Hill, A. V. (1910). The possible effects of the aggregation of the molecules of haemoglobin on its dissociation curves. *Journal of Physiology*, **40**(4), iv–vii.

Ionescu, C. M., De Keyser, R., Torrico, B. C., Smet, T. D., Struys, M. M. R. F., and Normey-Rico, J. E. (2008). Robust predictive control strategy applied for propofol dosing using BIS as a controlled variable during anesthesia. *IEEE Transactions on Biomedical Engineering*, **55**(9), 2161–2170.

Kahn, F. (1926). *Der Mensch als Industriepalast (Man as Industrial Palace)*. Number July. Stuttgart, chromolith edition.

Kalman, R. E. (1960). A New Approach to Linear Filtering and Prediction Problems. *Transactions of the ASME-Journal of Basic Engineering*, **82**(Series D), 35–45.

Kennedy, R. R. (2013). Effect-site estimation of volatile anaesthetic agents: Beyond MAC fractions as a target for anaesthesia delivery. *Trends in Anaesthesia and Critical Care*, **3**(4), 211–215.

Kent, C. D. and Domino, K. B. (2009). Depth of anesthesia. *Current Opinion in Anaesthesiology*, **22**(6), 782–7.

Kerrigan, E. C. and Maciejowski, J. M. (2004). Feedback min-max model predictive control using a single linear program: robust stability and the explicit solution. *International Journal of Robust and Nonlinear Control*, **14**(4), 395–413.

Kety, S. S. (1950). The physiological and physical factors governing the uptake of anesthetic gases by the body. *Anesthesiology*, **11**(5), 515–26.

Kety, S. S. (1951). The theory and applications of the exchange of inert gas at the lungs and tissues. *Pharmacological Reviews*, **3**(1), 1–41.

Kouramas, K. I., Sakizlis, V., and Pistikopoulos, E. N. (2008). Design of Robust Model-Based Controllers via Parametric Programming. *Encyclopedia of Optimization*, pages 667–687.

Kouramas, K. I., Panos, C., and Pistikopoulos, E. N. (2011). Algorithm for robust explicit/multi-parametric MPC in embedded control systems. In *18th IFAC World Congress*, pages 1344–1349, Milano, Italy.

Kouramas, K. I., Panos, C., Faísca, N. P., and Pistikopoulos, E. N. (2013). An algorithm for robust explicit/multi-parametric model predictive control. *Automatica*, **49**(2), 381–389.

Krieger, A., Panoskaltsis, N., Mantalaris, A., Georgiadis, M. C., and Pistikopoulos, E. N. (2011). A novel physiologically based compartmental model for volatile anaesthesia. In E. N. Pistikopoulos, M. C. Georgiadis, and A. C. Kokossis, editors, *21st European Symposium on Computer Aided Process Engineering*, volume 29, pages 1495 – 1499. Elsevier.

Krieger, A., Panoskaltsis, N., Mantalaris, A., Georgiadis, M. C., and Pistikopoulos, E. N. (2012). Analysis of an individualized physiologically based model for anesthesia control. In *IFAC Proceedings Volumes (IFAC-PapersOnline)*, pages 385–390.

Krieger, A., Panoskaltsis, N., Mantalaris, A., Georgiadis, M. C., and Pistikopoulos, E. N. (2013). Modelling and analysis of individualized pharmacokinetics and pharmacodynamics for volatile anaesthesia. *IEEE Transactions on Biomedical Engineering*, **61**(1), 25–34.

Lambert, R. S. C., Rivotti, P., and Pistikopoulos, E. N. (2013). A Monte-Carlo based model approximation technique for linear model predictive control of nonlinear systems. *Computers & Chemical Engineering*, **54**, 60–67.

Lemmens, H. J. M., Bernstein, D. P., and Brodsky, J. B. (2006). Estimating Blood Volume in Obese and Morbidly Obese Patients. *Obesity Surgery*, **16**(6), 773–776.

Lerou, J. G. C. and Booij, L. H. D. J. (2001a). Model-based administration of inhalation anaesthesia. 1. Developing a system model. *British Journal of Anaesthesia*, **86**(1), 12–28.

Lerou, J. G. C. and Booij, L. H. D. J. (2001b). Model-based administration of inhalation anaesthesia. 2. Exploring the system model. *British Journal of Anaesthesia*, **86**(1), 29–37.

Lerou, J. G. C. and Booij, L. H. D. J. (2002). Model-based administration of inhalation anaesthesia. 3. Validating the system model. *British Journal of Anaesthesia*, **88**(1), 24–37.

Lerou, J. G. C., Dirksen, R., Beneken Kolmer, H. H., and Booij, L. H. D. J. (1991a). A system model for closed circuit inhalation anesthesia I. Computer study. *Anesthesiology*, **75**, 345–335.

Lerou, J. G. C., Dirksen, R., Beneken Kolmer, H. H., Booij, L. H. D. J., and Borm, G. F. (1991b). A system model for closed circuit inhalation anesthesia II. Clinical validation. *Anesthesiology*, **75**(2), 230–237.

Lerou, J. G. C., Verheijen, R., and Booij, L. H. D. J. (2002). Model-based administration of inhalation anaesthesia. 4. Applying the system model. *British Journal of Anaesthesia*, **88**(2), 175–83.

Li, G., Wang, S.-W., Rabitz, H., Wang, S., and Jaffe, P. (2002). Global uncertainty assessments by high dimensional model representations (HDMR). *Chemical Engineering Science*, **57**, 4445–4460.

Liu, N., Chazot, T., Genty, A., Landais, A., Restoux, A., McGee, K., Laloe, P.-A., Trillat, B., Barvais, L., and Fischler, M. (2006). Titration of Propofol for Anesthetic Induction and Maintenance Guided by the Bispectral Index: Closed-loop versus Manual Control. *Anesthesiology*, **104**, 686–695.

Locher, S., Stadler, K. S., Boehlen, T., Bouillon, T., Leibundgut, D., Schumacher, P. M., Wymann, R., and Zbinden, A. M. (2004). A new closed-loop control system for isoflurane using bispectral index outperforms manual control. *Anesthesiology*, **101**(3), 591–602.

Lockwood, G. G. (1998). *The Systemic and Cerebral Kinetics of Inhalational Anaesthesia*. Ph.D. dissertation, Imperial College of Science, Technology and Medicine London, London.

Lortat-Jacob, B., Billard, V., Buschke, W., and Servin, F. (2009). Assessing the clinical or pharmaco-economical benefit of target controlled desflurane delivery in surgical patients using the Zeus anaesthesia machine. *Anaesthesia*, **64**(11), 1229–35.

Luginbühl, M., Bieniok, C., Leibundgut, D., Wymann, R., Geoffrey, A. S. J., and Schnider, T. W. (2006). Closed-loop control of mean arterial blood pressure during surgery with alfentanil: Clinical evaluation of a novel model-based predictive controller. *Anesthesiology*, **105**(3), 462–70.

Maeder, U. and Morari, M. (2010). Offset-free reference tracking with model predictive control. *Automatica*, **46**(9), 1469–1476.

Maeder, U., Borrelli, F., and Morari, M. (2009). Linear offset-free Model Predictive Control. *Automatica*, **45**(10), 2214–2222.

Mager, D. E., Wyska, E., and Jusko, W. J. (2003). Diversity of mechanism-based pharmacodynamic models. *Drug metabolism and disposition: the biological fate of chemicals*, **31**(5), 510–8.

Mansour, N. E. and Linkens, D. A. (1989). Pole-assignment self-tuning control of blood pressure in postoperative patients: a simulation study. *IEEE Proceedings*, **136**(1), 1–11.

Manthanwar, A. M., Sakizlis, V., and Pistikopoulos, E. N. (2005). Robust parametric predictive control design for polytopically uncertain systems. In *Proceedings of the American Control Conference, 2005*, pages 3994–3999, Portland, OR, USA. IEEE.

Mapleson, W. W. (1962). The rate of uptake of halothane vapour in man. *British Journal of Anaesthesia*, **34**(11), 11–18.

Mapleson, W. W. (1963). An electric analogue for uptake and exchange of inert gases and other agents. *Journal of Applied Physiology*, **18**(2), 197–204.

Mapleson, W. W. (1964a). Inert gas-exchange theory using an electric analogue. *Journal of Applied Physiology*, **19**, 1193–1198.

Mapleson, W. W. (1964b). Mathematical Aspects of the Uptake, Distribution and Elimination of Inhaled Gases and Vapours. *British Journal of Anaesthesia*, **36**, 129–139.

Mapleson, W. W. (1996). Effect of age on MAC in humans: a meta-analysis. *British Journal of Anaesthesia*, **76**(2), 179–85.

Mayne, D. Q., Raković, S. V., Findeisen, R., and Allgöwer, F. (2006). Robust output feedback model predictive control of constrained linear systems. *Automatica*, **42**(7), 1217 – 1222.

Mertens, M. and Vuyk, J. (1998). Interactions between intravenous anaesthetic agents. *Bailliere Clinical Anesthesia*, **12**(2), 247–261.

Miller, R. D., Eriksson, L. I., Fleisher, L. A., Wiener-Kronish, J. P., and Young, W. L. (2010). *Miller's Anesthesia*. Churchill Livingstone, 7th edition.

Minto, C. F., Schnider, T. W., Short, T. G., Gregg, K. M., Gentilini, A. L., and Shafer, S. L. (2000). Response surface model for anesthetic drug interactions. *Anesthesiology*, **92**, 1603–16.

MMSI (2006). Med Man Simulations, Inc. (MMSI), Gas Man®. `http://www.gasmanweb.com`.

Morari, M. and Gentilini, A. L. (2001). Challenges and opportunities in process control: Biomedical processes. *AIChE Journal*, **47**(10), 2140–2143.

Morley, A., Derrick, J., Mainland, P., Lee, B. B., and Short, T. G. (2000). Closed loop control of anaesthesia: an assessment of the bispectral index as the target of control. *Anaesthesia*, **55**(10), 953–9.

Muske, K. R. and Badgwell, T. A. (2002). Disturbance modeling for offset-free linear model predictive control. *Journal of Process Control*, **12**(5), 617–632.

Nadler, S., Hidalgo, J., and Bloch, T. (1962). Prediction of blood volume in normal human adults. *Surgery*, **51**(2), 224–32.

Nascu, I., Nascu, I., Ionescu, C. M., and De Keyser, R. (2012). Adaptive EPSAC predictive control of the hypnotic component in anesthesia. In *2012 IEEE International Conference on Automation Quality and Testing Robotics (AQTR)*, pages 103–108, Cluj-Napoca, Romania. IEEE.

Pannocchia, G. and Bemporad, A. (2007). Technical Notes and Correspondence. *IEEE Transactions on Automatic Control*, **52**(6), 1048–1053.

Pannocchia, G. and Rawlings, J. B. (2003). Disturbance models for offset-free model-predictive control. *AIChE Journal*, **49**(2), 426–437.

Panos, C., Kouramas, K. I., and Pistikopoulos, E. N. (2010). Robust Explicit/Multi parametric Model Predictive Control for Box-Constrained Linear Dynamic Systems. In *9th International Symposium on Dynamics and Control in Process Systems (DYCOPS 2010)*, pages 198–203, Leuven, Belgium.

Parker, R. S. and Doyle, F. J. (2001). Control-relevant modeling in drug delivery. *Advanced Drug Delivery Reviews*, **48**(2-3), 211–28.

ParOS (2004). Parametric Optimization Programming (POP). `http://www.parostech.co.uk`.

Pelosi, P., Croci, M., Ravagnan, I., Tredici, S., Pedoto, A., Lissoni, A., and Gattinoni, L. (1998). The Effects of Body Mass on Lung Volumes, Respiratory Mechanics, and Gas Exchange During General Anesthesia. *Anesthesia & Analgesia*, **87**, 654–660.

Pistikopoulos, E. N. (2009). Perspectives in Multiparametric Programming and Explicit Model Predictive Control. *AIChE Journal*, **55**(8).

Pistikopoulos, E. N., Faisca, N. P., and Kouramas, K. I. (2009). Explicit Robust Model Predictive Control. *International Symposium on Advanced Control of Chemical Processes (ADCHEM)*.

PSE (2011). Process Systems Enterprise (PSE), Model Validation Guide, Release v3.4.0. `http://www.psenterprise.com`.

Rawlings, J. B. and Mayne, D. Q. (2009). *Model Predictive Control: Theory and Design*. Nob Hill Publishing, LLC, Madison, Wisconsin.

Reboso, J. A., Méndez, J. A., Reboso, H. J., and León, A. M. (2012). Design and implementation of a closed-loop control system for infusion of propofol guided by bispectral index (BIS). *Acta Anaesthesiologica Scandinavica*, **56**(8), 1032–41.

Rehberg, B., Bouillon, T., Zinserling, J., and Hoeft, A. (1999). Comparative Pharmacodynamic Modeling of the Electroencephalography-slowing Effect of Isoflurane, Sevoflurane, and Desflurane. *Anesthesiology*, **91**(2), 397–405.

Rivotti, P., Wittmann-Hohlbein, M., and Pistikopoulos, E. N. (2012a). A combined multi-parametric and dynamic programming approach for model predictive control of hybrid linear systems. In *Proceedings of the 22nd European Symposium on Computer Aided Process Engineering*, pages 17–20.

Rivotti, P., Lambert, R. S. C., and Pistikopoulos, E. N. (2012b). Combined model approximation techniques and multiparametric programming for explicit nonlinear model predictive control. *Computers & Chemical Engineering*, **42**, 277–287.

Robayo, F., Sendoya, D., Hodrea, R., Ionescu, C. M., and De Keyser, R. (2010). Estimating the time-delay for predictive control in general anesthesia. In *Chinese Control and Decision Conference (CCDC)*, pages 3719–3724, Xuzhou, China. IEEE.

Röpcke, H., Rehberg, B., Koenen-bergmann, M., and Bouillon, T. (2001). Surgical Stimulation Shifts EEG Concentration Response Relationship of Desflurane. *Anesthesiology*, **94**(3), 390–399.

Rosow, C. E. (1997). Anesthetic Drug Interaction: An Overview. *Journal Clinical Anesthesia*, **9**(6 Suppl), 27S–32S.

Sakizlis, V., Kakalis, N. M. P., Dua, V., Perkins, J. D., and Pistikopoulos, E. N. (2002). Design of robust model-based tracking controllers via parametric programming. In *Proceedings. IEEE International Symposium on Computer Aided Control System Design*, pages 151–156, Glasgow, Scotland, UK. IEEE.

Sakizlis, V., Kakalis, N. M. P., Dua, V., Perkins, J. D., and Pistikopoulos, E. N. (2004a). Design of robust model-based controllers via parametric programming. *Automatica*, **40**(2), 189–201.

Sakizlis, V., Dua, V., Perkins, J. D., and Pistikopoulos, E. N. (2004b). Robust model-based tracking control using parametric programming. *Computers & Chemical Engineering*, **28**(1-2), 195–207.

Saltzman, W. M. (2001). *Drug Delivery Engineering Principles for Drug Therapy*. Oxford University Press.

Sartori, V., Schumacher, P. M., Bouillon, T., Luginbuehl, M., and Morari, M. (2005). On-line estimation of propofol pharmacodynamic parameters. In *Conference Proceedings of IEEE Engineering in Medicine and Biology Society*, pages 74–77, Shanghai, China.

Schnider, T. W., Minto, C. F., Shafer, S. L., Gambus, P. L., Anderson, C., Goodale, D. B., and Youngs, E. J. (1999). The Influence of Age on Propofol Pharmacodynamics. *Clinical Investigations*, **90**, 1502–16.

Schüttler, J. and Ihmsen, H. (2000). Population Pharmacokinetics of Propofol. *Anesthesiology*, **92**(3), 727–738.

Searle, R. and Hopkins, P. M. (2009). Pharmacogenomic variability and anaesthesia. *British Journal of Anaesthesia*, **103**(1), 14–25.

Sheiner, L. B., Stanski, D. R., Vozeh, S., Miller, R. D., and Ham, J. (1979). Simultaneous modeling of pharmacokinetics and pharmacodynamics: application to d-tubocurarine. *Clinical pharmacology and therapeutics*, **25**(3), 358–371.

Sieber, T. J., Frei, C. W., Derighetti, M. P., Feigenwinter, P., Leibundgut, D., and Zbinden, A. M. (2000). Model-based automatic feedback control versus human control of end-tidal isoflurane concentration using low-flow anaesthesia. *British Journal of Anaesthesia*, **85**(6), 818–25.

Singaravelu, S. and Barclay, P. (2013). Automated control of end-tidal inhalation anaesthetic concentration using the GE Aisys Carestation. *British Journal of Anaesthesia*, **110**(4), 561–6.

Smith, N. T., Zwart, A., and Beneken, J. E. (1972). Interaction between the Circulatory Effects and the Uptake and Distribution of Halothane. *Anesthesiology*, **37**(1), 47–57.

Sreenivas, Y., Yeng, T. W., Rangaiah, G. P., and Lakshminarayanan, S. (2009). A Comprehensive Evaluation of PID, Cascade, Model-Predictive, and RTDA Controllers for Regulation of Hypnosis. *Industrial & Engineering Chemistry Research*, **48**, 5719–5730.

Stadler, K. S. (2003). *Modelling and Control in Anaesthesia - From Design to Validation* -. Doctor of technical sciences, Swiss Federal Institute of Technology.

Stelfox, H. T., Ahmed, S. B., Ribeiro, R. A., Gettings, E. M., Pomerantsev, E., and Schmidt, U. (2006). Hemodynamic monitoring in obese patients: the impact of body mass index on cardiac output and stroke volume. *Critical Care Medicine*, **34**(4), 1243–6.

Struys, M. M. R. F., De Smet, T., Greenwald, S., Absalom, A. R., Bingé, S., and Mortier, E. P. (2004). Control Systems Using Bispectral Index Monitoring - A Simulation Study. *Anesthesiology*, **100**(3), 640–647.

Struys, M. M. R. F., Kalmar, A. F., De Baerdemaeker, L. E. C., Mortier, E. P., Rolly, G., Manigel, J., and Buschke, W. (2005). Time course of inhaled anaesthetic drug delivery using a new multifunctional closed-circuit anaesthesia ventilator. In vitro comparison with a classical anaesthesia machine. *British Journal of Anaesthesia*, **94**(3), 306–17.

Struys, M. M. R. F., Mortier, E. P., and Smet, T. D. (2006). Closed loops in anaesthesia. *Best Practice & Research Clinical Anaesthesiology*, **20**(1), 211–220.

Sui, D., Feng, L., and Hovd, M. (2008). Robust Output Feedback Model Predictive Control for Linear Systems via Moving Horizon Estimation. In *American Control Conference*, pages 453–458.

Tanner, G. (1982). Pharmacokinetics of Inhalation Anesthetics: A Three-Compartment Linear Model. *Anesthesia & Analgesia*, **61**(7), 587–594.

Tanner, G. E., Angers, D. G., Van Ess, D. M., and Ward, C. A. (1986). ANSIM: an anesthesia simulator for the IBM PC. *Computer Methods and Programs in Biomedicine*, **23**(3), 237–42.

Teorell, T. (1937a). Kinetics of distribution of substances administered to the body, I. *Archives Internationales de Pharmacodynamie et de Therapie*, **57**, 205–225.

Teorell, T. (1937b). Kinetics of distribution of substances administered to the body, II. *Archives Internationales de Pharmacodynamie et de Therapie*, **57**, 226–240.

Thompson, M. D. and Beard, D. a. (2011). Development of appropriate equations for physiologically based pharmacokinetic modeling of permeability-limited and flow-limited transport. *Journal of Pharmacokinetics and Pharmacodynamics*, **38**(4), 405–421.

Van Meurs, W. (2011). *Modeling and Simulation in Biomedical Engineering: Applications in Cardiorespiratory Physiology*. McGraw Hill Professional.

Vermeulen, P. M., Lerou, J. G. C., Dirksen, R., Booij, L. H. D. J., and Borm, G. F. (1995). A System Model for Halothane Closed Circuit Anesthesia. *Anesthesiology*, **83**, 515–527.

Voelker, A., Kouramas, K. I., and Pistikopoulos, E. N. (2010). Simultaneous design of explicit/multi-parametric constrained moving horizon estimation and robust model predictive control. *Computers & Chemical Engineering*, **54**, 24–33.

Voelker, A., Kouramas, K. I., and Pistikopoulos, E. N. (2013). Moving horizon estimation: Error dynamics and bounding error sets for robust control. *Automatica*, **49**, 943–948.

West, N., Dumont, G. a., van Heusden, K., Petersen, C. L., Khosravi, S., Soltesz, K., Umedaly, A., Reimer, E., and Ansermino, J. M. (2013). Robust closed-loop control of induction and maintenance of propofol anesthesia in children. *Paediatric Anaesthesia*, **23**(8), 712–9.

Westenskow, D. R., Zbinden, A. M., Thomson, D. A., and Kohler, B. (1986). Control of end-tidal halothane concentration. Part A: Anaesthesia breathing system and feedback control of gas delivery. *British Journal of Anaesthesia*, **58**(5), 555–62.

Yasuda, N., Lockhart, S. H., Eger, E. I., Weiskopf, R. B., Liu, J., Laster, J. M., Taheri, S., and Peterson, N. A. (1991a). Comparison of Kinetics of Sevoflurane and Isoflurane in Humans. *Anesthesia & Analgesia*, **72**, 316–324.

Yasuda, N., Lockhart, S. H., Eger, E. I., Weiskopf, R. B., Johnson, B. H., Freire, B. A., and Fassoulaki, A. (1991b). Kinetics of desflurane, isoflurane, and halothane in humans. *Anesthesiology*, **74**, 489–498.

Yelneedi, S., Lakshminarayanan, S., and Rangaiah, G. (2009). A comparative study of three advanced controllers for the regulation of hypnosis. *Journal of Process Control*, **19**(9), 1458–1469.

Yu, C., Roy, R. J., Kaufman, H., and Bequette, B. W. (1992). Multiple-Model Adaptive Predictive Control of Mean Arterial Pressure and Cardiac Output. *IEEE Transactions on Biomedical Engineering*, **39**(8), 765–778.

Zbinden, A. M., Frei, F., Westenskow, D. R., and Thomson, D. A. (1986). Control of end-tidal halothane concentration Part B: Verification in Dogs. *British Journal of Anaesthesia*, **58**, 563–571.

Ziehn, T. and Tomlin, A. S. (2009). Environmental Modelling & Software GUI - HDMR - A software tool for global sensitivity analysis of complex models. *Environmental Modelling & Software*, **24**(7), 775–785.

Zwart, A., Smith, N. T., and Beneken, J. E. (1972). Multiple Model Approach to Uptake Halothane: Use of an Analog Computer. *Computers and Biomedical Research*, **5**, 228–238.